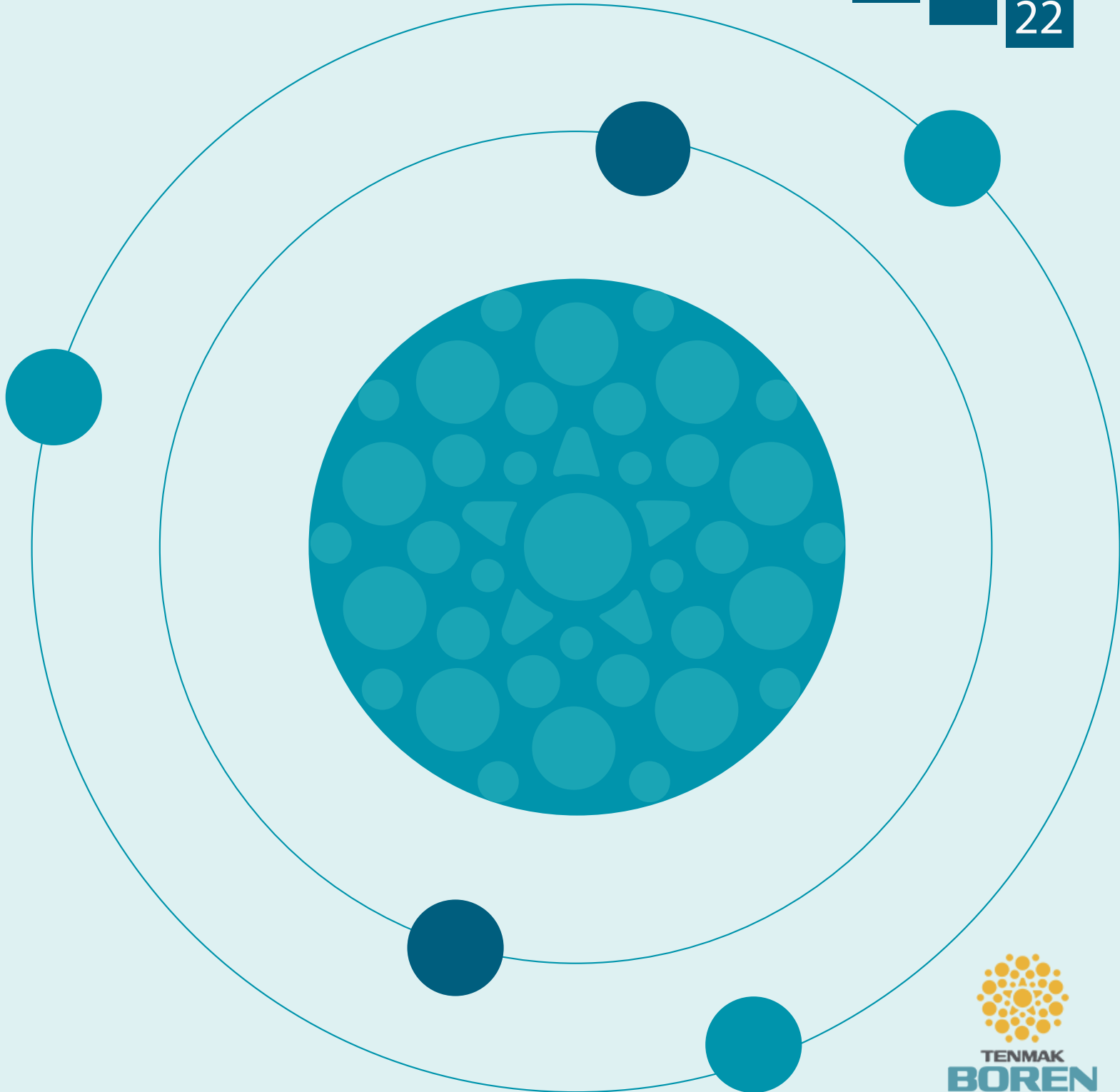


BOR DERGİSİ

JOURNAL OF BORON

CİLT/VOL	SAYI/ISSUE	YIL/YEAR
07	04	2022



BOR DERGİSİ

JOURNAL OF BORON

CİLT VOL 07 SAYI ISSUE 04 YIL YEAR 2022

**Türkiye Enerji Nükleer Maden Araştırma Kurumu (TENMAK) Adına İmtiyaz Sahibi
Owner on Behalf of Turkish Energy, Nuclear and Mining Research Authority (TENMAK)**

Başkan/President

Dr. Abdulkadir Balıkcı (Ankara, Türkiye)

Baş Editör/Editor in Chief

Dr. Zafer Evis (Ankara, Türkiye)

Editörler/Editors

Dr. Abdulkerim Yörükoğlu (Ankara, Türkiye)

Dr. Bengi Yılmaz (İstanbul, Türkiye)

DANIŞMA KURULU

ADVISORY BOARD

Dr. Ali Çırpan (Ankara, Türkiye)	Dr. İsmail Duman (İstanbul, Türkiye)
Dr. Arun K. Chattopadhyay (Pittsburgh, ABD)	Dr. İsmail Girgin (Ankara, Türkiye)
Dr. Atakan Peker (Washington, ABD)	Dr. Jamal Ahmad (Abu Dabi, BAE)
Dr. Ayşen Tezcaner (Ankara, Türkiye)	Dr. Mehmet Suat Somer (İstanbul, Türkiye)
Dr. Bilal Demirel (Kayseri, Türkiye)	Dr. Metin Gürü (Ankara, Türkiye)
Dr. Cahit Helvacı (İzmir, Türkiye)	Dr. Nalan Kabay (İzmir, Türkiye)
Dr. Çetin Çakanyıldırım (Çorum, Türkiye)	Dr. Nuran Ay (Eskişehir, Türkiye)
Derya Maraşlıoğlu (Ankara, Türkiye)	Dr. Olcay Şendil (Ankara, Türkiye)
Dr. Dursun Ali Köse (Çorum, Türkiye)	Dr. Onuralp Yücel (İstanbul, Türkiye)
Dr. Duygu Ağaoğulları (İstanbul, Türkiye)	Dr. Osman Okur (Kocaeli, Türkiye)
Dr. Emin Bayraktar (Paris, Fransa)	Dr. Rifaat Hussain (Islamabad, Pakistan)
Dr. Erol Pehlivan (Konya, Türkiye)	Dr. Rasim Yarım (Friedrichshafen, Almanya)
Dr. Fatih Akkurt (Ankara, Türkiye)	Dr. Raşit Koç (Illinois, ABD)
Dr. Fatih Algı (Aksaray, Türkiye)	Dr. Sait Gezgin (Konya, Türkiye)
Dr. Gülay Özkan (Ankara, Türkiye)	Dr. Sedat Sürdem (Ankara, Türkiye)
Dr. Gülhan Özbayoğlu (Ankara, Türkiye)	Dr. Şafak Gökhan Özkan (İstanbul, Türkiye)
Dr. Hatem Akbulut (Sakarya, Türkiye)	Dr. Şener Oktik (İstanbul, Türkiye)
Dr. Hüseyin Çelikkın (Ankara, Türkiye)	Dr. Taner Yıldırım (Maryland, ABD)
Dr. İhsan Efeoğlu (Erzurum, Türkiye)	Dr. Yuri Grin (Dresden, Almanya)
Dr. İsmail Çakmak (İstanbul, Türkiye)	

**Sorumlu Yazı İşleri Müdürü
Manager of Publication**

Dr. Serap Topsoy Kolukisa
Serap.Kolukisa@tenmak.gov.tr

Yayıncı/Publisher

TENMAK BOREN Bor Araştırma Enstitüsü

Yayın İdare Adresi/Address of Publication Manager

Dumlupınar Bulvarı (Eskişehir Yolu 7. km), No:166, D Blok,
Ankara, 06530, Türkiye
Tel: (0312) 201 36 00
Fax: (0312) 219 80 55
E-posta: boren.journal@tenmak.gov.tr
Web: <https://dergipark.org.tr/boron>

**Editöryal Teknik Personel
Editorial Technical Staff**

Dr. Abdulkadir Solak
Ayça Karamustafaoğlu
Sema Akbaba
Sinem Erdemir Guran

Yayın Türü/Type of Publication: Yaygın süreli yayın

Yayın Aralığı/Range of Publication: 3 Aylık

Yayın Tarihi/Publication Date: 31/12/2022

Bor Dergisi uluslararası hakemli bir dergidir. Dergi, ULAKBİM TR Dizin ve Google Scholar tarafından indekslenmekte olup yılda dört defa yayımlanmaktadır. Derginin yazım kılavuzuna, telif hakkı devir formuna ve yayınlanan makalelere <https://dergipark.org.tr/boron> adresinden ulaşılabilir. / Journal of Boron is International refereed journal. Journal of Boron is indexed by ULAKBİM TR Indexed and Google Scholar, published quarterly a year. Please visit the Journal website <https://dergipark.org.tr/boron> for writing rules, copyright form and published articles.

ANKARA

ARALIK 2022 / DECEMBER 2022

İÇİNDEKİLER/CONTENTS

Effects of different boron salt treatments on micropropagation and genetic stability in <i>in vitro</i> cultures of <i>Liquidambar orientalis</i> Miller	521
..... Taner Mercan, Selin Galatalı, Damla Ekin Ozkaya, Onur Çelik, Ergun Kaya	
Effect of soil application and foliar boron (Etidot-67) on hazelnut yield and kernel ratio	528
..... Faruk Özkutlu, Kürşat Korkmaz, Özlem Ete Aydemir, Mehmet Akgün, Fatmagül Akdin, Bayram Özcan, Özge Şahin, Mehmet Burak Taşkın	
B ₂ O ₃ katkısının PET'in kimyasal bozunma davranışı, termal ve mekanik performansı üzerine etkisi.....	535
..... Bilal Demirel, Ali Yaraş, Fatih Akkurt, Sedat Sürdem	
Investigation of the effects of borogypsum and silica fume on ceramic material's sintering and final properties.....	543
..... Çetin Öztürk, Atilla Evcin	
Co-synthesis of zirconium boride/silicide/oxide composite powders by magnesiothermic reduction	552
..... Didem Ovalı-Döndaş	

Effects of different boron salt treatments on micropropagation and genetic stability in *in vitro* cultures of *Liquidambar orientalis* Miller

Taner Mercan¹, Selin Galatalı¹, Damla Ekin Ozkaya^{1,2}, Onur Celik¹, Ergun Kaya^{1,*}

¹Mugla Sıtkı Kocman University, Faculty of Science, Molecular Biology and Genetic Department, Mugla, 48000, Türkiye

²Dogus University, School of Advanced Vocational Studies, Pathology Laboratory Techniques Program, Istanbul, 34775, Türkiye

ARTICLE INFO

Article history:

Received July 5, 2022

Accepted November 7, 2022

Available online December 31, 2022

Research Article

DOI: 10.30728/boron.1140926

Keywords:

Boric acid

Disodium octaborate

ISSR marker

Sodium metaborate

Sodium perborate

ABSTRACT

In the present study, the effects of different boron salts on the micropropagation of *Liquidambar orientalis* Mill., a relict-endemic plant species, were investigated and genetic stability of micro-shoots was determined by ISSR marker technique. Especially in species with low salinity and drought tolerance, salt stress may cause physiological and molecular changes such as plant growth and development, increase in secondary metabolite content in response to stress, and somaclonal variation. In this context, three different concentrations of boric acid, sodium perborate, sodium metaborate and disodium octaborate salts were applied to meristems isolated from *in vitro* clonal propagated *L. orientalis* and the effects of these boron salts on meristem regeneration and development were evaluated. When compared to the control group samples in which no salt application was applied, the best regeneration percentage was determined as 1 mgL⁻¹ disodium octaborate treatment with a value of 100%, while when the shoot forming capacity index was evaluated, 5 mgL⁻¹ sodium perborate treatment with a value of 4.94 gave the best results. However, when compared with the mother plant, it was observed that all salt treatments caused somaclonal variation on genetic stability, and in the light of the analyzed data, the lowest 30% (5 mgL⁻¹ disodium octaborate) and the highest 49% (1 mgL⁻¹ boric acid) somaclonal variation were determined in all applications.

1. Introduction

Liquidambar orientalis Miller, which is known as Anatolian sweetgum tree is a relict endemic and medicinal-aromatic tree belonging to the Altingiaceae family (Figure 1a) and spreading in the southwestern regions of Türkiye [1, 2]. In the IUCN list of hazard categories, Anatolian Sweetgum is listed in the category of "Highly Threatened in the Medium-Term Future in Nature" [3]. In addition, this species was included in the noble hardwood group by EUFORGEN (European Forest Genetic Resources Program) in 2001 and accepted as a species to be protected throughout

Europe. In addition, this plant species survives only in Fethiye, Marmaris and Köyceğiz districts as a natural forest area in the world, but it is a plant species that is in danger of extinction because of reasons such as climate and making room for agricultural production [4].

The main use of Anatolian sweetgum tree is its oil obtained from pathological balsam channels rather than wood production. Anatolian sweetgum oil, which has been used and traded for thousands of years, is an important source of raw materials for the cosmetics, pharmaceutical and chemical industries and is called "Turkish cytirax" in the world markets [5, 6].

Micropropagation is a tissue culture technique, and it is the name of the process of producing more than one plant with the same genetic characteristics as that plant from organs such as shoots, roots, and stems which capable of forming a new *in vitro* micro-shoots. It requires less material and is a faster production method compared to seed or cutting method production [7]. This technique, which has also been used in the commercial sector, is used in many plant species in park-garden crops, agriculture and forestry [8, 9].

L. orientalis is traditionally produced with seeds.

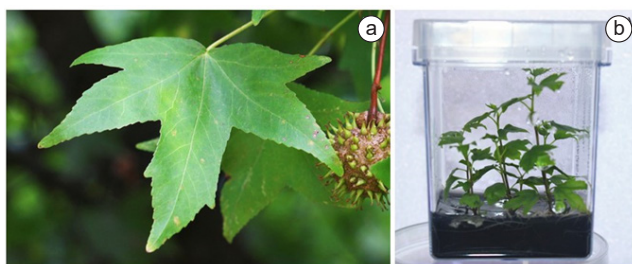


Figure 1. *L. orientalis* plant in natural population area (a); *in vitro* clonal propagated seedlings (b).

*Corresponding author: ergunkaya@mu.edu.tr

Sometimes seed germination can get to two years. Regeneration percentages are generally low. In addition, germ planting has to be done seasonally. For this reason, the mass production is chosen commercially. Clonal propagation by semi-mature shoot cuttings is limited and it is very difficult to collect propagation material from tall trees [10]. Micropropagation is an alternative production model of Anatolian Sweetgum for commercial and conservation purposes [11]. Existing *ex situ* and *in situ* techniques used in the plant genetic resources preservation are reinforced by *in vitro* techniques [12]. Axillary and/or apical shoot meristem-based *in vitro* propagation is one of the beneficial technology used in preservation of the plant biodiversity [13].

Although boron salts and other salinity stresses and their influence on seed germination, shoot growth and development have been studied in the literature [14, 15], there are still some uncertainties regarding the response of plants to the combined stress due to boron salts and other salinity stresses. Irrigation with water having high concentration of boron and other salts in cereals [15] or naturally occurring high levels of salinity and boron are usually found in arid and semi-arid areas [16]. At present, there are limited studies on the effects of boron toxicity and salt stress on plant growth and development and the responses of plants to these stresses, and there is no consensus on the reciprocal relationships between boron toxicity and salinity stress. In this context, the present study aimed to examine the effects of different boron salts on regeneration and development of micro-shoot in *in vitro* growing liquidamber plants.

The another aim of the current work is to analyze the influences of different boron salt treatments *in vitro* on genetic stability at the molecular level. For this purpose, inter simple sequence repeat (ISSR) method, one of the PCR-based molecular marker techniques, was used. This technique was preferred in the present study due to its advantages such as yielding results with a small number of samples, being the dominant marker, primer design without the need for sequence information, high level of allele variations, fast and low cost.

2. Materials and Methods

2.1. Plant Samples and *in vitro* Culture Establishment

The seeds of *L. orientalis* were collected from the natural sweetgum plantation located within the borders of Muğla Province Köyceğiz District Toparlar District (36°59'28.63"N, 28°38'49.07"E). The seeds were disinfected by the seed surface sterilization method (70% ethyl alcohol for five minutes, 10% hydrogen peroxide for five minutes, two times commercial bleach for ten minutes and, sterile distilled water until rinsed) developed by Kaya et al. [17] and transferred to woody plant medium (WPM) medium [18] that does not contain any

growth regulators.

2.2. Boron Salt Treatments

Four different boron salts (disodium octaborate, sodium metaborate, boric acid and sodium perborate) at three different concentrations (1, 3 and 5 mgL⁻¹) were separately combined with WPM nutrient medium supplemented with 1 mgL⁻¹ benzyl adenine, 7 gL⁻¹ (pH 5.8) and meristems cut from *in vitro* clonal propagated *L. orientalis* (Figure 1b) were transferred to these nutrient mediums separately. Ten meristems were used for each application, and each parameter was repeated at least three times. Each sample was incubated for 4 weeks in standard culture conditions (16/8-h photoperiod, 25±2 °C, 50 µmol⁻¹m⁻²s⁻¹ with white cool fluorescent light).

Each salt treatment was evaluated separately. Regeneration percentages, shoot numbers per meristem and stem lengths of meristems grown in nutrient media containing four different boron salts in three different concentrations were recorded separately for each repetition, and the data were then statistically analyzed. The rootstock plant without any salt application was used as the control group. Shoot Forming Capacity (SFC) index was calculated by Eq.1 [19]. Where AVN is average shoot number derived from each regenerating meristem and RMP is regenerating meristem percentage.

$$SFC = \frac{(AVN \times RMP)}{100} \quad (1)$$

2.2.1. Determination of genetic stability

After four weeks of incubation, the remaining *in vitro* material after data collection was individually packaged and stored at -20°C for use in genetic stability analysis. The CTAB-based method developed by Doyle and Doyle [20] was used for the isolation of genomic DNA from the samples. The genomic DNA was quantified spectrophotometrically and stored at -20°C to be used as a template in molecular analysis. Using total genomic DNA as template, PCR was performed with five primers giving the best band profile. Reactions were performed using 0.4 mM dNTP, 2.5 mM MgCl₂, 40 ng primer, 50 ng genomic DNA and 2 units Taq Polymerase in a 25 µl total reaction volume [21]. PCR products were migrated on a 1.5% agarose gel and the band profiles were visualized under UV. 1 kb and 100 bp DNA Ladders were used as guides and were coded as "1" if there is a band and "0" if there is no band." was analyzed using Eq.2. Where HB represents homologous bands and nHB stands for non-homologous bands.

$$\text{Similarity (\%)} = HB / HB + nHB \quad (2)$$

2.3. Statistical Analysis

The nonparametric data statistical analysis was achieved via SPSS (IBM SPSS Statistics 24.0).

Discrete data were subjected to ANOVA to compare means followed by the least significant difference test at $P \leq 0.05$.

3. Results and Discussion

3.1. Influences of Boron Salts on Meristem Regeneration and Shoot Development

When compared the control group with the samples incubated in WPM nutrient medium containing four different boron salts at different concentrations, the best results were obtained from 5 mgL^{-1} sodium perborate (Figure 2).

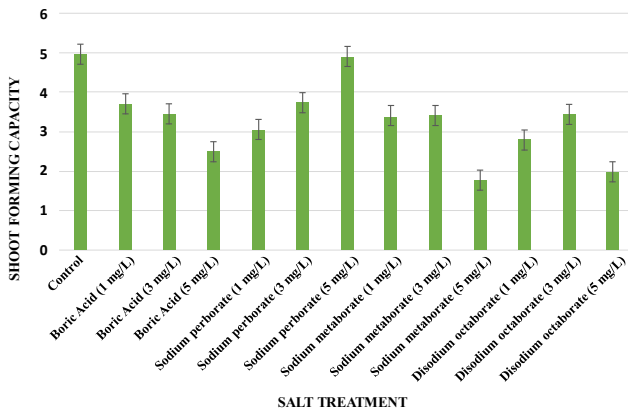


Figure 2. Calculated after salt application, meristem body forming capacities index.

However, the meristems cut from *L. orientalis* micro-shoots (Figure 3a) gave the best regeneration percentage (Figure 3b, Figure 4) in nutrient medium containing 1 mgL^{-1} disodium octaborate, while the maximum shoot numbers from per meristem were obtained from the application of 3 mgL^{-1} boric acid (Figure 5).

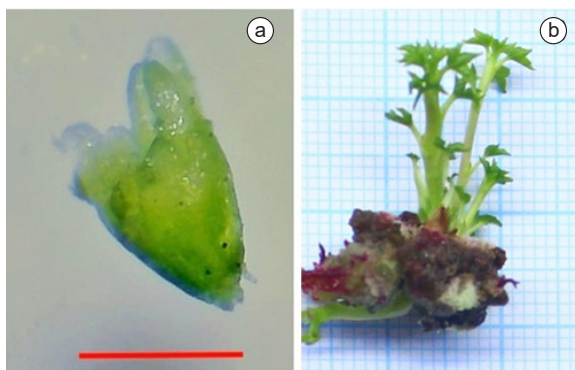


Figure 3. Meristem cut from *L. orientalis* micro-shoots (a), meristem grown in WPM nutrient medium containing 1 mgL^{-1} disodium octaborate (b), size bar 0.34 mm.

In vitro propagation of woody plants has some limitations due to genetic alteration in the process of development and aging of cultures. The *in vitro* cultures are the widely used method for multiplication of important species of woody plants [22] and cytokinin and/

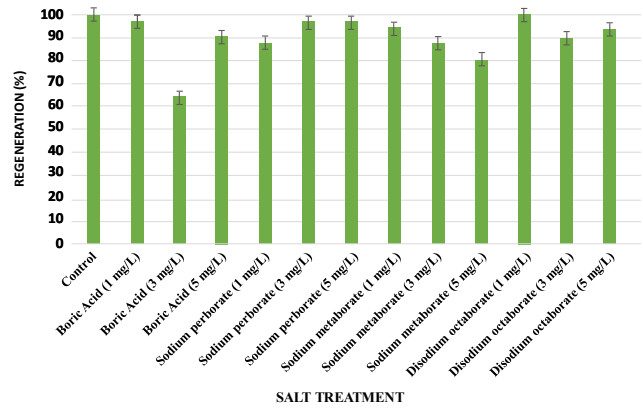


Figure 4. Meristem regeneration rates after different boron salt application.

or cytokinin and auxin growth regulators in optimized ratios are used for culture initiation. Nutrient media that do not contain plant growth regulators or contain auxin-like plant growth regulators for rooting [23] and indole butyric acid (IBA) are generally used to stimulate the roots of woody plants [24].

Micropropagation of woody plant species plays an important role in improving forest yields by supplying seedlings of high trading value. They also play an important role in inducing mineral nutrition, organogenic responses. In the current study, the different boron salt effects on the organogenesis of meristems from *L. orientalis* micro-shoots grown *in vitro* were evaluated. The culture media supplemented with different boron salts at different concentrations affected the *in vitro* organogenic control of *L. orientalis* differently. Boron-induced callus formation in explants let the initiation of well-developed micro-shoots that could be used for development of buds. Similarly, Brondani et al. [25] evaluated the calcium and boron effects on the nodal segments regeneration from *Eucalyptus grandis* micro-shoots. The Murashige and Skoog (MS) medium supplemented with different concentration of calcium and boron [26] was modified to induce regenerative responses in 45-day-old *E. grandis* nodal explants, and after 60 days, dry weight, fresh weight, fresh and dry

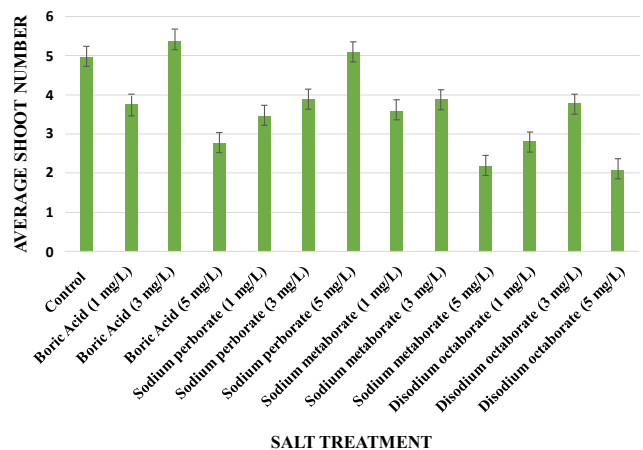


Figure 5. The shoot numbers obtained per meristem.

weight percentages, relative dry weight, fresh weight, fresh and dry weight accumulated by the explants, water content and relative substance content were evaluated. The culture medium supplemented with different concentrations of calcium and boron were found to affect the *in vitro* organogenic control of *E. grandis*.

It is known that the physical and superstructure features of cell walls are influenced by boron shortage [27]. In addition, when plants are developed with insufficient boron, boron is mainly accumulated in the cell wall [28]. Boron is not needed in large quantities by plants, but can cause critical plant development problems if not provided at essential amounts. Boron differs from other microelements in that it does not have chlorosis due to its shortage; however, it has similar toxicity effects as other microelements. Boron, along with calcium, is used in plant cell wall formation and is required for plant cell division. Other roles of boron include carbohydrate metabolism sugar translocation, potassium transport to the stoma, nitrogen metabolism, pollen germination, regulation of hormone levels and formation of certain proteins, regular functioning and growth of the apical meristems, membrane function and structure, and nucleic acid synthesis [29, 30]. In this study, four different boron salts (boric acid, sodium metaborate, sodium perborate, and disodium octaborate) at three different concentrations were used as a boron microelement source, and compared to the control group 3 mgL⁻¹ boric acid and 5 mgL⁻¹ sodium perborate applications, an increase was observed in the number of stems, while the application of 5 mgL⁻¹ disodium octaborate was also found to be effective on stem elongation. When boric acid levels in plant cells are insufficient, plant cells take up borate salts and boric acid as undissociated boric acid via active transport. On the other hand, higher soil concentrations of it are occurred passive diffusion. Boron and its salts are moved to the leaves via xylem, where the water vaporizes and the compounds are deposited on the leaves and left behind. In the phloem, boric acid and its salts are immobile and move little to other parts such as stem and fruit [31]. Boron is a necessary microelement for higher plant species, with the levels of interspecies variations requested for maximum plant development [32]. Studies on boron show that boron plays an important role in cell wall cross-linking, including complexation with specific pectin ingredient [28, 33].

The study of the functions of borax and boric acid on *Vicia faba* and other plant species has shown the effect of boron in plant nutrition [34]. The first large scale work of the functions of boron on plant development was achieved where fifty plant species were chosen and they were grown in sand cultures with normal nutrient solutions at different boron concentrations. The best plant growth, low concentrations that damage the plant, deficiency symptoms, trace boron levels were recorded for each species. The vast majority of plants showed best development up to 5 mgL⁻¹ of boron levels and approximately one third of them grown at trace boron levels were shown morphological deficiency

symptoms. It was concluded that the useful and harmful effects of boron salts overlap across plant species and therefore, he divided into the three broad categories of them sensitive, semi-tolerant and tolerant [35].

3.2. Effects of Boron Salts on Genetic Stability

It has been reported that phenotypic and genetic variations occur in *in vitro* cultures due to environmental conditions, prolongation of the subculture period, culture age, and nutrient media components [36]. The possibility of genetic variations induced by *in vitro* propagation processes requires exclusive consideration when the goal is to replicate special germplasms or to preserve genotypes. Therefore, it is especially critical to evaluate the genetic variation of main regenerants of *L. orientalis*, both because it is a relict endemic species and because of its medicinal aromatic properties. Molecular marker systems that can determine variations at the DNA level are progressively being used to access the genetic compatibility of micropropagated species with the parent material.

ISSR marker system includes the use of single simple sequence repeat (SSR) sequences to initiate the polymerase chain reaction (PCR) thus amplifying sequences between contiguous, but oppositely directional microsatellite regions [37]. ISSR markers have been successfully used in the determination of genetic stability in cauliflower [38], almond [39], banana [40] and *Swertia chirayita* [41] lines. Furthermore, ISSR marker system suggest many advantages, particularly in identifying somaclonal variation, a high degree of sensitivity, dominant representation of polymorphic genetic alleles and reproducibility. In the current thesis study, ISSR markers were used to evaluate the genetic stability of *in vitro* propagated *L. orientalis* microshoots with different concentrations of boron salt applied (Figure 6), and the current work is the first report on

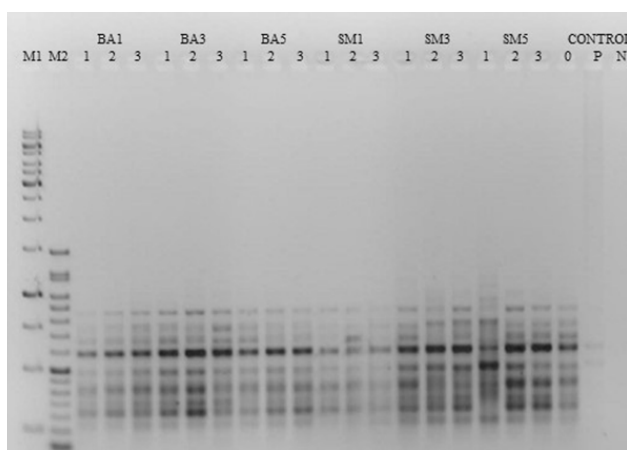


Figure 6. PCR band profiles obtained from ISSR 1 primer with DNA from the samples after application of three different concentrations of boric acid and sodium metaborate. M1: 1 kb gene ruler, M2: 100 bp gene ruler; BA boric acid (BA1: 1 mgL⁻¹; BA3: 3 mgL⁻¹; BA5: 5 mgL⁻¹); SM: sodium metaborate (SM1: 1 mgL⁻¹; SM3: 3 mgL⁻¹; SM5: 5 mgL⁻¹); Control 0: Control with no application; Control P: positive control of different plant; Control N: negative control without DNA template.

the determination of genetic variation as a result of application of different concentrations of boron salt in *in vitro* micro-shoots.

Salt stress due to combined effect of different minerals in the soil is within the important abiotic stresses that inhibit yield production worldwide [42], and the total area affected by salt stress is estimated to be ~80 mha [43]. Saltiness has profound influence on general plant morphology and physiology in different ways, ranging from metabolic, anatomic and physiological changes to molecular degradation [44, 45]. *L. orientalis* trees have moderate tolerance to various adverse environmental stresses, while their tolerance to salinity and drought may be low. *L. orientalis* is an economically important medicinal and aromatic plant that grows in wet and temperate regions. While sweetgum produces a limited number of shoots with traditional methods, *in vitro* tissue cultures are an excellent application for mass seedling production, but it is very critical to preserve the genetic stability of these and similar medicinal aromatic plants in *in vitro* propagated micro-shoots. The present study aimed to investigate the effects of different boron salts on the micropropagation of the plant in order to achieve genetically stable mass propagation in sweetgum and to produce genetically stable plants on a commercial scale. In ISSR PCR reaction analyzes using DNAs isolated from shoots of sweetgum plants after *in vitro* regeneration using meristem tissues as explant source, the lowest (30.77%) after 5 mgL⁻¹ disodium octaborate application, and the lowest after 1 mgL⁻¹ boric acid application. Polymorphism was determined with the highest rates (49.45%). Propagation of plants by tissue culture often undergoes genetic alterations among regenerated plant species, most likely due to stresses applied during micropropagation [46]. These alterations contain point mutations, chromosomal rearrangements and methylated DNA [47, 48]. The somaclonal variation is mostly due to genetic and/or epigenetic alterations during *in vitro* propagation of plants [49].

Somaclonal or culture-induced alterations have long-term been recognized as a source of beneficial or undesirable effects in plants cultured *in vitro*. Some of these undesirable effects contain anatomical and morphological features, secondary metabolite production, environmental stress tolerance, and other critical features of interest to the plant producer [50]. Many factors potentially responsible for somaclonal variation have been identified in the literature, such as desiccation, injury, inappropriate nutrient supply, and osmotic stress [51]. During micropropagation, micro-shoots are exposed to these stress conditions, which introduces both epigenetic and genetic alterations in the resulting multiplied shoots [52]. Genetic changes persist in following generations in the form of somatic recombination, chromosome rearrangements, addition of transposons, point mutations and ploidy variation. Epigenetic changes consist of histone modifications and DNA methylation. The molecular markers have commonly been used to determine genetic alteration

between source material and obtained somaclons in different plant species. In our study, three different concentrations of four different boron salts were tested for regeneration and micro-shoot development from meristem tissue. In woody species that are difficult to propagate *in vitro*, such as *L. orientalis*, some limitations are observed, such as necrosis formation on shoot tips, suppression of growth and development, suppressing *in vitro* culture. The cell development and *in vitro* regeneration of plants are an asexual process involving only mitotic cell divisions. In this context, the emergence of random spontaneous and uncontrolled alterations while *in vitro* clonal propagation is a critical limitation [53]. In such cases, *in vitro* cultures are treated by changing the concentration and/or variety of growth regulators, organic components, various amino acids, macro and micro elements in the nutrient medium composition. During these applications, application pressure from time to time, changing salt concentration and/or stress effects depending on the type cause somaclonal variations.

4. Conclusions

The tolerant species withstand a high concentrations of boron with little effect, and the sensitive species react strongly to too much or too little boron. In the light of the results obtained from our study, it can be said that it is in the semi-tolerant category for *L. orientalis*. There are many studies in the literature showing that various variations are noticed in plants propagated by *in vitro* tissue culture techniques [54, 55]. These variations, which are spontaneous in nature or caused by environmental factors, are stimulated by different stress conditions and biochemical compounds in *in vitro* cultures. Variation occurs from differentiated cells during embryogenesis and organogenesis using multiple or single cells, and also *in vitro* cultural condition induces the regulation of pre-existing variation expressions. The most of these variations are a big problem for seedling producers. However, these alterations are promising for the future studies focusing on plant quality.

Acknowledgement

This study is derived from Taner Mercan's master's thesis. Authors would like to thank Muğla Metropolitan Municipality Agricultural Services Department for providing plants and laboratory facilities during the thesis work.

References

- [1] Aslan, M. B., & Sahin, H. T. (2016). A forgotten forest product source: Anatolian sweetgum tree (*Liquidambar orientalis* Miller). *Journal of Bartın Faculty of Forestry*, 18(1), 103-117.
- [2] Alan, M., Velioglu, E., Ezen, T., Sıklar, S., & Ozturk, H. (2018). Diversity of some quantitative characters of oriental sweet gum (*Liquidambar orientalis* Mill.) for five-year-old seedlings. *Turkish Journal of Forestry Research*,

- 5(1), 74-81.
- [3] Ekim, T., Koyuncu, M., Vural, M., Duman, H., Aytac, Z., & Adıguzel, N. (2000). *Türkiye Bitkileri Kırmızı Kitabı (Eğrelti ve Tohumlu Bitkiler) [Red data book of Turkish plants (Pteridophyta and Spermatophyta)]*. Turkish Nature Conservation Association & Van 100. Yıl University.
- [4] Alan M, Kaya Z (2003). *Oriental sweet gum Liquidambar orientalis*. EUFORGEN technical guidelines. www.biodiversityinternational.org/publications.
- [5] Acar, M. I. (1989). Determination of composition of *Liquidambar orientalis* Mill. balm essential oil by analyzing it with GC-MS-DS system. *Forestry Research Institute Publications*, 33, 5-21.
- [6] Bozkurt, Y., Goker, Y., & Kurtoglu, A. (1989). Some properties of sweetgum tree. *Journal of the Faculty of Forestry Istanbul University*, 39(1), 43-52.
- [7] Ozkaynak, E., & Samancı, B. (2005). Acclimatization in micropropagation. *Selcuk Journal of Agriculture and Food Sciences*, 19(36), 28-36.
- [8] Pospisilova, J., Ticha, I., Kadlecek, P., Haisel, D., & Plzakova, S. (1999). Acclimatization of micro-propagated plants to ex vitro conditions. *Biologia Plantarum*, 42(4), 481-497.
- [9] Mansuroglu, S., & Gurel, E. (2001). Micropropagation. In Babaoglu, M., Gürel, E., & Ozcan, S. (Eds.), *Plant Biotechnology I. Tissue Culture and Applications* (8, 262-281), Selcuk University Foundation Publications.
- [10] Erdağ, B., & Emek, E. (2005). In vitro adventitious shoot regeneration of *Liquidambar orientalis* miller. *Journal of Biological Sciences*, 5(6), 805-808.
- [11] Bayraktar, M., Hayta, S., Parlak, S., & Gurel, A. (2015). Micropropagation of centennial tertiary relict trees of *Liquidambar orientalis* Miller through meristematic nodules produced by cultures of primordial shoots. *Trees*, 29(4), 999-1009.
- [12] Krishnan, P. N., Decruse, S. W., & Radha, R. K. (2011). Conservation of medicinal plants of Western Ghats, India and its sustainable utilization through *in vitro* technology. *In Vitro Cellular & Developmental Biology-Plant*, 47(1), 110-122.
- [13] Reed, B. M., Sarasan, V., Kane, M., Bunn, E., & Pence, V. C. (2011). Biodiversity conservation and conservation biotechnology tools. *In Vitro Cellular & Developmental Biology-Plant*, 47(1), 1-4.
- [14] Munns, R., & Termaat, A. (1986). Whole-plant responses to salinity. *Australian Journal of Plant Physiology*, 13, 143-160.
- [15] Nable, R. O., Banuelos, G. S., & Paull, J. G. (1997). Boron toxicity. *Plant and Soil*, 193, 181-198.
- [16] Keren, R., & Bingham, F. T. (1958). Boron in water, soils, and plants. In *Advances in Soil Science* (pp. 229-276). Springer, New York, NY.
- [17] Kaya, E., Souza, F. V. D., Yılmaz-Gokdogan, E., Ceylan, M., & Jenderek, M. (2017). Cryopreservation of citrus seed via dehydration followed by immersion in liquid nitrogen. *Turkish Journal of Biology*, 41, 242-248.
- [18] Lloyd, G., & McCown, B. H. (1980). Commercially feasible micropropagation of mountain laurel (*Kalmia latifolia*) by use of shoot tip culture. *The International Plant Propagators Society*, 30, 421427.
- [19] Lambardi, M., Sharma, K. K., & Thorpe, T. A. (1993). Optimization of *in vitro* bud induction and plantlet formation from mature embryos of Aleppo pine (*Pinus halepensis* Mill.). *In Vitro Cellular & Developmental Biology-Plant*, 29, 189-199.
- [20] Doyle, J. J., & Doyle, J. L. (1987). A rapid DNA isolation procedure for small quantities of fresh leaf tissue. *Phytochemistry Bulletin*, 19, 11-15.
- [21] Kaya, E. (2015). ISSR analysis for determination of genetic diversity and relationship in eight Turkish olive (*Olea europaea* L.) cultivars. *Notulae Botanicae Horti Agrobotanici Cluj-Napoca*, 43(1), 96-99.
- [22] Skirvin, R. M. (1986). Propagation of temperate fruits and nuts. In Conger, B. V. (Ed.), *Cloning of agricultural plants via in vitro techniques*. CRC Press.
- [23] George, E. F., Hall, M. A., & De Klerk, G. J. (Eds.). (2007). *Plant propagation by tissue culture: Volume 1. The background (Vol. 1)*. Springer Science & Business Media.
- [24] Kataeva, N. V., & Butenko, R. G. (1987). Clonal micropropagation of apple trees. *Acta Horticulturae*, 12, 585-588.
- [25] Brondani, G. E., Araujo, M. A. D., Alcântara, B. K. D., Carvalho, J. G. D., Gonçalves, A. N., & Almeida, M. D. (2012). In vitro organogenesis of *Eucalyptus grandis*: Effects of boron and calcium. *Acta Scientiarum. Agronomy*, 34, 403-411.
- [26] Murashige, T., & Skoog, F. A. (1962). Revised medium for rapid growth and bioassays with tobacco tissue cultures. *Physiologia Plantarum*, 15(3), 473-497.
- [27] Findekle, P., & Goldbach, H. E. (1996). Rapid effects of boron deficiency on cell wall elasticity modulus in *Cucurbita pepo* roots. *Botanica Acta*, 109(6), 463-465.
- [28] Hu, H., Brown, P. H., & Labavitch, J. M. (1996). Species variability in boron requirement is correlated with cell wall pectin. *Journal of Experimental Botany*, 47(2), 227-232.
- [29] Teng, C. C., & Zhang, Y. C. (2009). The Influence of boric acid and sucrose on the in vitro germination of Potato pollen. *Seed*, 28(2), 15-20.
- [30] Liang, G. J., Huang, G. P., & Deng L. (2011). Effect of boron, sugar, calcium and DA-6 on the growth of loquat pollen tube. *Journal of Zhaoqing University*, 32(2), 50-56.
- [31] Lank, P., & Wahl, M. (2014). Boric Acid. In Philip, W. (Ed.), *Encyclopedia of Toxicology* (Third Edition, 533-535). Academic Press.
- [32] Lovatt, C. J., & Dugger, W. M. (1984). Boron. In Frieden, E. (Ed.), *Biochemistry of the essential ultratrace*

- elements* (389-421). Plenum Press.
- [33] Loomis, W. D., & Durst, R. W. (1992). Chemistry and biology of boron. *BioFactors*, 3(4), 229-239.
- [34] Warrington, K. (1923). The effects of boric acid and borax on the bread bean and certain other plants. *Annals of Botany*, 37, 629-672.
- [35] Eaton, F. M. (1944). Deficiency, toxicity, and accumulation of boron in plants. *Journal of Agricultural Research*, 69(6), 237-277.
- [36] Larkin, P. J., & Scowcroft, W. R. (1981). Somaclonal variation—a novel source of variability from cell cultures for plant improvement. *Theoretical and Applied Genetics*, 60(4), 197-214.
- [37] Zietkiewicz, E., Rafalski, A., Labuda, D. (1994). Genome fingerprinting by simple sequence repeat (SSR)-anchored polymerase chain reaction amplification. *Genomics*, 20(2), 176-183.
- [38] Leroy, X. J., Leon, K., Charles, G., & Branchard, M. (2000). Cauliflower somatic embryogenesis and analysis of regenerant stability by ISSRs. *Plant Cell Reports*, 19(11), 1102-1107.
- [39] Martins, M., Sarmiento, D., & Oliveira, M. M. (2004). Genetic stability of micropropagated almond plantlets, as assessed by RAPD and ISSR markers. *Plant Cell Reports*, 23(7), 492-496.
- [40] Venkatachalam, L., Sreedha, R. V., & Bhagyalakshmi, N. (2007). Micropropagation in banana using high levels of cytokinins does not involve any genetic changes as revealed by RAPD and ISSR markers. *Plant Growth Regulation*, 51(3), 193-205.
- [41] Joshi, P., & Dhawan, V. (2007). Assessment of genetic fidelity of micropropagated Swerita chiraytia plantlets by ISSR marker assay. *Plant Biology*, 51(1), 22-26.
- [42] Gollack, D., Li, C., Mohan, H., & Probst, N. (2014). Tolerance to drought and salt stress in plants, unraveling the signaling networks. *Frontiers in Plant Science*, 5, 151.
- [43] El-Beltagi, H. S., Ahmed, S. H., Namich, A. A. M., & Abdel-Sattar, R. R. (2017). Effect of salicylic acid and potassium citrate on cotton plant under salt stress. *Fresenius Environmental Bulletin*, 26(1A), 1091-1100.
- [44] Wang, W. X., Barak, T., Vinocur, B., Shoseyov, O., & Altman, A. (2007). Abiotic resistance and chaperones, possible physiological role of SP1, a stable and stabilizing protein from *Populus*. In Vasil, K. (Ed.), *Plant Biotechnology 2000 and Beyond* (pp. 439-443). Dordrecht, Kluwer.
- [45] Flowers, T. J., & Colmer, T. D. (2015). Plant salt tolerance, adaptations in halophytes. *Annals of Botany*, 115(3), 327-331.
- [46] Matthes, M., Singh, R., Cheah, S. C., & Karp, A. (2001). Variation in oil palm (*Elaeis guineensis* Jacq.) tissue culture derived regenerants revealed by AFLPs with methylationsensitive enzymes. *Theoretical and Applied Genetics*, 102(6), 971-979.
- [47] Afify, A. M. R., El-Beltagi, H. S., Abd El-Salam, S. M., & Omran, A. A. (2012). Protein solubility, digestibility and fractionation after germination of sorghum varieties. *PLoS ONE*, 7(e31154), 1-6.
- [48] Krishna, H., Alizadeh, M., Singh, D., Singh, U., Chauhan, N., Eftekhari, M., & Sath, R. K. (2016). Somaclonal variations and their applications in horticultural crops improvement. *3 Biotech*, 6(1), 1-18.
- [49] Bhojwani, S. S., & Dantu, P. K. (2013). *Plant tissue culture, an introductory text*. Springer.
- [50] Veilleux, R. E., & Johnson, A. T. (1998). Somaclonal variation: Molecular analysis, transformation interaction, and utilization. *Plant Breeding Reviews*, 16, 229-268.
- [51] Filipecki, M., & Malepszy, S. (2006). Unintended consequences of plant transformation: A molecular insight. *Journal of Applied Genetics*, 47(4), 277-286.
- [52] Evans, D. A., & Sharp, W. R. (1988). Somaclonal and-gametoclonal variation. In Evans, D. A., Sharp, W. R., & Ammirato, P. V. (Eds.), *Handbook of Plant Cell Culture* (97-132). Macmillan Publishing Company.
- [53] Karp, A. (1994). Origins, causes and uses of variation in plant tissue cultures. In Vasil, I. K., & Thorpe, T. A. (Eds.), *Plant cell and tissue culture* (139-152). Dordrecht: Kluwer Academic Publishers.
- [54] Barret, P., Brinkman, M., & Beckert, M. (2006). A sequence related to rice Pong transposable element displays transcriptional activation by in vitro culture and reveals somaclonal variations in maize. *Genome*, 49(11), 1399-1407.
- [55] Baranek, M., Krizan, B., Ondrusikova, E., & Pidra, M. (2010). DNA-methylation changes in grapevine somaclones following in vitro culture and thermotherapy. *Plant Cell, Tissue and Organ Culture (PCTOC)*, 101(1), 11-22.



Effect of soil application and foliar boron (Etidot-67) on hazelnut yield and kernel ratio

Faruk Özkutlu^{1,*}, Kürşat Korkmaz¹, Özlem Ete Aydemir¹, Mehmet Akgün¹, Fatmagül Akdin¹, Bayram Özcan¹, Özge Şahin², Mehmet Burak Taşkın²

¹Ordu University, Faculty of Agriculture, Department of Soil Science and Plant Nutrition, Ordu, 52200, Türkiye

²Ankara University, Faculty of Agriculture, Department of Soil Science and Plant Nutrition, Ankara, 06000, Türkiye

ARTICLE INFO

Article history:

Received July 7, 2022

Accepted November 7, 2022

Available online December 31, 2022

Research Article

DOI: 10.30728/boron.1142160

Keywords:

Boron
Hazelnut
Quality
Yield

ABSTRACT

In this study, the effect of boron fertilizations of foliar and soil was investigated on the quality of hazelnuts (*Corylus avellana* L.) in two provinces in Turkey between 2013 and 2014. The experimental trials were carried out in soil application (0.0, 3.0 and 6.0 g per Ocak) and foliar spraying (0 and 300 mg B L⁻¹). Results show that compared with the control, soil and foliar application of boron increased hazelnut yield and quality. Due to the two-year average, the highest yield of the hazelnut in Samsun-Çarşamba was obtained from the application and dose of 36.70% increase in hazelnut yield was achieved by applying B (3g Ocak⁻¹) from the soil in comparison with the control application. It was a 20% increase in Ordu-Ulubey district. The highest kernel ratio of hazelnut was obtained from F1S2 applications for the two districts. Increases were observed at Samsun-Çarşamba (10%) and Ordu-Ulubey (7%). Results showed that there was also a positive association between the B leaf concentration and hazelnut yield and kernel ratio and no significant differences between foliar and soil applications on hazelnut quality. As a result of this study, and with increasing yield, foliar applications of B are an effective method of supplying sufficient B for the flowers. In addition, B leaf applications are more appropriate than soil B application.

1. Introduction

The hazelnut (*Corylus avellana* L.) is a hard-shelled fruit that has been known to man for about 5000 years. It originated in the Black Sea area and spread to the world from there. The main nut producers in the world are Türkiye, Italy, the United States, and Spain. Türkiye's hazelnut production is still on going in 705,445 hectares of cultivable land, especially on the Black Sea Coast [1]. Although Türkiye is the largest producer of hazelnuts in the world and accounting for about 70% of the world's supply, its production performance is quite low compared to other countries. Low lime content of the soil, slope, shallow soil depth, low water holding capacity, and high clay content are the main reasons for low hazelnut yield. In addition, the lack of macro and micro-nutrients in the soil is another cause.

Boron is an essential micronutrient for plant growth and fruit production. It affects pollen germination and pollen tube growth [2]. Boron deficiency in soils has been reported in 80 countries and 132 plant species [3]. It was also reported that 85% of areas in hazelnut orchards are insufficiently supplied with boron [4]. In

2019, deficiency of boron (B) has been identified as a current problem for plant growth in the Black Sea region of Türkiye, as well. On the other hand, many researchers reported that the application of B increased fruit quality and yield in hazelnuts [5, 6, 7].

The main aim of the study was to research the effect of soil and foliar applications of boron on the yield and quality of hazelnuts and give information about B fertilization to hazelnut producers.

2. Materials and Methods

2.1. Experimental Location and Treatments

Experiments were conducted in two different locations, Samsun-Carsamba and Ordu-Ulubey in the eastern Black Sea region of Türkiye (31°64'98"N and 45°77'44.08"E, height: 5m and 39°77'78"N and 45°27'50.09"E height: 397 m) in 2013 and 2014. The experiments were established in the "Tombul" (*Corylus avellana* L.) hazelnut orchard, which consists of four stemmed 25-year-old bushes called "Ocak" (a multi-rotated planting system specific to Türkiye) and conducted in a completely randomized block with a factorial combination of 3, 2 treatments (soil and foliar doses),

*Corresponding author: fozkutlu@odu.edu.tr

of which 5 were repeated. ($N=b*s*l*r=3*3*2*5=90$; b =number of blocks; s =number of soil borings; number of leaf borings; r =number of replicates).

Basal fertilization (nitrogen (N), phosphorus (P_2O_5), and potassium (K_2O)) was performed according to the results of soil analysis and 20 kg N da^{-1} as calcium ammonium nitrate (26% N), 10 kg da^{-1} P_2O_5 as triple superphosphate ($3Ca(H_2PO_4)_2 \cdot H_2O$ (42-44% P_2O_5)), and 10 kg K_2O da^{-1} as potassium sulfate (K_2SO_4 (48-50% K_2O)) in two consecutive years.

In the experiments, Etidot-67 ($Na_2B_8O_{13} \cdot 4H_2O$) was used as the B source, containing 20.96% B, and was applied as soil and foliar additives to the hazelnut Ocaks during the two-year period. Soil application of B was made in February of each year at three doses (Control, $S1=3.0$, $S2=6.0$ B g $ocak^{-1}$) and foliar application of B ($F1=300$ mg B L^{-1}) was made three times per year (i: after harvest in October, ii: at the "before flowering" stage in March, and iii: during fruit set in May) using a sprayer. Treatments were randomized, with five replicates per treatment. Foliar applications were made early in the morning or before sunset, and foliar applications of the drone fertilizer were sprayed with more than 0.25% nonionic wetting agent (Tween-20).

Technical and cultural practices such as pruning, weed control, disease and pest control were carried out in hazelnut orchards in both locations where the trials were held.

2.2. Preparation of Leaf Samples

After boron application, leaf samples were taken every other year from the third or fourth branch of each tree at the onset of maturity. Leaves were washed in deionized water for 1 minute and stored in air for 24 hours. They were then dried at 65°C for 48 hours. And then, boron concentrations of the leaves were analyzed.

2.3. Analysis of Soils and Plants

Before the experiments were established, some physical and chemical analyzes of the orchard soils were determined. Soil texture analysis was performed according to the hydrometer method [8]. pH and EC values of the soil were measured in saturated extracts as described by Jackson [9], and $CaCO_3$ content of the soil was determined as described by Hızalan [10]. Soil organic matter was determined by the Walkley-Black method of Schlichting and Blume [11]. Available phosphorus (P) was determined according to the method of Bray and Kurtz [12]. Available potassium (K) was determined by AAS; Pratt [13]. Available concentrations of Fe, Cu, Zn, Mn, and were determined by DTPA extraction according to metod of Lindsay and Norvell [14]. B available in soil was extracted with hot water 0.01 M $CaCl_2$ for 5 min (1:2) in water bath (95°C) and then filtered with Whatman No. 42 filter paper Measured by ICP-OES (Bingham F T; Boss and Fredeen) [15, 16]. The dried plant samples were then

crushed and approximately 0.2 g of the samples was digested at 550°C for 12 h to determined B concentration. The concentration of boron and other mineral elements in the leaves was determined by optical spectroscopy with inductively coupled plasma (ICP-OES - Perkin Elmer 2100V).

2.4. Measurements of the Yield

The hazelnut cultivation in the garden is carried out as an Ocak system and as a single body. The ocak system is a high bush cultivation system and is divided into single-rooted ocak and multi-rooted ocak. Multi-rooted ocak system is widely used in Turkiye and each ocak contains between 4-8 plants (branches) [17].

The planting system of the gardens selected for the experiment is 4x4m. Since there are 60 ocaks per decare area, the hazelnut yield (kg da^{-1}) in one ocak was calculated by multiplying the ... by 60. and expressed in kg da^{-1} . To ensure homogeneity in the experimental gardens, 4 branches were left in each ocak. Yield was calculated as kg da^{-1} over 4 branches in the ocaks.

Fruits were harvested by hand from four branches and fresh weights were determined. Then the nuts were separated from the husk by hand, dried at natural conditions (under sunlight) and the yield of the dried hazelnuts was determined.

2.5. Determination of Hazelnut Kernel Ratio (Quality)

Hazelnut quality characteristic (kernel ratio) were determined by analysing 100 randomly selected nuts. Three replicates of 100 nuts per treatment were used to calculate the percentage of empty and damaged nuts. And then kernel ratio percentages were calculated were calculated (See Eq. 1) [18, 19, 20]:

$$\text{kernel ratio (\%)} = \frac{\text{kernel weight (g)}}{\text{total nut weight (g)}} \times 100 \quad (1)$$

The Duncan multiple range test was used to determine further differences between groups. Significance was estimated at $p < 0.05$ for all tests. Statistical analyses were performed using SPSS 22.0. (SPSS, Inc., Chicago, Ill.).

3. Results

Statistically significant increases in the amount of B usable in the soil were obtained based on the amounts of B applied in both years compared to the initial B concentration in the soil (Table 1).

After soil and foliar application, hazelnut leaves were highly statistically significant in the B concentration in both years compared to controls. B concentration in hazelnut leaves was ($75, 69.0 \pm 14.0$ mg kg^{-1}) in Samsun-Çarşamba location, ($48.0 \pm 7.2, 50.1 \pm 7.0$ mg kg^{-1}) in Ordu-Ulubey location in both years, when F1 dosage

Table 1. Physical and chemical properties of soil in hazelnut orchards.

Soil Properties	Location	
	Samsun-Çarşamba	Ordu-Ulubey
Texture	Clay	Clay
Soil PH	6.79	6.73
Salinity (dS.m ⁻¹)	0.02	0.08
CaCO ₃ (%)	1.11	0.89
Organic matter (%)	1.13	2.71
Available phosphorus (mg.kg ⁻¹)	2.0	5.0
Available potassium (mg.kg ⁻¹)	85	141
Available boron (mg.kg ⁻¹)	0.02	0.22

was applied. The B concentration of hazelnut leaf was 82.0±8.2, 99.0±14.0 mg kg⁻¹ in Samsun-Çarşamba, and 37.0±5.1, 61.0±10.2 mg kg⁻¹ in Ordu-Ulubey district when S1 was applied. In Samsun-Çarşamba (103.0±10.1, 119.0±19.7 mg kg⁻¹) and Ordu-Ulubey (54.0±8.0, 67.0±5.0 mg kg⁻¹) the results were obtained by applying F1+S1. After the application of S2, the B concentrations in hazelnut leaves were determined in Samsun-Çarşamba (84±7.1, 109.0±16.4 mg kg⁻¹) and Ordu-Ulubey (54.0±4.3, 95.0±15.1 mg kg⁻¹). Boron concentrations in hazelnut leaves were measured in Samsun-Çarşamba (149.0±9.1, 158.0±20.1 mg kg⁻¹) and Ordu-Ulubey (69.0±8.3, 90.0±9.1 mg kg⁻¹), after the treatment of soil by F1+S2 (Table 2).

There were statistically significant differences between B applications and hazelnut yield for both years and the two locations (p<0.05) (Table 3).

In the first year, hazelnut yield (94.5±7.8, 75.1±4.3, 79.9±2.7 kg da⁻¹) was observed in Samsun-Çarşamba by the applications of S1, F1, F1+S1. Hazelnut yield

(76.5±2.1, 54.5±1.8 kg da⁻¹) was determined by the applications of S2, F1+S2. The lowest hazelnut yield was obtained with the control dose (67.1±5.1 kg da⁻¹). In the second year, hazelnut yields determined in Samsun-Çarşamba by the applications of S1, F1, F1+S1, S2 and F1+S2 were 124.9±6.3, 113.7±2.6, 117.8±5.3, 111.1±03.0, 94.9±2.0 kg da⁻¹, respectively. The lowest hazelnut yield was measured in control samples (92.5±4.2 kg da⁻¹).

In the first year, hazelnut yields determined in Ordu-Ulubey by the applications of S1, F1, F1+S1, S2 and F1+S2 were 20.3±1.9, 19.9±1.8, 17.5 ±1.5, 19.3±1.6 and 19.2±2.6 kg da⁻¹, respectively. The lowest hazelnut yield was obtained with the control dose (18.6±1.6 kg da⁻¹). In the second year, hazelnut yield in Ordu-Ulubey district (41.0±1.9, 35.5±1.8, 38.3±2.3 kg da⁻¹) was determined by applying S1, F1, and F1+S1. Hazelnut yield (36.1±1.8, 39.4±1.9 kg da⁻¹) was determined by the application of S2 and F1+S2. The lowest hazelnut yield was obtained with the control dose (32.5±2.7 kg da⁻¹).

The first year, kernel ratio in Samsun-Çarşamba district, was determined respectively (53.6, 51.7, and 52.5%) by applications of S1, F1, and F1+S1. It was hazelnut kernel ratio (51.2- 52.4%) determined by both applications of S2, and F1+S2. The lowest hazelnut kernel ratio was obtained with the control dose (48.0%). In the second year, the kernel quotient in Samsun-Çarşamba district was determined by the application of S1, F1, and F1+S1 (49.6-48.3-49.6%). The kernel ratio of hazelnuts was determined by the application of S2 and F1+S2 (51.4-51.8%). The lowest kernel ratio was obtained with the control dose (46.3%) (Table 4).

In 2013, with the applied dosages of S1, F1, F1+S1, S2 and F1+S2 the kernel ratios in Ordu-Ulubey district

Table 2. Effect of B (Etidot-67) fertilizer application on leaf B concentration (mg kg⁻¹).

Location		Control	F1	S1	F1+S1	S2	F1+S2
Samsun Çarşamba	Leaf B ₍₂₀₁₃₎	33.0 ±4.2d	75.0±10.2c	82.0±8.3c	103.0±10.1b	84.0±7.1c	149.0±9.1a
	Leaf B ₍₂₀₁₄₎	29.0±2.0d	69.0±14.0c	99.0±14.0b	119.0±19.7b	109.0±16.4b	158.0±20.1a
	Leaf B _{avg}	31.0±3.7d	72.0±12.1b	90.5±14.1c	111.0±18.0b	96.5±17.6c	153.5±15.5a
Ordu Ulubey	Leaf B ₍₂₀₁₃₎	25.0±4.2d	48.0±7.2b	37.0±5.1c	54.0±8.0b	54.0±15.1b	69.0±8.3a
	Leaf B ₍₂₀₁₄₎	23.0±2.1d	50.1±7.0c	61.0±10.2c	67.0±5.0b	95.0±15.1a	90.0±9.1a
	Leaf B _{avg}	24.0±3.3c	49.5±6.9b	49.0±14.7b	60.7±9.2b	74.5±24.0a	79.5±13.8a

Table 3. Effect of B (Etidot-67) fertilizer application on nut yield (kg da⁻¹).

Location		Control	F1	S1	F1+S1	S2	F1+S2
Samsun Çarşamba	Yield ₍₂₀₁₃₎	67.1±5.1c	75.1±4.3b	94.5±7.8a	79.9±2.7b	76.5±2.1b	54.5±1.8d
	Yield ₍₂₀₁₄₎	92.5±4.2d	113.7±2.6bc	124.9±6.3a	117.8±5.3b	111.1±3.0c	94.9±2.0d
	Yield _{avg}	80.2±13.7bc	94.8±20.2ab	109.7±16.9a	98.9±20.3a	93.8±18.4ab	74.7±21.42c
Ordu Ulubey	Yield ₍₂₀₁₃₎	18.6±1.6ab	19.9±1.8ab	20.3±1.9a	17.5±1.5b	19.3±1.6ab	19.2±2.6ab
	Yield ₍₂₀₁₄₎	32.5±2.7c	35.5±1.8b	41.0±1.9a	38.3±2.3ab	36.1±1.8b	39.4±1.9a
	Yield _{avg}	25.6±7.7	27.7±8.4	30.6±11.1	27.9±11.1	27.7±9.1	29.3±10.8

Table 4. Effect of B (Etidot-67) fertilizer application on Kernel ratio (%).

Location		Control	F1	S1	F1+S1	S2	F1+S2
Samsun Çarşamba	Kernel ratio ₍₂₀₁₃₎	48.5±4.8	51.7±2.8	53.6±6.1	52.5±2.3	51.2±2.2	52.4±3.3
	Kernel ratio ₍₂₀₁₄₎	46.3±3.2	48.3±5.5	49.6±3.1	49.6±7.9	51.4±5.9	51.8±1.2
	Kernel ratio _{avg}	47.4±4.0b	50.0±4.5a	51.7±5.0ab	51.0±5.7ab	51.3±4.2ab	52.1±2.4a
Ordu Ulubey	Kernel ratio ₍₂₀₁₃₎	49.5±2.1	51.6±2.8	51.9±2.9	51.4±3.1	51.8±1.9	51.2±2.6
	Kernel ratio ₍₂₀₁₄₎	47.6±1.6b	52.0±4.2a	51.9±3.5a	52.3±1.9a	52.0±2.9a	52.8±2.5a
	Kernel ratio _{avg}	48.5±2.0b	51.8±3.3a	51.9±3.1a	51.8±2.5a	51.9±2.4a	51.9±2.5a

was calculated as 51.9%, 51.6%, 51.4%, 51.8%, and 51.2%, respectively. The kernel ratio percentage was obtained with the control dose (49.5%). In 2014, with the applied dosages of S1, F1, F1+S1, S2 and F1+S2 the kernel ratios in Ordu-Ulubey district was calculated as 51.9%, 52.0%, 52.2%, 52.0%, and 52.8%, respectively. The lowest kernel ratio was obtained with the control dose (47.6%) (Table 4).

4. Discussion

Boron deficiency is the most common nutritional disorder and is easily washed out as $B(OH)_3$ in places with heavy rainfall. In regions with high annual precipitation, B deficiency occurs in sandy and highly decomposed, acidic soils by leaching. It has been reported that there is a decrease in flower formation in plants grown under B deficiency and metabolic damage in plants during vegetative growth [21]. Insufficient B supply in hard-shelled fruit production, may have a negative impact on yield and quality. A number of researchers have found that boron fertilization has a positive effect on yield by reducing cavity formation in nuts, almonds, and pistachios. For example, in walnut [22], almond [23, 24], and pistachio [25], B fertilization increased fruit set and more fruits were reported accordingly.

There are several studies on the positive effects of boron fertilizer applications on the yield and quality of hazelnuts. There are studies that find that fertilization with B generally reduces empty formation in hazelnuts and increases fruit set, leading to an increase in yield. For example, in one of the first studies on this topic by Okay et al. [26], vacant fruit formation was found to decrease by 41.5% when leaves were sprayed with 0.1% boric acid; Korkmaz et al. [27] found that dosage across leaves increased in the garden dominated by Palaz hazelnut cultivars. In the application of 0, 0.2 and 0.4% B, 0.2% dose increased the hazelnut yield and yield, and in Samsun Terme, 0-6-12-18-24 g B oca^k⁻¹ and 0.2% solubor application from the leaf, 12 g B oca^k⁻¹ application increased the hazelnut yield by 55.5%, and the application of 600 mg B L⁻¹ over two years in the orchard with the hazelnut cultivar Barcelona by Shrestha et al. [28] increased the fruit set by 23% in the first year and 17% in the second year, respectively.

In the study conducted by Erdogan and Aygun [29], 300 and 600 mg kg⁻¹ B were applied over the leaves to the hazelnut cultivar "Tombul" in the third week from

January to May 1 over a period of two years. It was reported that leaf B content increased with increasing B application and fruit set was higher with 300 mg kg⁻¹ B application than with 600 mg kg⁻¹ B application in both years. In the study conducted by Tarakcioglu et al. [30], 0-6-12 g B from Oca^k⁻¹ soil and 0-250-500-750 mg B L⁻¹ were applied to leaves. According to the results, 6 g B oca^k⁻¹ from soil increased total wet weight, shell yield, kernel weight, and kernel weight compared to the control, and 500 mg L⁻¹ B from leaves; it was found that total fresh weight, shell yield, shell weight, and kernel weight increased, and foliar application of B increased hazelnut yield and leaf B content.

The highest boron concentration in hazelnut leaves in Samsun-Çarşamba district was achieved by the application and dosage of F1+S2 in two-year average. According to the observations made during the trials, no toxic damage caused by boron to the leaves was observed. The boron concentration of hazelnut leaves was increased by 390% by the application of F1+S2 compared to the control application. In Ordu-Ulubey district, the highest boron concentration in hazelnut leaves was determined by the application and dose of F1+S2. Boron concentration in hazelnut leaves was increased by 231% by the application of F1+S2 compared to the control.

The study found that the yield and kernel ratio of hazelnuts were positively affected by the application of fertilizer B in hazelnuts from the soil and leaves compared to controls. According to the two-year average, the highest yield of hazelnut in Samsun-Çarşamba was obtained by the application and dosage of S1. Hazelnut yield was increased by 36.70% by the application of S1 compared to the control application. However, there were no significant differences between the doses of S1 and F1, F1+S1, S2 with yield. In Ordu-Ulubey district, also had not occurred a significant difference between the application and doses in the yield of hazelnut. However, the application of B increased the hazelnut yield by 20% compared to the control. Some authors indicated that fruit yield and quality of hazelnuts could be improved by the application of boron, while others found no effect [31, 32]. The application of boron had no significant effect in certain trials under Mediterranean conditions [31, 33, 34]. In contrast, foliar and soil application of B in hazelnuts has been shown to favour fruit quality and fruit set [32]. It was also reported that although 300 and 600 ppm B were

sprayed only once on trees in Ocak, positive effects of B application on fruit set in Tombul were obtained and an annual increase was observed [6]. However, one study found that B-based treatments had significant effects on fruit set when tested in cooler spring climates such as Oregon. These results suggest that climatic conditions may be related on the translocation of boron [32]. As a result, cooler spring conditions should promote better utilization of this mineral and higher fruit production to support higher metabolic rates [35]. The beneficial effect depends on the average air temperature during flowering (June-July) and increases as temperatures drop. As a result of increased fruiting, nut yield increases [36]. According to TUIK [37], average hazelnut yields in Türkiye in 2013 and 2014 were 78 and 64 kg da⁻¹, respectively. These yield values correspond to an average of 8 to 10 branches of hazelnut ocaks in growers' orchards. Considering the fact that the yield values in our trials were determined on four branches, it was found that fertilization with B has a positive effect on yield.

This experiment with different boron applications on hazelnuts showed that there was a positive and very significant correlation ($p < 0.001$, $r = 0.433$) between leaf B concentration and yield in Ordu-Ulubey district ($p < 0.001$). On the other hand, in Samsun-Çarşamba district, there was no significant correlation between leaf B concentration and yield. It is possible that climatic differences are responsible for this significance, and this result was also confirmed in other studies.

The two-year average hazelnut kernel ratio was statistically significant between the B applications and the control ($p < 0.05$). The highest proportion of hazelnut kernels was obtained in F1+S2 applications in the two districts. These increases were found in Samsun-Çarşamba (10%) and Ordu-Ulubey (7%). There was also a positive correlation in Samsun ($p < 0.05$, $r = 0.296$), Ordu ($p < 0.05$, $r = 0.305$) between B leaf concentration and hazelnut kernel ratio. These correlations occurred at both district levels ($p < 0.05$). The technical reports stated that the optimal B-leaf concentration for good fruit and hazelnut yield was between 25 and 30 mg kg⁻¹ DW [38]. Soil and foliar applications were reported to have a considerable effect on yield, quality, and peanut content compared to controls, and foliar applications were reported to have significant increases in leaf B concentration and kernel to nut ratio [39]. Similar to our results, the kernel size of hazelnut cultivar 'Negret' was also reported to increase with boron application [7]. Similar results were reported in the literature [40, 41, 42, 43].

5. Conclusion

Foliar-B fertilization generally increases fruit set and yield in various fruit varieties. For this reason, foliar fertilization is usually applied to plants such as walnut, almond, hazelnut, etc. Our study showed that foliar fertilization statistically increased the yield and quality of hazelnut. Depending on the yield increase, foliar

fertilization with B is an efficient method to provide sufficient B for the flowers. In addition, foliar fertilization of B is a more suitable method because it reduces the toxicity of boron as it does not mix with groundwater and does not enter the environment. It also shows that there are differences in yield and quality at two different locations where the study was conducted, and that the application of B to increase B concentration in leaves is related to different factors. Therefore, the timing and weather conditions are also important for foliar application. As a result, fertilization of crop products with B is necessary for high yield when the plant-available B concentration in the soil determined by hot water extraction is < 0.5 mg B kg⁻¹. When hazelnut yield is in the range of 0.5-1.0 mg B kg⁻¹, fertilization with B may be recommended.

Acknowledgement

This research is the part of a research project (project no: 2012.Ç0366) supported by TENMAK-BOREN Boron Research Institute.

Kaynaklar (References)

- [1] Erdogan, V. (2017, August). Hazelnut production in Turkey: current situation, problems and future prospects. In *IX International Congress on Hazelnut 1226* (pp. 13-24).
- [2] De Silva, A. L., Kämper, W., Wallace, H. M., Ogbourne, S. M., Hosseini Bai, S., Nichols, J., & Trueman, S. J. (2022). Boron effects on fruit set, yield, quality and paternity of macadamia. *Agronomy*, 12(3), 684.
- [3] Shorrocks, V. M. (1997). The occurrence and correction of boron deficiency. *Plant and Soil*, 193(1), 121-148.
- [4] Ozkutlu, F., Aydemir, Ö. E., Akgün, M., & Özcan, B. (2019). Determination of potential nutritional problems and Zinc (Zn) status of hazelnut (*Corylus avellana* L.) grown soils in Ordu province *Academic Journal of Agriculture*, 8(Special Issue), 131-140.
- [5] Duran, P., Barra, P. J., Mora, M. d. I. L., Nunes-Nesi, A., & Merino-Gergichevich, C. (2022). Boron and zinc diminish grey necrosis incidence by the promotion of desirable microorganisms on hazelnut orchards. *Agronomy*, 12(4), 868.
- [6] Erdogan, V., & Aygun, A. (2008). *Effect of foliar boron application on fruit set in 'Tombul' hazelnut*. In *VII International Congress on Hazelnut 845*.
- [7] Tous, J., Romero, A., Plana, J., Sentis, X., & Ferrán, J. (2004). *Effect of nitrogen, boron and iron fertilization on yield and nut quality of Negret hazelnut trees*. In *VI International Congress on Hazelnut 686*.
- [8] Bouyoucos, G. J. (1962). Hydrometer method improved for making particle size analyses of soils 1. *Agronomy Journal*, 54(5), 464-465.
- [9] Jackson, M. L. (1958). *Soil chemical analysis*. Prentice Hall, England.
- [10] Allison, L. E., & Moodie, C. D. (1965). *Carbonate. Methods of Soil Analysis: Part 2 Chemical and Microbiological Properties* (pp. 1379-1396).
- [11] Schlichting, E., and Blume, H.P. (1966). *Bodenkundliches*

- Praktikum* (Hamburg, Berlin: Springer).
- [12] Bray, R. H., Kurtz, L. T. (1945). Determination of total, organic and available forms of phosphorus in soils. *Soil Science*, 59, 39-45.
- [13] Pratt, P. F. (1965). *Potassium methods of soil analysis*. (Editor: C. A. Black) part-2. Agron. Series No:9: 1010-1022 Am. Soc. of Agron., Inc. Madison, Wisconsin, USA.
- [14] Lindsay, W. L. & Norvell, W. A. (1978). Development of a DTPA soil test for zinc, iron, manganese and copper. *Soil Science Society of America Journal*, 42, 421-428.
- [15] Bingham, F. T. (1983). Boron. *Methods of Soil Analysis: Part 2 Chemical and Microbiological Properties*, 9, 431-447.
- [16] Charles, B., & Fredeen, K. J. (1997). Concepts, instrumentation and techniques in inductively coupled plasma optical emission spectrometry. *Perkin Elmer Corp*, 3(2).
- [17] İslam, A. (2021). *Fındık [Hazelnut]*. Nobel Yayınları [Nobel Publishing], Türkiye ISBN:978-625-417-388-2.
- [18] Ayfer, M., Uzun, A. & Baş, F. (1986). *Türk Fındık Çeşitleri [Turkish Hazelnut Varieties]*. Karadeniz Bölgesi Fındık İhracatçılar Birliği Yayınları [Black Sea Region Hazelnut Exporters Association Publications], Türkiye, p. 95.
- [19] Demir, T., & Beyhan, N. (1998). Research on the Selection of Hazelnuts Grown in Samsun. *Turkish Journal of Agriculture and Forestry*, 24(2000), 173-183.
- [20] Köksal, A. İ. (2002). *Türk Fındık Çeşitleri [Turkish Hazelnut Varieties]*. Fındık Tanıtım Grubu [Hazelnut Promotion Group], ISBN 975- 92886-0-5, Ankara.
- [21] Herrera-Rodriguez, M. B., Gonzalez-Fontes, A., Rexach, J., Camacho-Cristobal, J. J., Maldonado, J. M., & Navarro-Gochicoa, M. T. (2010). Role of boron in vascular plants and response mechanisms to boron stress. *Plant Stress* 4(2), 115-122.
- [22] Keshavarz, K., Vandati, K., Samar, M., Azadegan, B., & Brown, P. H. (2011). Foliar application of zinc and boron improves vegetative and reproductive growth. *HortTechnology*, 21(2), 181-186.
- [23] Rufat, J., & Arbonés, A. (2005). Foliar applications of boron to almond trees in dryland areas. In *V International Symposium on Mineral Nutrition of Fruit Plants 721* (pp. 219-226).
- [24] Sotomayor, C., Silva, H., & Castro, J. (2001). Effectiveness of boron and zinc foliar sprays on fruit setting of two almond cultivars. In *III International Symposium on Pistachios and Almonds 591* (pp. 437-440).
- [25] Meli, M., Delfini, M., Capuani, G., Di Cocco, M. E., Sciubba, F., Tzareva, I., ... & Terziev, I. (2009). Effect of boron treatment on 'bianca' and 'gloria' pistachio cultivars. In *V International Symposium on Pistachios and Almonds 912* (pp. 143-149).
- [26] Okay, A. N., Koç, N., & Kılavuz, F. H. (1987). Boş fındık oluşum sebepleri ve giderilmesi üzerine araştırmalar [Researches on the causes of empty hazelnut formation and removal]. *Sonuç raporu [Result Report] TC. TOKB. Fındık Araş.Enst.Müd. [Republic of Türkiye Ministry of Agriculture and Forestry Hazelnut Research Institute]*, Giresun.
- [27] Korkmaz, A., Özdemir, N., Kızılkaya, R., Gülser, C., Sürücü, A., Horuz, A., ... & Yirmibeşoğlu, B. (2001). Fındık, ayçiçeği, şeker pancarı ve mısır bitkilerinde borlu gübre kullanımını üzerine araştırmalar [Studies on the use of boron fertilizer in hazelnut, sunflower, sugar beet and corn plants]. *Sonuç raporu [Result Report]*. Ondokuz Mayıs Üniversitesi Ziraat Fakültesi, Toprak Bölümü [Ondokuz Mayıs University, Faculty of Agriculture, Department of Soil], Samsun.
- [28] Shrestha, G. K., Thompson, M. M., & Rigetti, T. L. (1987). Foliar-applied boron increases fruit set in 'Barcelona' hazelnut. *American Society for Horticultural Science*, 112(3), 412-416.
- [29] Erdogan, V., & Aygun, A. (2009). Effect of foliar boron application on fruit set in 'tombul' hazelnut, *Acta Horticulturae*, 845, 331-336.
- [30] Tarakcıoğlu, C., Taban, N., Askin, T., & Taban, S. (2005). Fındık bitkisine topraktan ve yapraktan uygulanan borun verim ile yaprakların bazı besin maddesi içerikleri üzerine etkisi [The effect of boron applied to the hazelnut plant, from the soil and leaves, on the yield and some nutrient contents of the leaves.]. *II.Ulusal Bor Çalıştayı [II.National Boron Workshop]* 637-642, Ankara
- [31] Llavaneres, J. R. P. (1994). *Aplicacions de bor i llur efecte en cultius d'avellaner (Corylus avellana L.) al camp de Tarragona* [Ph. D. Thesis, Universitat de Lleida].
- [32] Paula Silva, A., Rosa, E., & Haneklaus, S. H. (2003). Influence of foliar boron application on fruit set and yield of hazelnut. *Journal of Plant Nutrition*, 26(3), 561-569.
- [33] Ferran, X., Tous, J., Romero, A., Lloveras, J., & Pericon, J. (1997). Boron does not increase hazelnut fruit set and production. *HortScience*, 32(6), 1053-1055.
- [34] Germain, E. (1992). The reproduction of hazelnut (*Corylus avellana* L.): A review. In *III International Congress on Hazelnut 351*.
- [35] Özenç, N., Bender Özenç, D., & Duyar, Ö. (2014). Nutritional composition of hazelnut (*Corylus avellana* L.) as influenced by basic fertilization. *Acta Agriculturae Scandinavica, Section B-Soil & Plant Science*, 64(8), 710-721.
- [36] Portela, E., Ferreira-Cardoso, J., Louzada, J., & Gomes-Laranjo, J. (2015). Assessment of boron application in chestnuts: nut yield and quality. *Journal of Plant Nutrition*, 38(7), 973-987.
- [37] Turkish Statistical Institute (2015). Retrieved from <https://biruni.tuik.gov.tr/medas/?kn=92&locale=tr>.
- [38] Silvestri, C., Bacchetta, L., Bellincontro, A., & Cristofori, V. (2021). Advances in cultivar choice, hazelnut orchard management, and nut storage to enhance product quality and safety: An overview. *Journal of the Science of Food and Agriculture*, 101(1), 27-43.
- [39] Acar, I., Doran, I., Aslan, N., & Kalkancı, N. (2016). Boron affects the yield and quality of nonirrigated pistachio (*Pistacia vera* L.) trees. *Turkish Journal of Agriculture and Forestry*, 40(5), 664-670.
- [40] Bhatia, B., & Yadav, R. (2005). Effect of foliar spray of urea and NAA on fruit yield and quality of ber (*Z. mauritiana* Lamk.). In *National Seminar on Commercialization of Horticulture in Nontraditional Areas*.
- [41] Bybordi, A., & Malakouti, M. (2005). Effects of foliar applications of nitrogen, boron and zinc on fruit setting

and quality of almonds. In *IV International Symposium on Pistachios and Almonds* 726.

- [42] Farid, A., Halder, N., & Shahjahan, M. (2007). Effect of boron for correcting the deformed shape and size in Jackfruit. *Indian Journal of Horticulture*, 64(2), 144-149.
- [43] Tomar, C., & Singh, N. (2007). Effect of foliar application of nutrients and bio-regulators on growth, fruit set, yield and nut quality of walnut. *Indian Journal of Horticulture*, 64(3), 271-273.



B₂O₃ katkısının PET'in kimyasal bozunma davranışı, termal ve mekanik performansı üzerine etkisi

Bilal Demirel^{1,*}, Ali Yaraş², Fatih Akkurt³, Sedat Sürdem⁴

¹Erciyes Üniversitesi, Mühendislik Fakültesi, Malzeme Bilimi ve Mühendisliği Bölümü, Kayseri, 38039, Türkiye

²Bartın Üniversitesi, Mühendislik, Mimarlık ve Tasarım Fakültesi, Metalurji ve Malzeme Mühendisliği Bölümü, Bartın, 74110, Türkiye

³Gazi Üniversitesi, Mühendislik Fakültesi, Kimya Mühendisliği Bölümü, Ankara, 06570, Türkiye

⁴Gazi Üniversitesi, Fen Bilimleri Enstitüsü, Çevre Bilimleri Ana Bilim Dalı, Ankara, 06500, Türkiye

MAKALE BİLGİSİ

Makale Geçmişi:
İlk gönderi 25 Temmuz 2022
Kabul 12 Kasım 2022
Online 31 Aralık 2022

Araştırma Makalesi

DOI: 10.30728/boron.1148497

Anahtar kelimeler:

B₂O₃
Kimyasal bozunma
PET şişe
Termal ve mekanik özellik

ÖZET

Bu çalışmada, ekstrüzyon yöntemiyle bor oksit (B₂O₃) farklı miktarlarda (kütlece %0,05-0,8) polietilen tereftalat'a (PET) katkılanarak önce PET/B₂O₃ granülleri sonrasında ise sırasıyla enjeksiyon ve gerdirme-şişirme-kalıplama (SBM) yöntemleriyle şişe üretimi gerçekleştirilmiştir. Üretilen PET/B₂O₃ kompozitler mekanik performans, kimyasal ve termal özellikler açısından karakterize edilmiştir. B₂O₃ içeriğinin artmasıyla PET kompozitin viskozitesi azaldı ve en düşük viskozite değeri %0,8 B₂O₃ katkısı için 0,385 dL/g olarak ölçülmüştür. %0,2'den daha yüksek B₂O₃ içeriği viskozitenin düşük olmasına neden olduğundan şişe üretimi gerçekleştirilememiştir. PET kompozitlerin kristalleşme sıcaklığı (T_c), B₂O₃ miktarının artışına bağlı olarak yaklaşık 8,2°C yükselmiştir. PET'in bozunması sonucu açığa çıkan izofoalik asit (IPA) üzerinde B₂O₃ katkısının herhangi bir etkisi görülmezken asetaldehit (AA) miktarında azalma, karboksilik asit (COOH) ve dietilen glikol (DEG) miktarında ise artış meydana gelmiştir. PET kompozit şişelerin mekanik performanslarının saf PET şişelerden daha yüksek olduğu tespit edilmiştir. Dolayısıyla, %0,05 ve %0,1 oranlarında B₂O₃ kullanımı PET şişelerin taşınması ve depolanması sırasında oluşabilecek sorunların azaltılmasına katkı sağlayabilir.

Effect of B₂O₃ additive on chemical decomposition behavior, thermal and mechanical performance of PET

ARTICLE INFO

Article History:

Received July 25, 2022
Accepted November 12, 2022
Available online December 31, 2022

Research Article

DOI: 10.30728/boron.1148497

Keywords:

B₂O₃
Chemical decomposition
PET bottle
Thermal and mechanical properties

ABSTRACT

In this study, different amounts of boron oxide (B₂O₃) (0.05-0.8% by mass) were incorporated to polyethylene terephthalate (PET) by extrusion method, followed by production of PET/B₂O₃ granules and bottles using the injection and stretch-blow-molding (SBM) methods, respectively. The produced PET/B₂O₃ composites were characterized in terms of mechanical performance, chemical and thermal properties. With the increase of B₂O₃ content, the viscosity of PET composite decreased and the lowest viscosity value was measured as 0.385 dL/g for %0.8 B₂O₃ additive. Bottle could not be produced since B₂O₃ content higher than 0.2% caused low viscosity. The crystallization temperature (T_c) of PET composites increased by about 8.2°C due to the increase in the amount of B₂O₃. While there was no effect of B₂O₃ additive on isophthalic acid (IPA) released as a result of the degradation of PET, there was a decrease in the amount of acetaldehyde (AA) and an increase in the amount of carboxylic acid (COOH) and diethylene glycol (DEG). It was determined that the mechanical performances of PET composite bottles were higher than that of pure PET bottles. Therefore, the use of 0.05% and 0.1% B₂O₃ can contribute to reducing the problems that may occur during the transportation and storage of PET bottles.

1. Giriş (Introduction)

Gıda ambalaj sektöründe kullanılan polietilen tereftalat (PET), etilen glikol (EG) ve tereftalik asit (TA) veya dimetil tereftalat (DMT) polimerizasyonu ile üretilen bir termoplastiktir. Gaz bariyer performansının iyi olması,

yüksek şeffaflık, kolay işlenebilirlik ve nispeten düşük maliyet nedeniyle PET gıda ambalaj uygulamalarında en fazla tercih edilen üçüncü polimerdir. En popüler kullanım alanı şişe üretimi olup genellikle gazlı/gazsız içecekler, meyve suları, su gibi içeceklerin paketlenmesinde kullanılmaktadır [1, 2].

*Corresponding author: bilaldemirel@erciyes.edu.tr

PET hidrolitik, termal, kimyasal ve mekanik etki ile çeşitli mekanizmalar sonucu bozunabilir ve bu durum gıda ürünleri için ciddi bir tehdittir [3-5]. Nitekim, bu bozunma süreçleri sonunda PET bünyesinde renk değişimi, çatlak oluşumu gibi makro/mikro seviyede deformasyonlar meydana gelebilir [6]. Örneğin, PET'in hidrolitik bozunması ile amorf bölgedeki ester bağlarının kopması sonucu alkol ve asit fonksiyonel grupları açığa çıkar ve polimerin molekül ağırlığı azalır. Bu ise PET'in nem, karbondioksit ve oksijen geçirgenliğini olumsuz etkiler [7]. Termal bozunmada ise yaklaşık 250-350°C sıcaklık aralığında oksijen yokluğunda ester gruplarının parçalanmasıyla karbonil ve vinil esterler oluşur ki bu süreç önce vinil alkol sonra AA oluşuncaya kadar devam eder [8]. Bununla birlikte, etilen ve benzen'in yanı sıra çeşitli aromatiklerin ve aldehytlerin açığa çıkması da muhtemeldir [4]. Termal bozunmanın oksijen varlığında gerçekleşmesi durumunda ise bozunma PET ana zincirinde hidroperoksitlerin oluşmasıyla başlar ve farklı radikal reaksiyonlarla devam eder [3]. Yukarıda bahsi geçen bozunma türlerinin meydana gelmesi PET'in mekanik performansını, camı geçiş sıcaklığını (T_g) ve erime sıcaklığını (T_m) etkileyebilir [9].

PET'in bozunması sonucu özelliklerinde gözlenen olumsuzlukları en aza indirgeyebilmek amacıyla literatürde çok sayıda çalışma yer almaktadır. Örneğin; çok tabakalı bor nitrür kullanılarak PET'in termal ve mekanik özellikleri iyileştirilmiştir [10]. PET'e antibakteriyel özellik kazandırmak için titanyum dioksit (TiO_2) ve demir (III) oksit (Fe_2O_3), PET'in UV ışık geçirgenliğini artırmak için ise çinko oksit (ZnO) katkı maddesi olarak kullanılmıştır [11, 12]. Nano boyuttaki hidroksiapatit'in (nHAp) farklı oranlarda (kütlece %0,1'den %0,8'e) PET'e katıldığı bir diğer çalışmada, nHAp miktarının artmasıyla açığa çıkan COOH miktarı üzerinde katalitik etki gösterirken AA miktarı üzerinde ise inhibisyon etkisi gösterdiği bildirilmiştir. Diğer taraftan, açığa

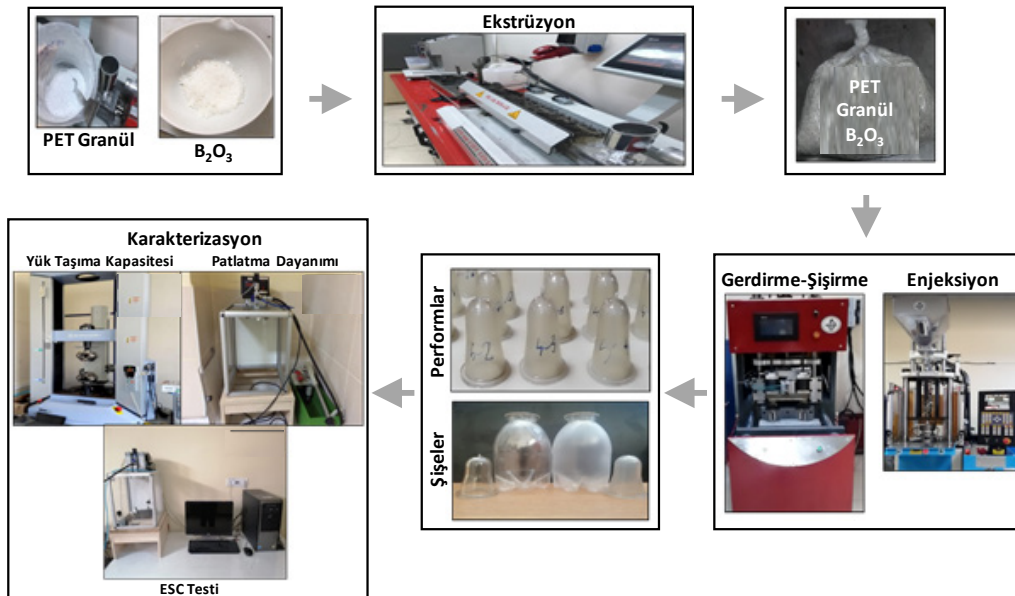
çıkan DEG ve IPA seviyelerinde saf PET'e nazaran önemli bir fark gözlenmemiştir [13].

Bor bileşikleri bir takım karakteristik özelliklerinden dolayı farklı uygulamalarda kullanılabilir. Alev geciktirici olarak çinko borat [14], piezoelektrik özellikteki lityum borat, yüksek optik performans özelliğine sahip baryum borat, ferroelektrik özellikteki kalsiyum borat [15] ve lüminesans özellik gösteren magnezyum borat [16] bileşikleri bunlardan bazılarıdır. Bir diğer bor bileşiği de borik asit (H_3BO_3) dehidrasyonu sonucu elde edilen bor oksit'tir (B_2O_3). Bu çalışmada, PET polimer matrisine farklı oranlarda B_2O_3 eklenerek üretilen PET/ B_2O_3 kompozitlerinden şişe üretimi gerçekleştirilmiştir. Üretilen şişelerin termal, mekanik ve kimyasal özelliklerine B_2O_3 katkısının etkisi incelenmiştir.

2. Malzemeler ve Yöntemler (Materials and Methods)

Deneylerde katkı maddesi olarak kullanılan B_2O_3 analitik saflıkta olup Kimetsan Kimya'dan (Ankara/Türkiye) temin edilmiştir. 0,84 dL/g gerçek viskozite ve 1 ppm (maksimum) AA içeriğine sahip PET ise Köksan Plastik ambalaj firmasından (Gaziantep/Türkiye) granül formunda temin edilmiştir.

PET granülleri ve B_2O_3 tozları ekstrüzyon işleminden önce 80°C'de 24 saat süreyle kurutuldu. PET/ B_2O_3 kompozitler, uzunluk/çap oranı 40:1 olan birlikte dönen çift vidalı ekstrüderde (Gülmar Makina, Türkiye) 100 rpm vida dönme hızında eritilerek harmanlandı. Besleme bölgesinden nozula doğru ekstrüder sıcaklıkları 50, 200, 205, 210, 215 ve 220°C olarak ayarlandı. Kurutulmuş B_2O_3 tozları kütlece beş farklı oranda (kütlece %0,05, %0,1, %0,2, %0,4 ve %0,8) PET granülleri ile birlikte ekstrüdere beslendi. PET/ B_2O_3 kompozitleri ekstrüderden granül halinde alındı ve enjeksiyon prosesinde kullanılmak üzere kapalı bir kap içinde muhafaza edildi. PET/ B_2O_3 şişe üretimine ait proses akış diyagramı Şekil 1'de görülmektedir.



Şekil 1. PET/ B_2O_3 şişe üretimine ait proses akış diyagramı (Process flow diagram of PET/ B_2O_3 bottle production).

Enjeksiyon kalıplama öncesinde üretilen PET/B₂O₃ granülleri 80°C'de 12 saat kurutuldu. Şişe üretimi için kurutulan granüller dikey enjeksiyon cihazına (YH-15V, Yuhdak Makina, Tayvan) beslenerek önkalıp (preform) kalıba enjekte edildi. Dikey enjeksiyon cihazının kalıp sıcaklığı 15°C, kovan bölgesel sıcaklıkları sırasıyla 260°C, 275°C ve 280°C olarak ayarlandı. Üretilen preformlara şişe üretimi için gerdirme-şişirme-kalıplama yöntemi uygulandı.

Yarı otomatik olan SBM makinesinde ısıtma işlemi sekiz adet IR lambaları tarafından sağlandı. SBM sürecinde önkalıbın yüzey sıcaklığı 90°C ile 95°C aralığında değişmektedir. Gerdirme ve şişirme sırasında basınç 0,5 saniye süreyle 0,09 MPa'da tutuldu. Ardından basınç 2 saniyede 1,5 MPa'a yükseltildi ve 1,5 MPa basınçta 2 saniye beklendi. Gerdirme çubuğunun hızı 0,75 m/s olup 1,13 saniyede şişe tabanına ulaştı. Şişirme işlemi boyunca kalıp sıcaklığı ve kalıpta kalma süresi sırasıyla 20°C ve 2 saniye olarak ayarlandı.

2.1. Karakterizasyon ve Analizler (Characterization and Analyses)

Deneylerde kullanılan B₂O₃ tozlarının partikül boyut dağılımı yaş yönteme göre Mastersizer 3000 (Malvern Instruments Ltd. UK) kullanılarak gerçekleştirildi. Saf PET ve PET/B₂O₃ kompozitlerin Fourier Dönüşümlü Kızılötesi Spektroskopisi (FTIR) analizleri (Perkin Elmer 400) 4000-400 cm⁻¹ dalga sayısı aralığında, 4 cm⁻¹ çözünürlükte ve 20 taramanın ortalaması alınarak gerçekleştirildi. B₂O₃, PET ve PET/B₂O₃ kompozitlerin faz yapıları 2 θ =5° ile 90° aralığında gerçekleştirilen X-Işını Kırınımı (XRD) analizleri (Bruker AXS D8) ile belirlendi. Numunelerin yüzey morfolojik özellikleri de Taramalı Elektron Mikroskobu (SEM) analizi (ZEISS LS-10) ile karakterize edildi.

Numunelerin termal özellikleri Diferansiyel Taramalı Kalorimetre (DSC) (Perkin Elmer Diamond) ve Termogravimetrik Analiz (TGA) (Hitachi-High TechSTA-7300) analizleri ile belirlendi. DSC ve TGA analizleri 10°C/dk ısıtma hızında ve azot atmosferinde gerçekleştirildi.

Viskozite ölçümleri için 50 mL'lik balon jøjeye 250 mg PET ve 25 mL çözücü karışımı (fenol/1,2-diklorbenzen) eklendi. Ardından PET'in çözelti içerisinde 110°C sıcaklıkta 30 dakika karıştırılarak çözülmesi sağlandı. Çözeltinin ortam sıcaklığına kadar soğuması beklendi. Viskozimetre ölçümleri Lauda viskozimetresi kullanılarak alındı ve sonuçlar dL/g olarak elde edildi.

AA, COOH, IPA ve DEG'in kimyasal bozunma analizleri sırasıyla F2013-01, DIN/ISO 2114, IQ10694 ve IQ10687 standartlarına göre yapıldı. COOH analizi için 4 g ve 50 mL (1:1 fenol/kloroform) bir behere alındı ve berrak çözelti elde edilinceye kadar 1 saat reflux yapıldı. Daha sonra çözeltiye oda sıcaklığında 0,5 mL %0,1 Etanolik tetrabromofenol blue çözeltisi eklendi ve karıştırıldı.

Hazırlanan çözeltinin rengi sarı renkten mavi renge dönünceye kadar 0,1 N Benzilalkolik KOH çözeltisi ile titre edildi. AA analizi için PET/B₂O₃ numuneleri sıvı azot ile soğutulduktan sonra öğütülerek 750 μ m'lik bir elekten geçirildi. Numunelerin oda sıcaklığına gelmesi için yaklaşık 10 dk beklendi, 0,2 g tartılan öğütülmüş numune analiz kabına (headspace) konuldu ve AA miktarı gaz kromatografisinde analiz edildi.

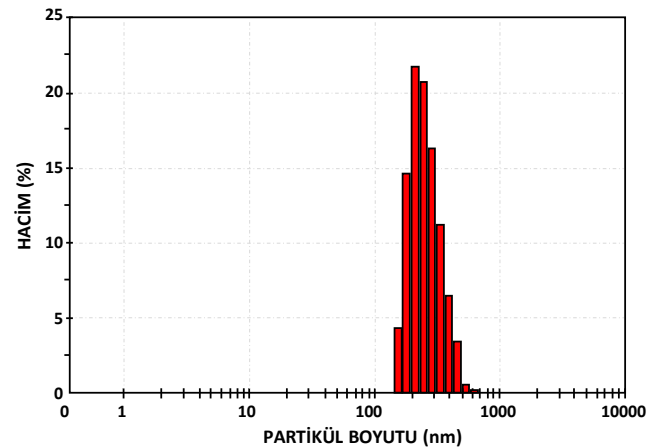
IPA ve DEG'nin analiz prosedürüne göre öğütülmüş numune 50 mL'lik ağzı kapalı bir kaba konulduktan sonra üzerine 10 mL standart çözelti ve 1 mg çinko asetat ilave edildi. Kap 22°C'deki fırında 2 saat boyunca bekletildi. Kabın sıcaklığı ortam sıcaklığına ulaştıktan sonra üzerine 15 mL kloroform ilave edildi. Numune membran filtreden geçirildi, süzüntü analiz kabına (headspace) alındı ve gaz kromatografisinde analizi gerçekleştirildi. Analizler üç tekrarlı gerçekleştirildi ve hesaplamalarda ortalama değerler kullanıldı.

Mekanik testler, EN ISO 527-3 standardına göre 100 mm/dk hızında çekme cihazı (DVT GP E NN) kullanılarak gerçekleştirildi. Her numune için çekme testi üç kez tekrarlandı ve ortalama değerler alındı.

3. Sonuçlar ve Tartışma (Results and Discussion)

3.1. XRD, FTIR ve Partikül Boyut Analizleri (XRD, FTIR and Particle Size Analysis)

B₂O₃'ün partikül boyut dağılımı analiz sonucu Şekil 2'de verilmiştir. Buna göre deneylerde kullanılan B₂O₃'ün ortalama partikül boyutunun 234,5 nm olduğu belirlenmiştir.

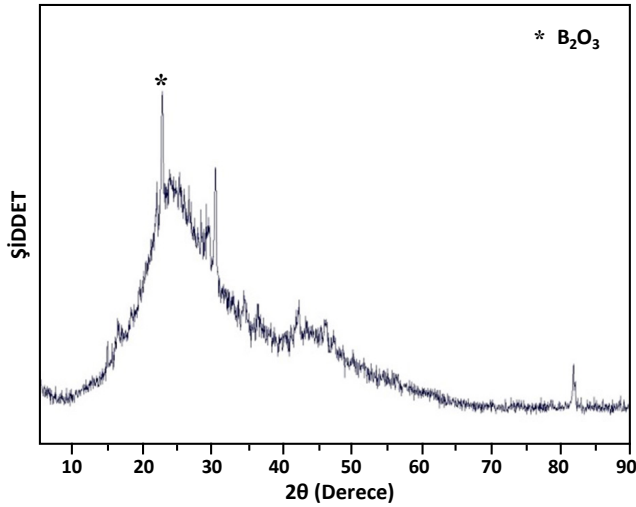


Şekil 2. B₂O₃'ün partikül boyut analizi (Particle size analysis of B₂O₃).

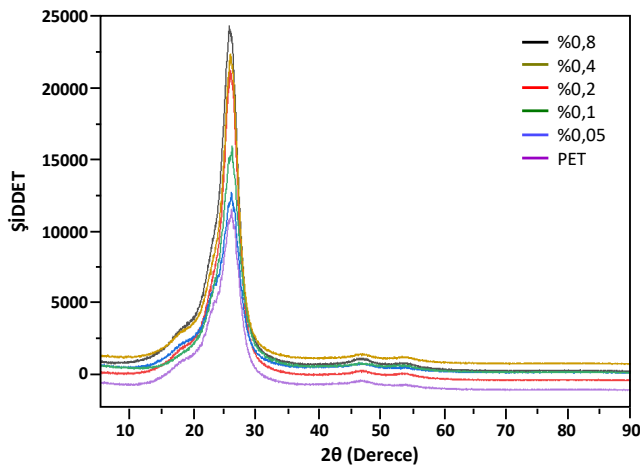
Şekil 3'de B₂O₃ tozlarının XRD grafiği verilmiştir. Buna göre; yaklaşık 24°'de B₂O₃'ün karakteristik piki gözlemlenmiştir. Şekil 4'deki saf PET ve PET/B₂O₃ kompozitlerin XRD verilerinde ise, yaklaşık 26,5°'de gözlenen pik PET'e aittir [13, 17, 18] ve pik şiddeti B₂O₃ ilavesiyle artmıştır.

Şekil 5'de görüldüğü üzere, 3100-2800 cm⁻¹ dalga sayısındaki IR spektrumları, PET'in karakteristik aromatik ve alifatik C-H gerilmelerine aittir. 1712 cm⁻¹ deki

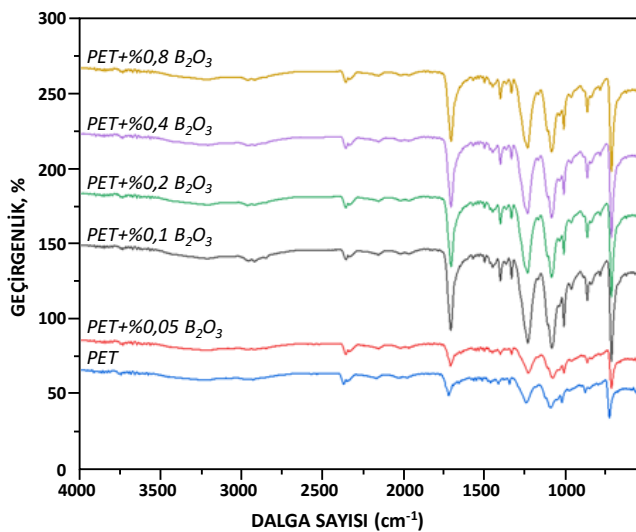
pik ve 1300 cm^{-1} civarındaki pikler sırasıyla PET bün-yesindeki karbonil grubuna (C=O gerilmesi) ve ester gruplarına karşılık gelir. 1100 cm^{-1} ve 1165 cm^{-1} 'deki pikler sırasıyla metilen gruplarına ait gerilmelerden ve



Şekil 3. B_2O_3 'ün XRD grafiği (XRD graph of B_2O_3).



Şekil 4. Saf PET ve PET/ B_2O_3 kompozitlerin XRD grafikleri (XRD plots of pure PET and PET/ B_2O_3 composites).

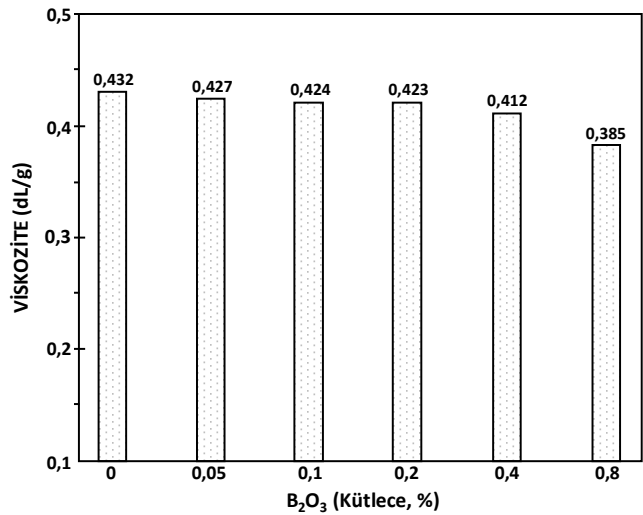


Şekil 5. Saf PET ve PET/ B_2O_3 kompozitlerin FTIR analiz sonuçları (FTIR analysis results of pure PET and PET/ B_2O_3 composites).

C-O-C asimetrik gerilme titreşimlerinden kaynaklanmaktadır [19, 20]. Ayrıca, B-O gerilme titreşimine ve B-O-B eğilme titreşimine ait pikler sırasıyla yaklaşık 722 cm^{-1} ve 1404 cm^{-1} 'de görülmektedir [21-23].

3.2. Viskozite Ölçümleri (Viscosity Measurements)

Şekil 6'da B_2O_3 'ün PET matrise dahil edilmesi durumunda viskozitenin azaldığı görülmektedir. Kütlece %0,8 B_2O_3 ilavesiyle saf PET'e göre viskozite %10,8 oranında azalarak $0,385\text{ dL/g}$ olarak ölçülmüştür. Bu duruma, PET yapısındaki H atomlarının B_2O_3 molekülü ile etkileşime girerek PET zincir hareketliliğini (dönme, itme, çekme vb.) arttırmasının neden olduğu düşünülmektedir. Benzer şekilde; TiO_2 , montmorillonit ve SiO_2 gibi inorganik katkı maddelerinin PET'in viskozitesini azalttığını gösteren çalışmalara literatürde rastlamak mümkündür [24, 25].



Şekil 6. B_2O_3 katkısının viskoziteye etkisi (Effect of B_2O_3 additive on viscosity).

3.3. Mekanik Özellikler (Mechanical Properties)

Tablo 1'de görüldüğü üzere saf PET şişenin yük taşıma kapasitesi ($86,49\text{ N}$), kütlece %0,05 ve %0,1 B_2O_3 içeren PET şişelere kıyasla daha düşüktür. Saf PET şişe ile karşılaştırıldığında %0,1 B_2O_3 katkısıyla şişenin yük taşıma kapasitesi %27,76 oranında bir

Tablo 1. B_2O_3 katkısının PET şişelerin yük taşıma kapasitesi, büzülme, çevresel stres dayanımı ve iç basınç dayanımına etkisi (Effect of B_2O_3 additive on load carrying capacity, shrinkage, environmental).

B_2O_3 (%)	Yük Taşıma Kapasitesi (N)	Büzülme (%)	Çevresel Stres Çatlaması (dk.)	İç Basınç Dayanımı (MPa)
0,00	86,49	26,90	0,3	6,61
0,05	134,80	28,04	4,0	5,44
0,10	110,5	29,39	-	4,14
0,20	68,40	-	-	-
0,40			Şişe üretilmedi	
0,80			Şişe üretilmedi	

artış göstermiştir. Bu artış B_2O_3 ilavesinin PET polimer zincirlerinin hareket kabiliyetini sınırlandırmasına atfedilebilir [13]. Demirel vd. kütlece %0,05'den %0,8 oranına kadar farklı CaB_2O_4 oranları için PET şişelerin yük taşıma kapasitelerini ölçmüşler ve %0,8 CaB_2O_4 içeren şişelerin yük taşıma kapasitesinin saf PET şişeye nazaran yaklaşık %208 daha yüksek olduğunu bildirmişlerdir [26]. Bu çalışmada ise %0,4 ve %0,8 B_2O_3 katkılı PET kompozit granüller üretilmiştir ancak bu katkı oranlarında viskozite düşük olduğundan dikey enjeksiyon cihazı ile şişe üretimi gerçekleştirilememiştir (Şekil 6). Ayrıca, %0,2 B_2O_3 içeren şişenin yük taşıma kapasitesi saf PET şişesinden daha düşüktür (68,4 N). Bunun daha yüksek B_2O_3 oranlarında PET yapısının bozulmasından kaynaklandığı düşünülmektedir. Tablo 3'deki kimyasal bozunma ürünlerinden COOH miktarındaki artış buna işaret etmektedir.

Saf PET ve B_2O_3 katkılı şişelerin büzülme değerleri %26,9 ile %31,97 arasında değişim göstermektedir. Saf PET şişeye kıyasla B_2O_3 katkısının büzülmeyi artırdığı açıktır. Bu artışta şişe ağırlığının ve şişe gövde kalınlığının etkili olduğu düşünülmektedir. Bu, şişenin birim ağırlığının (ağırlık/alan) artışı anlamına gelir ki böylece gerdirme işlemi sırasında şişe tabanına daha fazla malzeme taşınır (Tablo 2) [26].

Tablo 2. Şişelerin baş, gövde ve taban bölgelerindeki ağırlık dağılımları (Weight distribution of bottles in the head, body and base regions).

B_2O_3 (%)	Baş (g)	Gövde (g)	Taban (g)
0,00	5,8	113	2,3
0,05	5,6	1,1	2,5
0,10	5,8	1,0	2,6
0,20	5,6	0,9	2,8
0,40	-	-	-
0,80	-	-	-

PET şişeler, kullanım ve uygulama alanlarına bağlı olarak aynı anda hem mekanik gerilmelere hem de içinde bulunan çeşitli akışkanlara maruz kalabilir [27]. Bu olayların şişelerin mekanik performansları üzerindeki etkileri "çevresel stres çatlama testi (ESC)" ile belirlenebilir. Bu test, sodyum hidroksit (NaOH) gibi agresif çözeltiler kullanılarak gerçekleştirilir. Bu test yönteminde, kimyasal bozunma sonucu PET zincirlerini kısaltarak daha düşük molekül ağırlığına sahip makromoleküllerin oluşumuna neden olduğundan NaOH çözeltisi kullanıldı [28]. Bu çalışmadaki ESC testleri, test süresini kısaltmak amacıyla %2'lik NaOH çözeltisi kullanılarak gerçekleştirildi [29]. Tablo 1'deki verilere göre, %0,05 B_2O_3 ilavesiyle PET şişenin ESC değeri 4 dakika olarak ölçülürken %0,1 ve %0,2 B_2O_3 katkı oranlarındaki şişelerin ESC değeri ölçülemedi. Bu durumun, NaOH çözeltisinin varlığından dolayı sudaki OH gruplarına karşı ilgisi yüksek olan bor elementinin reaksiyona girerek borik asite dönüşmesinden ve bu nedenle PET zincir bütünlüğünün kaybolmasından kaynaklandığı düşünülmektedir.

B_2O_3 katkılı şişelerde iç basınç dayanımı açısından saf PET şişeye göre azalma meydana gelmiştir. B_2O_3 katkı oranına bağlı olarak iç basınç dayanımındaki azalmaya PET ve B_2O_3 arasındaki zayıf etkileşim ve B_2O_3 'ün polimer matristeki homojen olmayan dağılımı neden olabilir [30, 31].

3.4. Kimyasal Bozunma (Chemical Decomposition)

Isıl ve oksidatif bozunma esnasında PET bünyesinde meydana gelen esterleşme tepkimeleri ortamdaki karboksil uç gruplarının miktarında artışa sebep olur. Diğer bir ifadeyle, PET'in ısıl kararlılığı karboksil uç gruplarının varlığından etkilenir. Tablo 3'deki numunelerin kimyasal bozunma verilerine göre; saf PET'in COOH⁻ bozunma değeri 60,05 mmol/kg olup B_2O_3 ilavesiyle bu değer artarak en yüksek 85,19 mmol/kg seviyesine ulaşmıştır. Bu durum, B_2O_3 varlığında PET zincirlerinin kırılarak uç grupların açığa çıkmasından kaynaklanabilir. Nitekim, PET'in hidrolizi ile açığa çıkan COOH⁻ miktarının artması beklenen bir durumdur [7]. Benzer şekilde, CaB_2O_4 [26] ve nHAp'ın [13] PET'e katkılı olduğu literatürdeki çalışmalarda artan katkı oranlarının COOH⁻ degradasyonu üzerinde katalitik etkisinin olduğu bildirilmiştir.

Tablo 3. Saf PET ve PET/ B_2O_3 kompozitlerin kimyasal bozunma sonuçları (Chemical degradation results of pure PET and PET/ B_2O_3 composites).

B_2O_3 (%)	DEG (kütlece %)	IPA (%)	AA (ppm)	COOH (mmol/kg)
0,00	1,52	1,81	6,36	60,05
0,05	1,76	1,76	6,30	65,91
0,10	1,79	1,77	5,79	77,86
0,20	1,79	1,79	5,23	79,58
0,40	1,80	1,80	4,98	83,69
0,80	1,81	1,81	4,46	85,19

Saf PET'in AA değeri 6,36 ppm iken artan B_2O_3 katkı oranıyla bu değerde kısmi bir azalma kaydedilmiştir. Bu azalmanın açığa çıkan AA bünyesindeki hidrojen iyonlarının B_2O_3 yapısındaki bor iyonları ile yer değiştirmesinden kaynaklandığı düşünülmektedir. Benzer şekilde, kimyasal bozunma sonucu açığa çıkan DEG miktarı da B_2O_3 içeriğine bağlı olarak artış göstermiştir. Diğer taraftan, B_2O_3 katkısı IPA'nın kimyasal bozunması üzerinde herhangi bir katalitik veya inhibisyon etki göstermemiştir. Katkı maddesi olarak nHAp'ın PET matrisine katkılı olduğu çalışmada da kimyasal bozunma ürünleri için benzer sonuçlar elde edilmiştir [13].

3.5. Termal Özellikler (Thermal Properties)

Saf PET ve PET/ B_2O_3 kompozitlerin T_g , T_m ve T_c Tablo 4'de verilmiştir. Buna göre; T_m sıcaklıklarında herhangi bir değişim olmazken T_g sıcaklığı saf PET'e kıyasla en fazla 1,2°C azalmıştır. Polimer matrisine katkı maddelerin ilave edilmesinin polimer kompozitin kristalleşme sıcaklığını etkilediği bilinmektedir [32, 33]. Bu

çalışmada, PET/B₂O₃ kompozitlerin kristalleşme sıcaklıkları saf PET'e kıyasla daha yüksektir. Daha önceki çalışmalarda çeşitli katkı maddelerinin PET bünyesine dahil edilmesiyle kristalleşme sıcaklıklarının arttığı bildirilmiştir [34-36].

Tablo 4. Saf PET ve PET/B₂O₃ kompozitlerin T_m, T_g ve T_c değerleri (T_m, T_g and T_c values of pure PET and PET/B₂O₃ composites).

B ₂ O ₃ (%)	T _m (°C)	T _g (°C)	T _c (°C)
0,00	249,3	81,2	188,4
0,05	249,4	80,9	192,2
0,10	249,2	80,8	193,6
0,20	249,4	80,0	195,7
0,40	249,4	80,3	196,1
0,80	249,8	80,0	196,6

3.6. SEM Analizi (SEM Analysis)

Şekil 7'deki SEM görüntülerinde, saf PET ve B₂O₃ katkılı PET kompozitlerin yüzeylerinde farklı boyutlarda mikro çatlaklar görülmektedir. Saf PET'e kıyasla PET/B₂O₃ kompozitlerdeki çatlakların azaldığı görülmektedir. Bu, ambalajların bariyer özelliklerinin geliştirilmesi açısından önemlidir. Böylece, B₂O₃ bileşiğinin PET bünyesindeki mikro çatlakları azaltarak H₂O, CO₂ ve O₂ geçirgenliğini de azaltacağı düşünülmektedir.

4. Sonuçlar (Conclusions)

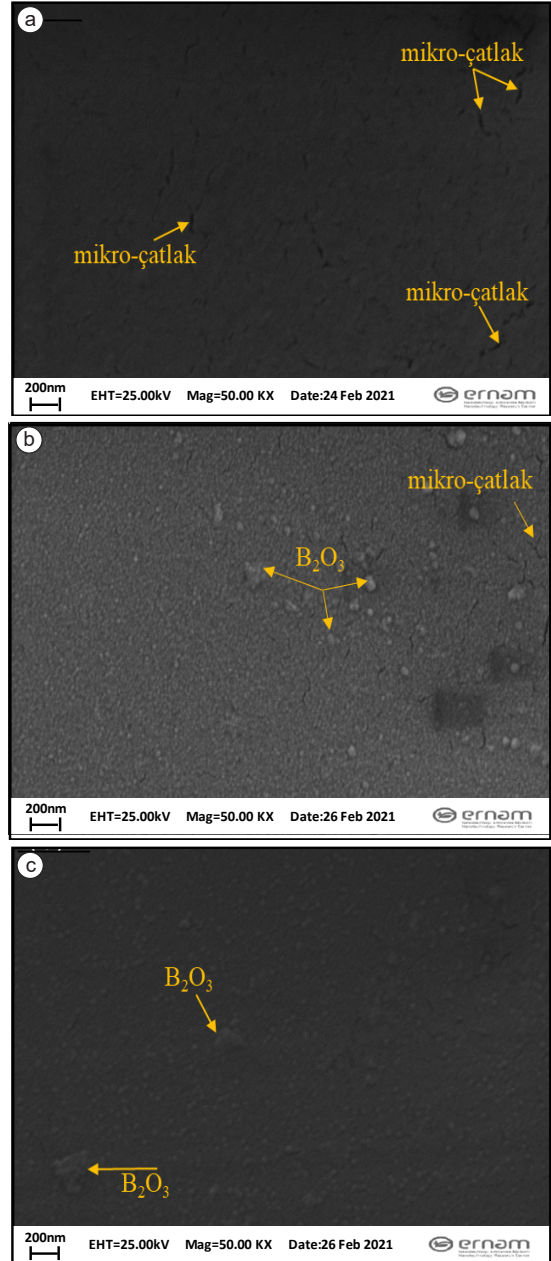
Bu çalışma kapsamında elde edilen deneysel bulgular aşağıda listelenmiştir;

Artan B₂O₃ katkı oranı ile viskozite azalma eğilimindedir. En düşük viskozite değerine (0,385 dL/g) %0,8 B₂O₃ içeriğinde ulaşılmıştır. Viskozite de meydana gelen bu düşüş nedeniyle dikey enjeksiyon cihazı kullanılarak şişe üretimi gerçekleştirilememiştir. Dolayısıyla, şişe üretiminin gerçekleştirilebilmesi için %0,2'den daha yüksek B₂O₃ katkı oranlarında çalışılmaması önerilmektedir.

T_m sıcaklığında ciddi bir değişim söz konusu değilken saf PET'e kıyasla %0,8 B₂O₃ katkı oranı için T_g sıcaklığı 1,2°C azalmış ve T_c sıcaklığı yaklaşık 8,2°C artış göstermiştir.

B₂O₃ katkısının PET'in bozunması sonucu açığa çıkan IPA üzerinde herhangi bir etkisi gözlenmemiştir. Diğer taraftan, artan B₂O₃ içeriği AA miktarını azaltırken DEG ve COOH miktarında artışa neden olmuştur. Bu şekilde, B₂O₃ varlığının PET'in bazı kimyasal bozunma reaksiyonlarını inhibe edebilmesi gıda kalitesine ve dolayısıyla da halk sağlığına önemli katkılar sağlayabilir.

Sonuçlar, PET kompozit şişelerin mekanik performanslarının saf PET şişeden üstün olduğunu göstermektedir. Dolayısıyla belirtilen oranlarda B₂O₃



Şekil 7. Saf PET (a), %0.05 B₂O₃ katkılı PET (b) ve %0.1 B₂O₃ katkılı PET numunelerin SEM görüntüleri (SEM images of pure PET (a), 0.05% B₂O₃ added PET (b), and 0.1% B₂O₃ added PET samples).

kullanımı gıda ihtiva eden PET şişelerin taşınması ve depolanması sırasında oluşabilecek sorunları azaltabilir.

Teşekkür (Acknowledgement)

Bu çalışma TENMAK-BOREN Bor Araştırma Enstitüsü (Proje No: 2019-31-07-25-004) tarafından finansal olarak desteklenmiştir.

Kaynaklar (References)

- [1] Gerassimidou, S., Lanska, P., Hahladakis, J. N., Lovat, E., Vanzetto, S., Geueke, B., ... Lacovidou, E. (2022). Unpacking the complexity of the PET drink bottles value

- chain: A chemicals perspective. *Journal of Hazardous Materials*, 430, 128410.
- [2] Kawai, F. (2021). Emerging strategies in polyethylene terephthalate hydrolase research for biorecycling. *ChemSusChem*, 14(19), 4115-4122.
- [3] Venkatachalam, S., Nayak, S. G., Labde, J. V., Gharal, P. R., Rao, K., & Kelkar, A. K. (2012). Degradation and recyclability of poly (ethylene terephthalate). In *Polyester* (pp. 75-98). *InTech Rijeka, Croatia*.
- [4] Das, P., & Tiwari, P. (2019). Thermal degradation study of waste polyethylene terephthalate (PET) under inert and oxidative environments. *Thermochimica Acta*, 679, 178340.
- [5] Mutsuga, M., Tojima, T., Kawamura, Y., & Tanamoto, K. (2005). Survey of formaldehyde, acetaldehyde and oligomers in polyethylene terephthalate food-packaging materials. *Food Additives and Contaminants*, 22(8), 783-789.
- [6] Frache, A., & Camino, G. (2012). *Degradazione, stabilizzazione e ritardo alla fiamma di polimeri, Collana AIM testi*, Edizioni Nuova Cultura, Roma (Italy), ISBN 978886134817.
- [7] Golike, R. C., & Lasoski Jr, S. W. (1960). Kinetics of hydrolysis of polyethylene terephthalate films. *The Journal of Physical Chemistry*, 64(7), 895-898.
- [8] McIntyre, J. E. (2005). *Synthetic fibres: nylon, polyester, acrylic, polyolefin*. Taylor & Francis US.
- [9] Demirel, B., Kılıç, E., Yaraş, A., Akkurt, F., Daver, F., & Gezer, D. U. (2022). Effects of magnesium borate on the mechanical performance, thermal and chemical degradation of polyethylene terephthalate packaging material. *Journal of Plastic Film & Sheeting*, 38(4), 589-607.
- [10] Sahoo, A., Gayathri, H. N., Sai, T. P., Upasani, P. S., Raje, V., Berkman, J., & Ghosh, A. (2020). Enhancement of thermal and mechanical properties of few layer boron nitride reinforced PET composite. *Nanotechnology*, 31(31), 315706.
- [11] Hwang, S. H., Kim, Y. K., Seo, H. J., Hong, S. H., Lim, S. K., Lee, S. H., & Kim, D. K. (2019). The morphological effects of ZnO upon the antimicrobial and deodorant activities of polyethylene terephthalate/ZnO composite filaments. *Journal of Nanoscience and Nanotechnology*, 19(12), 7721-7728.
- [12] Calvo, M. E., Castro Smirnov, J. R., & Míguez, H. (2012). Novel approaches to flexible visible transparent hybrid films for ultraviolet protection. *Journal of Polymer Science Part B: Polymer Physics*, 50(14), 945-956.
- [13] Demirel, B., Inaner, N. B., Gezer, D. U., Daver, F., Yaras, A., & Akkurt, F. (2021). Chemical, thermal, and mechanical properties and ultraviolet transmittance of novel nano-hydroxyapatite/polyethylene terephthalate milk bottles. *Polymer Engineering & Science*, 61(7), 2043-2054.
- [14] Mergen, A., Tektas, E., Karakoc, G., & Gündüz, M. (2003). Effect of process variables on the fabrication of zinc borate by a wet chemical method. *CFI. Ceramic Forum International* (Vol. 80, E40-E50).
- [15] Li, J., Gao, S., Xia, S., Li, B., & Hu, R. (1997). Thermochemistry of hydrated magnesium borates. *The Journal of Chemical Thermodynamics*, 29(4), 491-497.
- [16] Furetta, C., Kitis, G., Weng, P. S., & Chu, T. C. (1999). Thermoluminescence characteristics of MgB4O7: Dy, Na. *Nuclear Instruments and Methods in Physics Research Section A: Accelerators, Spectrometers, Detectors and Associated Equipment*, 420(3), 441-445.
- [17] Vedula, J., & Tonelli, A. E. (2007). Reorganization of poly (ethylene terephthalate) structures and conformations to alter properties. *Journal of Polymer Science Part B: Polymer Physics*, 45(7), 735-746.
- [18] Zhang, G. Q., Sun, F., Gao, L. P., Wang, L. N., Shao, M., & Liu, J. Q. (2007). Thermodynamics properties and isothermal crystallization kinetics of carbon black/poly (ethylene terephthalate) composites. *Journal of Composite Materials*, 41(12), 1477-1485.
- [19] Ganeshan, G., Shadangi, K. P., & Mohanty, K. (2018). Degradation kinetic study of pyrolysis and co-pyrolysis of biomass with polyethylene terephthalate (PET) using Coats-Redfern method. *Journal of Thermal Analysis and Calorimetry*, 131(2), 1803-1816.
- [20] Holland, B. J., & Hay, J. N. (2002). The thermal degradation of PET and analogous polyesters measured by thermal analysis-Fourier transform infrared spectroscopy. *Polymer*, 43(6), 1835-1847.
- [21] Rojas, S. S., Yukimitu, K., De Camargo, A. S. S., Nunes, L. A. O., & Hernandez, A. C. (2006). Undoped and calcium doped borate glass system for thermoluminescent dosimeter. *Journal of Non-Crystalline Solids*, 352(32-35), 3608-3612.
- [22] Özdemir, Z., Özbayoğlu, G., & Yilmaz, A. (2007). Investigation of thermoluminescence properties of metal oxide doped lithium triborate. *Journal of Materials Science*, 42(20), 8501-8508.
- [23] Pekpak, E., Yilmaz, A., & Özbayoğlu, G. (2011). The effect of synthesis and doping procedures on response of lithium tetraborate. *Journal of Alloys and Compounds*, 509(5), 2466-2472.
- [24] Harris, B. (1999). *Engineering composite materials*, (2nd Edition). The Institute of Materials.
- [25] Ari, A. G. (2009). Investigation of the effects of various nanoparticles on properties of polymer nanocomposites. [Ph.D. Thesis, İstanbul University]. Council of Higher Education Thesis Center (Thesis Number 283157). Doktora Tezi, İstanbul Üniversitesi Fen Bilimleri Enstitüsü, İstanbul, 4-7 .
- [26] Inaner, N. B., Demirel, B., Yaras, A., Akkurt, F., & Daver, F. (2022). Improvement of environmental stress cracking performance, load-carrying capacity, and UV light barrier property of polyethylene terephthalate packaging material. *Polymers for Advanced Technologies*, 33(7), 2352-2361.
- [27] Barros, A. B. D. S., Farias, R. D. F., Siqueira, D. D., Luna, C. B. B., Araújo, E. M., Rabello, M. S., & Wellen, R. M. R. (2020). The effect of ZnO on the failure of PET by environmental stress cracking. *Materials*, 13(12), 2844.
- [28] Wright, D. C. (1996). *Environmental stress cracking of plastics*, Rapra Technology Limited.
- [29] Moskala, E. J. (1998). A fracture mechanics approach

to environmental stress cracking in poly (ethyleneterephthalate). *Polymer*, 39(3), 675-680.

- [30] Leong, Y. W., Ishak, Z. A. M., & Ariffin, A. (2004). Mechanical and thermal properties of talc and calcium carbonate filled polypropylene hybrid composites. *Journal of Applied Polymer Science*, 91(5), 3327-3336.
- [31] Thio, Y. S., Argon, A. S., Cohen, R. E., & Weinberg, M. (2002). Toughening of isotactic polypropylene with CaCO₃ particles. *Polymer*, 43(13), 3661-3674.
- [32] Wan, T., Chen, L., Chua, Y. C., & Lu, X. (2004). Crystalline morphology and isothermal crystallization kinetics of poly (ethylene terephthalate)/clay nanocomposites. *Journal of Applied Polymer Science*, 94(4), 1381-1388.
- [33] Farhoodi, M., Mousavi, S. M. A., Sotudeh-Gharebagh, R., Emam-Djomeh, Z., & Oromiehie, A. (2014). Effect of spherical and platelet-like nanoparticles on physical and mechanical properties of polyethylene terephthalate. *Journal of Thermoplastic Composite Materials*, 27(8), 1127-1138.
- [34] Guan, G., Li, C., Yuan, X., Xiao, Y., Liu, X., & Zhang, D. (2008). New insight into the crystallization behavior of poly (ethylene terephthalate)/clay nanocomposites. *Journal of Polymer Science Part B: Polymer Physics*, 46(21), 2380-2394.
- [35] Farhoodi, M., Mohammadifar, M. A., Mousavi, M., Sotudeh-Gharebagh, R., & Emam-Djomeh, Z. (2017). Migration kinetics of ethylene glycol monomer from pet bottles into acidic food simulant: effects of nanoparticle presence and matrix morphology. *Journal of Food Process Engineering*, 40(2), e12383.
- [36] Bandyopadhyay, J., Ray, S. S., & Bousmina, M. (2007). Thermal and thermo-mechanical properties of poly (ethylene terephthalate) nanocomposites. *Journal of Industrial and Engineering Chemistry*, 13(4), 614-623.



Investigation of the effects of borogypsum and silica fume on ceramic material's sintering and final properties

Çetin Öztürk^{1,*}, Atilla Evcin²

¹*Necmettin Erbakan University, Department of Old Tile Repairs, Konya, 42090, Türkiye*

²*Afyon Kocatepe University, Department of Material Science and Engineering, Afyonkarahisar, 03200, Türkiye*

ARTICLE INFO

Article history:

Received August 3, 2022

Accepted December 1, 2022

Available online December 31, 2022

Research Article

DOI: 10.30728/boron.1153669

Keywords:

Borogypsum

Silica Fume

Firing

Waste

ABSTRACT

The present study aims to investigate the utilization of two crucial industrial wastes, borogypsum, and silica fume, as the primary raw materials in the production of ceramic materials. For this purpose, different receipts were designed from boron waste (borogypsum) belonging to the Emet boric acid factory (Kütahya/Türkiye) and silica fume, which was taken from the electrometallurgy facilities (Antalya/Türkiye). Mixtures were prepared by mixing 90% waste material and 10% binder clay. The samples, prepared at different mixing ratios from both wastes, were pressed uniaxially at 10 MPa, and the shaped samples were then fired at 1000, 1050, 1100, and 1150°C. Physical and mechanical tests, as well as mineralogical and microstructural analyses, were carried out on the fired samples. The technical properties of the samples derived from the wastes were evaluated depending on the type of waste material and its usage amounts, and firing temperatures. It was found that using high borogypsum caused high firing loss, which negatively affects the material's dimensional stability. Moreover, it was determined that adding silica fume to borogypsum increased water absorption (WA) and porosity values, and decreased strength (BS) values accordingly. As a result, the water absorption and bending strength values obtained in the samples prepared from a mixture of 70% borogypsum and 20% silica fume sintered at 1050°C (WA:12.39%, BS:13.45 MPa) and 1100°C (WA:10.25%, BS:15.18 MPa) coincide with the technical specifications defined in EN ISO 10545-3 (WA>10%) and EN ISO 10545-4 (BS≥12 MPa) standards, so it can be considered possible to use as wall tiles.

1. Introduction

Industrialization, urbanization, and technological developments benefit human life, but they also bring along problems such as the reduction of natural resources over time and the generation of substantial amounts of waste. Protecting the environment from industrial wastes is very important for living creatures because the health of all living things and their environment are adversely affected by this waste and pollution. For this purpose, many scientists continue to explore alternative ways to recycle waste, protect living creatures and the environment, and limit the consumption of natural resources [1-6].

The production of engineering materials from waste materials and their possibilities of application for alternative purposes is an essential interest for engineers. Research on waste products will help solve many environmental problems and create new valuable findings in the engineering field. The production of ceramic materials is one of the possible ways to dispose of industrial wastes of organic and inorganic origin.

Since high-temperature heating >1000°C is required to produce ceramic materials, organics and volatile compounds in waste burn out and cause porosity in the structure. The porous structure dominates many properties of the material, such as lightness and insulation [1-2].

Boron minerals are Türkiye's most essential and strategic underground asset, with the world's largest boron deposits. Türkiye has approximately 73% of the world's boron reserves and the first boron production capacity followed USA. Although there are many boron minerals in nature, colemanite, tincal, and ulexite are the boron minerals widely used industrially. These minerals are concentrated to produce boron compounds. Colemanite is reacted with sulfuric acid to produce boric acid. The main product of the reaction is boric acid, and gypsum is collected in the filters as a by-product of the boric acid production process [6-10]. Since the gypsum sludge contains about 3-6 % B₂O₃, it is called borogypsum (BG). Approximately 3.3×10⁵ tons per year of boric acid and 6.5-7×10⁵ tons per year of BG are produced in the factories located in Bandırma and

*Corresponding author: rcozturk@erbakan.edu.tr

Emet of Etimaden Inc. in Türkiye [4, 11]. BG discarded from the plant is stored in open areas. It is a valuable industrial waste for its B_2O_3 content. However, boron compounds in BG can be dissolved by rain, which can lead to soil and water pollution. Also, the high amount of boron content leads to economic loss [4, 5, 12].

Utilization of industrial wastes and by-products has become an exciting issue for scientists to investigate. There are several studies in the literature investigating mechanical, physical, and chemical properties of materials containing by-products and wastes such as phosphogypsum, tincal ore waste, colemanite ore waste, BG, etc., [7-10].

In recent years, BG has been widely used in various fields, such as material science, chemical, agricultural, and civil engineering applications, since it offers cost reduction, energy savings, and arguably superior products. Boncukcuoglu et al. [7] and Elbeyli et al. [17] investigated using BG instead of natural gypsum in cement mortar. It was reported that concrete containing BG exhibited better mechanical strength than one containing natural gypsum. Sevim and Tumen [18] and Alp et al. [19] noted that using BG as a set retarder in the cement industry might be possible. Kutuk-Sert and Kutuk [20] reported that it was possible to use BG as infill aggregate in asphalt concrete for road and highway construction. Abi [11] reported that it was possible to use 10% BG to increase mechanical strength in brick compositions. Demir and Keles [21] and Evcin and Yahsi Çelen [22] reported that BG was suitable for gamma-ray shielding material.

Silica fume (SF), also known as microsilica, is a sub-product of the foundry process in the elemental silicon and ferrosilicon alloys. This by-product, produced in the electric arc furnace during the production of metallurgical silicon and ferrosilicon alloys, is a fine, amorphous, spherical silica powder with a SiO_2 content of 85-95%. The fume produced at the furnace condenses into fine particles and is recovered from the process exhaust gases by classification and filtration. Submicron particle size ($<1 \mu m$), flabby nature (thus behaving like a fume or smoke when dispersed in the air), high surface area ($\sim 13.000-30.000 m^2/kg$), spherical shape, and glassy structure make SF very reactive in hydrous and anhydrous reaction environments. The worldwide production of SF waste is estimated to be over 1 million tons annually. It is known that about 500,000 tons of this is in the USA, and 200,000 tons are in Norway. In Türkiye, SF productions from one ferrosilicon production plant are around 1,000 tonnes annually. Fumed silica is a compelling material due to its ultra-fineness and high silica content. It is mainly used as a mineral additive in materials such as cement and concrete to improve properties such as strength, permeability, corrosion resistance, and others [1, 23-27].

Most of the studies on the evaluation of waste are for the use of single waste material as a substitute in the composition of a product, and the amount of

waste used is relatively low. The present study aims to investigate the possible use of BG and SF, which are two important industrial wastes, as primary raw materials in the production of ceramic materials. For this purpose, samples were produced from mixtures containing BG belonging to the Emet Boric Acid factory (Kütahya/Türkiye) and SF, which was taken from the Electrometallurgy facilities (Antalya/Türkiye) and these were fired at different temperatures. Physical and mechanical tests, as well as mineralogical and microstructural analyses, were carried out on the fired samples. Technical properties of the samples derived from the wastes were evaluated depending on the type of waste material and its usage amounts and firing temperatures.

2. Materials and Methods

2.1. Materials

In the present study, the fabrication of ceramic materials from two industrial wastes was investigated. The BG was provided by the Eti Mine Works and the representative wastes were taken from the outlet of the thickener unit at the plant in Emet (Türkiye). The particle size of BG is the fine (d_{10}) and coarse (d_{90}) fractions, and the median particle size (d_{50}) is 0.96, 3.4, and 14.88 μm . SF was provided by Etibank Ferro-Alloy Production. SF powders were taken from a plant in Antalya (Türkiye) and then used as received without any treatment being applied. The particle size of SF is the fine (d_{10}) and coarse (d_{90}) fractions, and the median particle size (d_{50}), 1, 6.6, and 16 μm , respectively. Chemical analyses of waste materials used were performed by using an X-ray fluorescence spectroscopy (XRF; Rigaku, ZSX Primus II, Japan). The chemical analysis of waste materials used in the bodies determined by the XRF method is presented in Table 1. The mineralogical phase analysis of both wastes was performed by an X-ray diffractometer (XRD; Bruker-D8 Advance, Germany), with $CuK\alpha$ radiation, to determine their present crystalline phases. The determined crystalline phases of waste materials used in the bodies are presented in Figure 1.

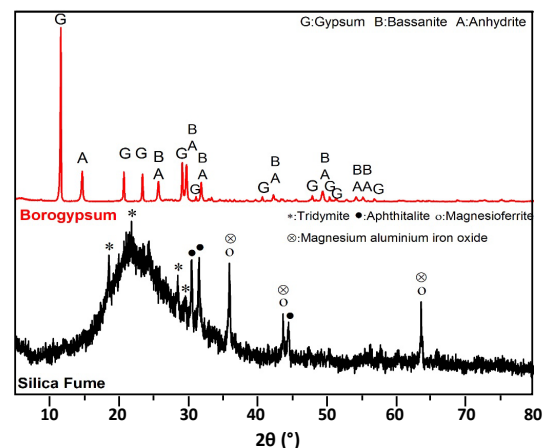


Figure 1. XRD analysis of waste materials as-received.

Table 1 show that BG consists mainly of calcium oxide (CaO), silicon oxide (SiO₂), and sulphur trioxide (SO₃) with relatively small and variable amounts of iron oxide (Fe₂O₃), magnesium oxide (MgO), aluminium oxide (Al₂O₃), and boron oxide (B₂O₃). Up to 20% ignition loss in the chemical composition of BG is remarkable. SF predominantly contains the SiO₂ component as well as relatively small and variable amounts of alkali and alkaline earth oxides, CaO, Al₂O₃, and Fe₂O₃. Its SiO₂ content is over 96%, as presented in Table 1. Kaolin has a typical aluminosilicate composition but, on the other hand, has a high loss on ignition (LOI).

Table 1. The chemical analysis of raw and waste materials used.

Composition (wt. %)	Borogypsum	Silica Fume	Kaolin
SiO ₂	9.96	96.02	57.15
Al ₂ O ₃	1.66	0.20	21.36
Na ₂ O	0.03	0.08	2.40
K ₂ O	0.92	0.08	1.24
CaO	36.70	1.40	0.55
MgO	2.33	-	0.80
Fe ₂ O ₃	2.64	0.20	0.23
TiO ₂	0.11	-	-
SO ₃	22.57	0.21	-
SrO	2.27	-	-
B ₂ O ₃	1.21	-	-
MnO	0.10	-	-
L.O.I.*	19.50	1.81	16.27

*L.O.I.: Loss on Ignition

According to the XRD patterns presented in Figure 1, it was determined that BG contains bassanite (2CaSO₄·H₂O) (Pdf: 00-047-0964) and anhydrite (CaSO₄) (Pdf: 01-076-6906) crystalline phases besides gypsum (CaSO₄·2H₂O) (Pdf: 01-070-0982) mineral. On the other hand, in the XRD pattern of SF, it was observed that the structure was mainly amorphous, as expected. The crystalline phases detected in the SF structure were as follows; tridymite (SiO₂) (Pdf: 01-086-0681), apthitalite ((K,Na)₃Na(SO₄)₂) (Pdf: 00-020-0928), magnesioferrite (MgFe₂O₄) (Pdf: 01-0754392) and magnesium aluminium iron oxide (MgAlFeO₄) (Pdf: 01-071-4392).

2.2. Composition Design

In this study, five different recipes were designed in which the amount of BG and SF were varied, and the kaolin was kept constant. In the designed recipes, the amount of kaolin was kept constant at 10 wt. %, the amount of BG was systematically reduced, and the amount of SF was increased as much as the decreasing amount of BG as given in Table 2. The B_x-SF_y formulation was used to symbolize the samples prepared from these designed recipes. Here 'B' stands for BG

while X stands for weight percentage of BG. The second index value, SF, was assigned to SF, and its weight percentage was encoded as Y. The mineralogical compositions and their chemical analysis of designed receipts are given in Tables 2 and 3, respectively.

Table 2. The chemical analysis of raw and waste materials used.

Sample Code	Borogypsum (wt. %)	Silica Fume (wt. %)	Kaolin (wt. %)
B90-SF0	90	0	10
B70-SF20	70	20	10
B45-SF45	45	45	10
B20-SF70	20	70	10
B0-SF90	0	90	10

Table 3. The chemical analysis of raw and waste materials used.

Composition (wt. %)	B90-SF10	B70-SF20	B45-SF45	B20-SF70	B0-SF90
SiO ₂	14.68	31.89	53.41	74.92	92.13
Al ₂ O ₃	3.63	3.34	2.97	2.61	2.32
Na ₂ O	0.27	0.28	0.29	0.30	0.31
K ₂ O	0.95	0.78	0.57	0.36	0.20
CaO	33.09	26.03	17.20	8.38	1.32
MgO	2.18	1.71	1.13	0.55	0.08
Fe ₂ O ₃	2.40	1.91	1.30	0.69	0.20
TiO ₂	0.10	0.08	0.05	0.02	0.00
SO ₃	20.31	15.84	10.25	4.66	0.19
SrO	2.04	1.59	1.02	0.45	0.00
B ₂ O ₃	1.09	0.85	0.54	0.24	0.00
MnO	0.09	0.07	0.05	0.02	0.00
L.O.I.*	19.18	15.64	11.22	6.79	3.26

*L.O.I.: Loss on Ignition

2.3. Sample Preparations

BG, taken from the facility as a cake, was first oven-dried and then crushed using a laboratory-type roll crusher with an opening of 1 mm, then sieved through a 250 µm sieve. The other raw materials were also first dried in an oven to keep the correct mixing ratio. The weighing of raw materials was performed using an electronic balance with a precision of 0.01 grams, according to the amounts given in Table 2. Mixtures of 500 grams were prepared to represent each recipe, as presented in Table 2. A dry grinding process was then performed using a planetary ball mill until a homogeneous mixture was obtained and until the particle size of the prepared mix decreased to the desired ratio. The grinding time required for the desired homogeneity and grain size was kept constant at 30 minutes for all series. The mixtures obtained in the desired grain size were sieved through a 100 µm sieve and dried in

an oven (Elektromag, Türkiye) at 110°C for 24 hours until they reached a constant weight. The dried mixtures were next hand-milled with an agate mortar and pestle. The ground mixtures were moisturized with sprayed water to between 5 and 5.5% moisture, and all mixtures were formed into granules. The granulated powders were shaped as prismatic (10×10×70 mm) test samples by a hydraulic press by applying 100 kg/cm². The test samples were dried in an oven at 110°C for 2 hours. The dried specimens were fired at 1000, 1050, 1100, and 1150°C in an electrically heated kiln at a heating rate of 5°C min⁻¹, holding the firing temperature for 1 hour.

3. Characterization

Test samples were prepared with five different recipes using two different types of industrial waste from the metallurgical and mining sectors. 10 samples from each group were measured to obtain reliable values for all tests performed to evaluate the physical properties of the test samples. The test results were made by taking the mean values of 10 measurements.

The linear shrinkage percentage of samples, shaped in rectangular prism geometry and then fired, was calculated by dividing the difference between the sample sizes measured before and after the firing stage by the value before firing and multiplying by 100. The water absorption values were determined by the ratio of the mass increase caused by water immersion, calculated by weighing the dry and water-saturated mass of the samples to the dry sample's weight. Bulk density values were determined by proportioning the weight of the relevant examples in the air to the mass difference between their water-saturated and water-suspended weights. Apparent porosity values were calculated by dividing the difference in mass caused by immersion of the samples in water to the value of the mass difference between the water-saturated and water-suspended weights of the relevant pieces and then multiplying by 100. The physical properties of fired samples (water absorption, porosity, firing shrinkage, etc.) were measured and evaluated according to TS EN ISO 10545-3 standards.

The bending strength (σ_F) of fired samples was measured according to EN ISO 10545-4 standards using a three-point bending test instrument (Shimadzu AG-IS, Japan). Five representative fired samples were used for the three-point bending test and the average fired strength values were calculated to represent the results better. The standard deviation was less than 1% of the average values.

The crystal structures of fired samples were characterized by an X-ray diffractometer (XRD; Bruker-D8 Advance) using Cu-K α radiation ($\lambda=1.5406 \text{ \AA}$) scanning from 10° to 90° at a scanning rate of 2°/min, and the divergence and scattering slit widths were set at 0.30 mm. After a first visual inspection of the XRD patterns, the mineral spectral search and match

confirmation were analysed. Basic data processing and phase identification were performed by Bruker EVA software and the ICDD PDF-2 database.

Using scanning electron microscopy (SEM; Leo 1430 VP, Germany), the microstructure of fired samples has been examined in terms of formed phases, porosity, etc. During the observation, secondary electron images (SEI) at different magnifications of the fractured surface of the fired sample were used. The particle sizes of grains and pore sizes in microstructure were manually measured using the scale bar on the SEM micrographs. At least five measurements for each sample were performed. EDX (Energy Dispersive X-ray) analyses were also performed to identify crystalline phases.

4. Results and Discussion

4.1. Physical and Mechanical Properties of the Material Produced from Wastes

The results of characterization work on fired samples of encoded B90-SF10, B70-SF20, B45-SF45, B20-SF70, and B0-SF90 are given in Table 4. The linear shrinkage (LS), water absorption (WA), apparent porosity (AP), bulk density (BD), and bending strength (BS) values of fired samples are presented in Table 4, depending on the change in both firing temperature and amount of BG.

The effect of firing temperature and BG amount on the linear shrinkage of the samples fired at different temperatures is shown in Figure 2. It is seen that the linear shrinkage values of the fired samples gradually decreased with the decreasing BG amount at all temperatures. This decreasing trend in linear shrinkage values coincides with the LOI values of the compositions presented in Table 3. As seen in Table 3, as the amount of BG in the recipes decreases, the fire loss values decrease. Since SF has a much lower LOI values than BG (Table 1) and the replacement of BG by SF reduces the LOI values of the mixture.

Reducing linear shrinkage values with SF addition is considered favourable for the dimensional stability of material during firing. Because the high shrinkage

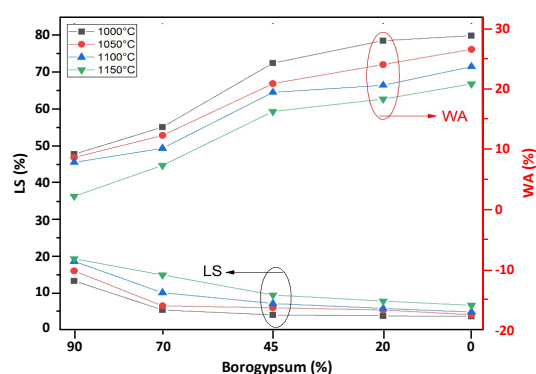


Figure 2. Linear shrinkage (LS) and water absorption (WA) in the samples as a function of firing temperature.

Table 4. Some properties of samples prepared from borogypsum and silica fume wastes.

Temperature (°C)	Borogypsum (%)	LS (%)	WA (%)	AP (%)	BD (g/cm ³)	BS (MPa)
1000	90	13.54	9.29	18.57	1.99	13.27
	70	5.68	13.77	25.93	1.72	11.36
	45	4.32	24.39	35.61	1.60	9.84
	20	4.05	28.10	39.04	1.55	7.25
	0	3.96	28.93	39.30	1.35	4.66
1050	90	16.23	8.72	17.78	2.04	16.06
	70	6.75	12.39	22.33	1.78	13.48
	45	6.22	20.99	33.47	1.66	12.09
	20	5.67	24.13	39.25	1.64	9.86
	0	4.38	26.66	39.34	1.57	6.18
1100	90	18.83	7.92	16.91	2.13	19.23
	70	10.34	10.25	20.52	1.83	15.18
	45	7.41	19.53	32.10	1.74	13.26
	20	6.08	20.71	39.34	1.68	11.07
	0	5.13	23.79	40.06	1.62	9.64
1150	90	19.57	2.32	9.64	2.44	23.64
	70	15.14	7.42	17.53	2.24	16.41
	45	9.72	16.36	24.67	1.84	14.71
	20	8.06	18.42	39.95	1.71	11.89
	0	6.90	20.93	40.27	1.65	10.15

results in a lack of dimensional stability in materials, which leads to an important loss of end-product quality (deformation, size mismatch, etc.), as well as problems in the application of materials (tiling, brick-laying, etc.). Producing materials free of dimensional defects is required using appropriate control of the body composition and temperature distribution in the firing process. The most important precaution that can be taken for body composition is to avoid using the raw materials in high amounts that can cause high shrinkage.

From this point of view, the high shrinkage values obtained in the series with the highest BG content (B90-SF0) are considered not suitable for the dimensional stability of the final product. On the other hand, it can be observed that there is a severe decrease in shrinkage values with the incorporation of SF in their body compositions (Figure 2). This situation is related to the fact that silica preserves its dimensional stability at firing temperatures reducing the distortion and shrinkage of the bodies, as expressed in many previous studies [28-31].

As indicated in Table 4, the water absorption values measured in the samples prepared using waste materials are above 10% in all samples except for the samples with 90% BG content for 1000, 1050, and 1100°C temperatures and 70% and 90% BG content for 1150°C. SF addition increased the values of the water absorption of the samples at all firing temperatures (Figure 2). However, at all firing temperatures,

samples containing the maximum amount of SF have at least 15% higher water absorption values than those without SF. This observation can be attributed to the decreasing shrinkage and low packing density induced by the use of SF, resulting in increased water absorption values.

Water absorption is an essential factor in ceramic materials' durability and liquid permeability. Water absorption is directly proportional to apparent porosity [2]. Therefore, similar trends were observed in water absorption and apparent porosity (Figure 3).

As presented in Table 4, the lowest bulk density value which was to be 1.35 g/cm³ was obtained in the sample that did not have BG and was fired at 1000°C,

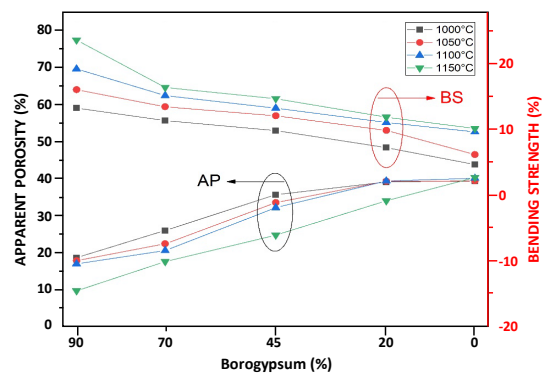


Figure 3. Apparent porosity (AP) and bending strength (BS) in the samples as a function of firing temperature.

while the highest bulk density value of 2.44 g/cm³ was obtained in the sample that did not have SF and was fired at 1150°C. The bulk density values of the bodies increased with the increase in temperature. This can be associated with the reduction of porosity in number and size. On the other hand, with the increase of SF, the bulk density values of the bodies decreased. This observation can be attributed to the reduced shrinkage and lower packing density caused by the use of SF, as discussed in the water absorption results.

Due to the increase in the degree of sintering, the size and number of internal pores in the material decreases, and the degree of packing increases, resulting in higher bulk density values. Conversely, under poor sintering conditions, porosity increases, and the material becomes less dense; as a result, the bulk density of the body is reduced, resulting in an underdeveloped microstructure. As a result, the use of SF in waste-containing bodies resulted in an increase in porosity, a reduction in firing shrinkage, and a decrease in bulk density values as a result of these, which is an indication that the sintering process is negatively affected.

It can be seen that the apparent porosity values presented in Table 4 are below 20% in all samples without SF and above 20% in samples containing SF, except B70SF20. Parallel to the increase in SF usage, AP values increased in all samples (Figure 3). On the other hand, except for the series in which SF is used at the amount of 70 and 90%, it can be seen that the AP values of the samples decrease with increasing temperature in the other series. On the contrary, it was observed that AP increased with the increase in temperature in the series in which SF was used at a high rate (>70%). High apparent porosity (AP) and associated high water absorption (WA) result in reduced material mechanical strength. When evaluated within this framework, the addition of SF at increasing rates to BG adversely affected the mechanical strength of the material produced from these wastes.

As presented in Table 4, the lowest bending strength value to be 4.66 MPa was obtained in the sample that did not have BG and was fired at 1000°C, while the highest bending strength value to be 23.64 was obtained in the sample that did not have SF and was fired at 1150°C. The bending strength values of the bodies increased with the increase in temperature (Figure 3). This can be attributed to a decrease in porosity in number and size, as discussed earlier in the evaluation of bulk density results. On the other hand, with the increase of SF, the bending strength values of the bodies decreased. This observation can also be attributed to the reduced shrinkage and lower packing density caused by the use of SF, as discussed in the water absorption and bulk density results.

4.2. Microstructural Evaluation

After the determination of the physical and mechanical properties, the samples belonging to the B70SF20

coded series, sintered at 1000 and 1100°C were selected for phase analysis, since they have low LS and WA, and high BS values. The XRD analysis of the sample (B70SF20) of materials produced from the industrial wastes is given in Figure 4. There was no remarkable change in the phase structure of samples with the increasing firing temperature, and it was found that the phase structure of the samples included similar phases, i.e., calcium sulphate (Ca(SO₄)₂), calcium silicate (Ca₂O₄Si), and augite (Si, Al)₂O₆. As the difference in XRD patterns drawn for two different temperatures; in the sample fired at 1100°C, a cristobalite peak was detected at 2θ:21.8° in the XRD pattern, while an increase in the number of augite peaks was detected.

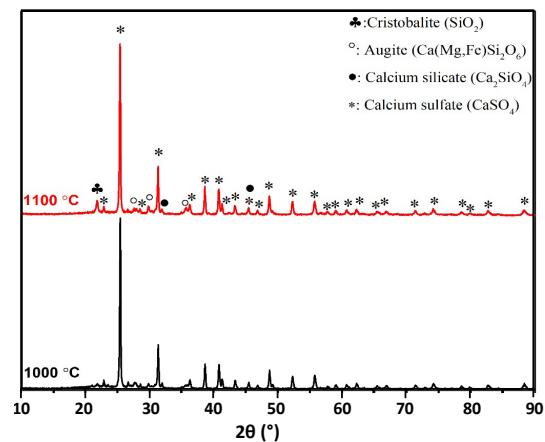


Figure 4. XRD analysis patterns of fired samples at two different temperatures.

According to XRD analysis, it can be seen that the main phase forming the microstructure of the waste originating material consists of calcium sulphate from BG. In the composition (B70SF20), where 70% BG and 20% SF are used, it can be understood that calcium silicate and augite compounds are formed depending on the reactions between BG and SF.

The secondary electron images (SEI) taken from the fractured surfaces of the sample belonging to the bodies incorporated 20% SF (B70SF20) and which were fired at 1100°C are given in Figure 5. From the SEI images presented in Figure 5, the presence of crystalline phases such as calcium sulphate and calcium silicate, and also glassy phase in the microstructure of the waste-based material was determined. In SEM figures, letters indicate CSu: calcium sulphate, CSi: calcium silicate, G: glassy phase, P: porosity.

In the micrographs taken at low magnification of the sample examined in the SEM analysis, it can be understood that the general microstructure image is homogeneous and dense but also contains pores. In the micrographs taken at high magnifications, it can be seen that the grains of calcium sulphate, which are 1-3 µm in size, are both embedded in the glass phase and the form of independent grains outside the glass

phase. In addition, needle-like calcium silicate crystals showing an aspect ratio in the 10:1 interval (~1 µm long and ~0.1 µm wide) were also observed in the micrograph taken at the highest magnification of the sample, which was exposed to microstructure examination. On the other hand, it has been determined that the majority of the pores in the microstructure are not

spherical but hollow and pitted, and the largest pores are around 1-2 µm.

In this study, which was carried out to investigate the effects of BG and SF on the sintering and final properties of ceramic materials, heat microscopy analysis of SF was carried out to explain its effect on the sintering, microstructural development, and technical properties.

The melting behaviour of SF was determined by the Optonom Scientific Instruments brand heat microscope (Optonom Scientific Instruments, Türkiye) in Figure 6. By using the heat microscope, the physical changes of the sample with the increase in temperature (sintering temperature, softening temperature, sphere temperature, hemisphere temperature, yield temperature) and the temperatures at which these changes occur can be determined. It is seen that the sintering temperature, softening temperature, hemisphere temperature and yield temperature determined by the heat microscope of SF are 933, 1032, 1196 and 1199°C, respectively.

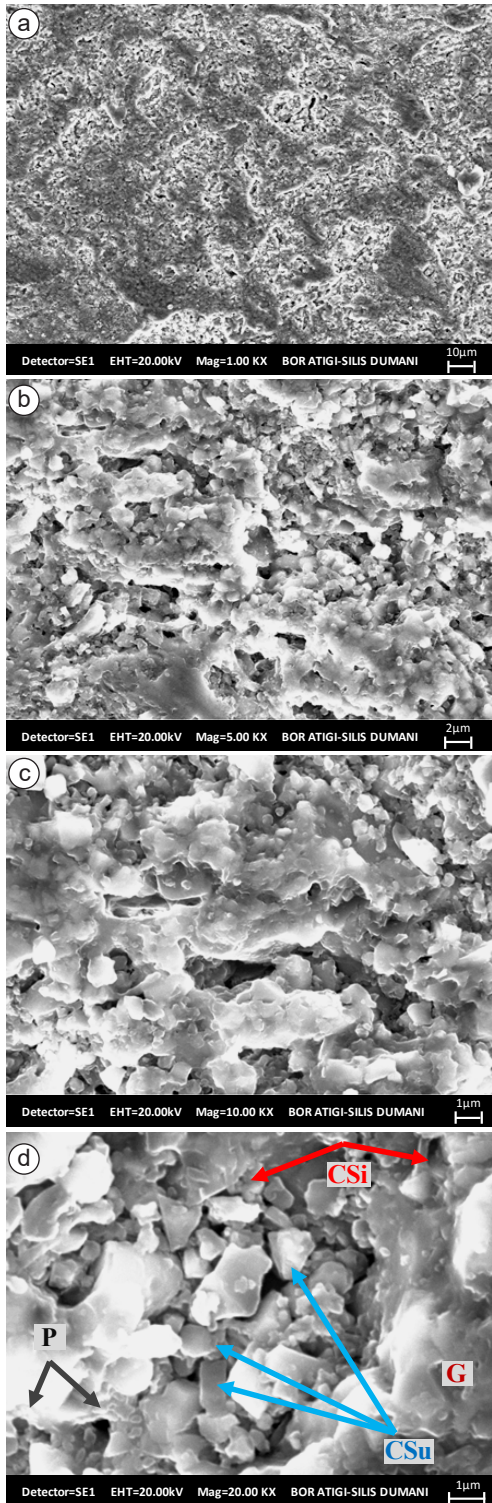


Figure 5. Secondary electron image of B70SF20 at different magnifications; (a) 1000X, (b) 5000X, (c) 10000X, and (d) 20000X.

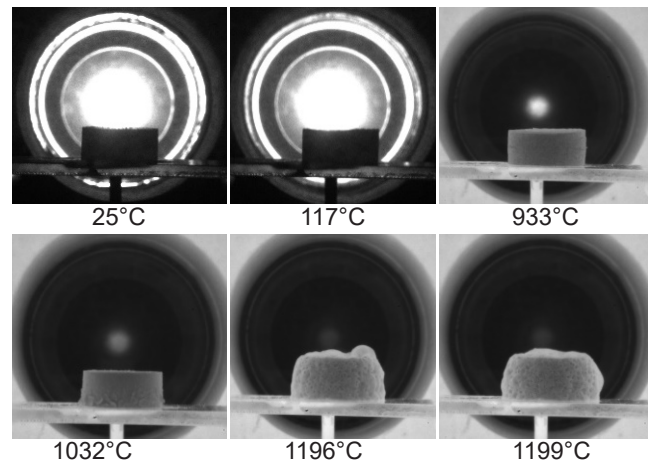


Figure 6. Heat microscope analysis of silica fume.

According to the results of the physical and mechanical properties, the B70SF20 coded samples, which were determined to have the best properties, during the sintering process at 1000-1150°C, the SF did not completely pass into the molten phase (because it began to soften at 1032°C and flow at about 1200°C). It is thought that this molten phase has a high viscosity. In the SEM micrograph of the sample sintered at 1100°C, code B70SF20, it is understood that the partial molten phase formed from SF partially encloses the grains of the other components, while the parts that the liquid phase does not wrap remain in the structure as open porosity. Additionally, it can be understood that the gas releases originating from BG and kaolin, which have higher heating loss than SF, do not cause foaming in this high-viscosity melt phase. On the other hand, although gas escape is provided from the remaining (not surrounded by amorphous) openings, it can be said that some of them are trapped in the glassy phase (as closed porosity) due to the increase in porosity.

5. Conclusion

From the two industrial wastes used, it can be understood that the high ignition loss of BG will cause more firing shrinkage in the samples to be produced entirely using BG, thus posing a problem in terms of material dimensional stability. For this reason, it can be understood that using additional raw materials to reduce LOI originating from BG is required. On the other hand, it was determined that with the increase of SF addition to BG, the water absorption and porosity values increased, and the strength values decreased accordingly. The effects on the material properties of usage of both BG and SF in the composition together or individually were evaluated. It can be understood that the optimum composition should be adjusted by using a minimum amount of SF that will not adversely affect the technical properties and in an amount that will reduce the LOI originating from BG and thus shrinkage. In this context, it has been shown that the technical properties obtained in the samples prepared from a mixture of 70% BG and 20% SF can be considered wall tile since they coincide with the water absorption and strength values defined in the EN ISO 10545-3 (WA%>10) and EN ISO 10545-4 (BS \geq 12 MPa) standards, respectively.

As a result, when all the technical properties are evaluated, it can be concluded that the usage of BG and SF for producing wall tiles materials will be possible through optimizations in body composition and/or operational conditions.

References

- [1] Baspinar, S., Demir, I. & Orhan M. (2010). Utilization potential of SF in fired clay bricks. *Waste Management & Research*, 28, 149-157.
- [2] Bahtli, T., & Erdem Y. (2022). The use of foundry waste sand from investment casting in the production of porcelain tiles. *Ceramics International*, 48(19A), 27967-27972.
- [3] Zaimoglu, S. A. (2011). Engineering properties of sand stabilised with borogypsum. *Proceedings of the Institution of Civil Engineers-Geotechnical Engineering*, 164, 277-282.
- [4] Simsek, H. M., Guliyev, R., & Bese, A. V. (2018). Dissolution kinetics of borogypsum in di-ammonium hydrogen phosphate solutions. *International Journal of Hydrogen Energy*, 43(44), 20262-20270.
- [5] Elbeyli, I. Y., & Piskin, S. (2004). Kinetic study of the thermal dehydration of borogypsum. *Journal of Hazardous Materials*, 116(1-2), 111-117.
- [6] Kunt, K, Dur, F., Yildirim, M., & Derun, E. M. (2017). Effect of chemical admixtures on borogypsum containing cement mortar. *Main Group Chemistry*, 16(4), 227-239.
- [7] Boncukcuoglu, R., Yilmaz, M. T., Kocakerim, M. M., & Tosunoglu, V. (2002). Utilization of borogypsum as set retarder in Portland cement production. *Cement and Concrete Research*, 32(3), 471-475.
- [8] Ozdemir, M., & Ozturk, N. U. (2003). Utilization of clay wastes containing boron as cement additives. *Cement and Concrete Research*, 33(10), 1659-1661.
- [9] Sevim, U. K., Ozturk, M., Onturk, S., & Bankir, M. B. (2019). Utilization of boron waste borogypsum in mortar. *Journal of Building Engineering*, 22, 496-503.
- [10] Ozturk, M., Sevim, U. K., Akgol, O., Unal, E., & Karaaslan, K. (2020). Investigation of the mechanic, electromagnetic characteristics and shielding effectiveness of concrete with boron ores and boron containing wastes. *Construction and Building Materials*, 252, 119058, 1-11.
- [11] Abi, C. B. E. (2014). Effect of borogypsum on brick properties. *Construction and Building Materials*, 59, 195-203.
- [12] Delfini, M., Ferrini, M., Manni, A., Massacci, P., & Piga, L. (2003). Arsenic leaching by Na₂S to decontaminate tailings coming from colemanite processing. *Minerals Engineering*, 16, 45-50.
- [13] Holanda, F. C., Schmidt, H., & Quarcioni, V. A. (2017). Influence of phosphorus from phosphogypsum on the initial hydration of Portland cement in the presence of superplasticizers. *Cement and Concrete Composites*, 83, 384-393.
- [14] Abali, Y., Bayca, S. U., & Targan, S. (2006). Evaluation of blends tincal waste, volcanic tuff, bentonite and fly ash for use as a cement admixture. *Journal of Hazardous Materials*, 131(1-3), 126-130.
- [15] Kaman, D. O., Koroglu, L., Ayas, E., & Guney, Y. (2017). The effect of heat-treated boron derivative waste at 600°C on the mechanical and microstructural properties of cement mortar. *Construction and Building Materials*, 154, 743-751.
- [16] Sevim, U. K. (2011). Colemanite ore waste concrete with low shrinkage and high split tensile strength. *Materials and Structures*, 44, 187-193.
- [17] Elbeyli, I. Y., Derun, E. M., Gulen, J., & Piskin S. (2003). Thermal analysis of borogypsum and its effects on the physical properties of Portland cement. *Cement Concrete Research*, 33, 1729-1735.
- [18] Sevim U. K., & Tumen Y. (2013). Strength and fresh properties of borogypsum concrete. *Construct Build Mater*, 48, 342-347.
- [19] Alp I., Deveci, H., Sungun, Y. H., Yazici, E. Y., Savas, M., & Demirci, S. (2009). Leachable characteristics of arsenical borogypsum wastes and their potential use in cement production. *Environmental Science & Technology*, 43, 6939-6943.
- [20] Kutuk-Sert T., & Kutuk, S. (2013). Physical and marshall properties of borogypsum used as filler aggregate in asphalt concrete. *Journal of Materials in Civil Engineering*, 25(2), 266-273.
- [21] Demir, D, & Keles, G. (2006). Radiation transmission of concrete including boron waste for 59.54 and 80.99 keV gamma rays. *Nuclear Instruments and Methods in Physics Research Section B: Beam Interactions with Materials and Atoms*, 245(2), 501-504.

- [22] Celen, Y. Y., & Evcin, A. (2020). Synthesis and characterizations of magnetite-borogypsum for radiation shielding. *Emerging Materials Research*, 9(3), 1-7.
- [23] Muller, A. C. A., Scrivener, K. L., Skibsted, J., Gajewicz, A. M., & McDonald, P. J. (2015). Influence of SF on the microstructure of cement pastes: new insights from H NMR relaxometry. *Cement and Concrete Research*, 74, 116-125.
- [24] Sanjuán, M. A., Argiz, C., Gálvez, J. C., & Moragues, A. (2015). Effect of SF fineness on the improvement of Portland cement strength performance. *Construction and Building Materials*, 96, 55-64.
- [25] Siddique, R. (2011). Utilization of SF in concrete: review of hardened properties. *Resources, Conservation and Recycling*, 55, 923-932.
- [26] Khan, M. I., & Siddique, R. (2011). Utilization of SF in concrete: review of durability properties. *Resources, Conservation and Recycling*, 57, 30-35.
- [27] Ávalos-Rendón, T. L., Chelala, E. A. P., Mendoza Escobedo, C. J., Figueroa, I. A., Lara, V. H., & Palacios-Romero, L. M. (2018). Synthesis of belite cements at low temperature from SF and natural commercial zeolite. *Materials Science and Engineering: B*, 229, 79-85.
- [28] Ozturk, C., Akpınar, S., & Tığ, M. (2022). Effect of calcined colemanite addition on properties of porcelain tile. *Journal of the Australian Ceramic Society*, 58, 321-331.
- [29] Ozturk, C., Akpınar, S., & Tarhan, M. (2021). Investigation of the usability of Silice stone as additive in floor tiles. *Journal of the Australian Ceramic Society*, 57(2), 567-577.
- [30] Ozdemir, Y., Akpınar, S., & Evcin, A. (2017). Effect of calcined colemanite additions on properties of hard porcelain body. *Ceramics International*, 43(11), 8364-8371.
- [31] Turkmen, O., Kucuk, A., & Akpınar, S. (2015). Effect of wollastonite addition on sintering of hard porcelain. *Ceramics International*, 41(4), 5505-5512.



Co-synthesis of zirconium boride/silicide/oxide composite powders by magnesiothermic reduction

Didem Ovalı-Döndaş ^{1,*}

¹Osmaniye Korkut Ata University, Department of Mechanical Engineering, Osmaniye, 80000, Türkiye

ARTICLE INFO

Article history:

Received September 20, 2022

Accepted December 1, 2022

Available online December 31, 2022

Research Article

DOI: 10.30728/boron.1177551

Keywords:

ZrB₂

ZiSi

High-energy ball milling

Magnesiothermic reduction

X-ray diffraction

ABSTRACT

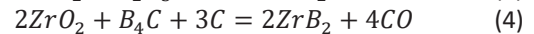
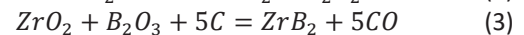
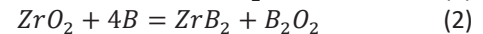
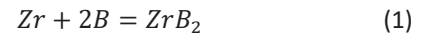
This study uses a magnesiothermic reduction method to investigate the co-synthesis of zirconium boride, silicides, and oxide powder composites using ZrO₂, B₂O₃, Si, and Mg powders. Synthesis of high-temperature ceramic powders was examined through milling durations, reduction temperatures, and excess magnesium addition. Thermochemical analysis of probable reaction products was conducted by the Factsage software. According to the results, the thermochemical predictions and resultant powder phases showed good coherency. High-energy milling has a significant effect on the formation of the zirconium boride phase after annealing. However, extended milling time and higher annealing temperature had no significant effect on composition of the constituted composite powders according to the X-ray diffraction results. An annealing temperature of 600°C was enough to obtain ZrB₂-based ceramic composite powders. In the final powder phases, the excess magnesium addition to the stoichiometric displays an important feature. After the milling, annealing, and leaching procedure, the stoichiometric powder composition comprises ZrB₂, ZrSi, ZrSi₂, ZrO₂, and MgSiO₂, and excess Mg added powders have the ZrB₂, ZrSi, ZrSi₂, ZrO₂ phases in their structure. Scanning electron microscopy analysis was utilized to observe the morphologies of the powders throughout each step of the synthesis procedure and revealed the finely structured morphology of synthesized powders.

1. Introduction

Ultra high-temperature ceramics (UHTCs) are well known for their extreme resistance in high-temperature environments and their melting temperatures above 3000°C [1, 2]. Different borides, nitrides, carbides, and silicides of IV and V group elements in the periodic table have gained recognition of UHTC. Their common advanced properties are high thermal conductivity, high hardness, low coefficient of thermal expansion, good thermal shock resistance, good oxidation resistance, and stability in extreme environments [3]. One of them, zirconium borides, has been seen as a promising compound for different applications as cutting tools, wear-resistant coatings, hypersonic flights, and rocket propulsion systems. Therefore, researchers have published many works about synthesizing or applying zirconium boride-based materials because of their supreme properties [4].

Zirconium-boron binary phase diagram presents three different crystal structures of zirconium boride as ZrB (stable up to 927°C), ZrB₁₂ (stable between 1720-2030°C), and ZrB₂ (stable up to 3227°C) [5]. The synthesis of zirconium boride is possible in many methods using high-temperature reactions, including elemental

Zr and B powder. The zirconium borides are commonly obtained through high-temperature methods such as the direct reaction of elemental powders (Eq.1), borothermal (Eq.2), and carbothermal (Eq.3 and Eq.4) reduction of ZrO₂ [4, 6]. However, the synthesis process of ZrB₂ from elemental powders cannot be commercially produced because of the expensive charge materials.



The production process of zirconium borides involves a high-temperature step over 1200°C due to their strong covalent bonding and low self-diffusion coefficient values. In order to enhance the structural integrity of zirconium borides, reinforcement materials were used as high-temperature borides, silicides, carbides, and oxides [7]. Especially, the initial powder conditions such as size, shape, and homogeneity play a critical role in the consolidation process and final properties of products [8]. On the other hand, aiming to obtain zirconium

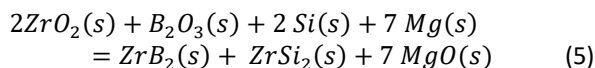
*Corresponding author: didemovali@osmaniye.edu.tr

boride composite powders could lead to a simplified synthesis process or a lowered annealing temperature for the reduction process of ZrO_2 . Therefore, many researchers conducted various works on the *in situ* synthesis of composites of zirconium boride together with other zirconium-based ceramic phases [1, 3, 9]. So far, ZrB_2 - ZrO_2 (Zirconium diboride-zirconium dioxide) [10-12], ZrB_2 - $ZrSi_2$ (Zirconium diboride-zirconium disilicite) [13-21], and ZrB_2 - ZrC (Zirconium diboride-zirconium carbide) [22, 23] binary systems were obtained using different starting compositions. Some of them resulted in ternary compositions such as $ZrSi_2$ - $MoSi_2$ - ZrB_2 [24], ZrB_2 - ZrC - SiC [25, 26], ZrB_2 - $ZrSi_2$ - SiC [27]. Having assessed the binary (e.g. boride-carbide) and ternary ceramic systems (e.g. boride-silicide-oxide), ternary systems could result in altered physical and mechanical properties due to their diverse microstructures [28]. And this may lead to the development of alternative materials for various applications. Among published papers about ternary ceramic systems, ZrB_2 - $ZrSi_2$ - ZrO_2 systems have not been attempted before, to our knowledge.

In this study, the synthesis of UHTC composite powders comprising zirconium boride/silicide/oxide was investigated through a magnesiothermic reduction process using ZrO_2 , B_2O_3 (Boron trioxide), Si, and Mg initials. Thermochemical software also examined the thermodynamic calculations for existence and probable by-products using initial batches. The synthesis procedures using ZrO_2 , B_2O_3 , Si, and Mg system were investigated in terms of different milling durations, excess Mg initial addition, and annealing temperatures. The outcomes of this study can contribute well to the existing literature for obtaining zirconium boride/silicide/oxide composite powders.

2. Materials and Methods

The initial materials were ZrO_2 (Alfa Aesar™, >99% purity), Si (ABCR™, >99% purity), Mg (Mg, Sigma Aldrich™, >99% purity), and B_2O_3 (Sigma Aldrich™, >99.9% purity) powders in this study. Each powder batch was calculated in Eq.5 and mixed in a Turbula blender for 2h.



Following Turbula blender, initial powder batches were subjected to high-energy ball milling (SPEX™ 8000D) for 3h, 6h, and 15h of milling durations. The initial powders were solely mixed using a blender mentioned as 0h. Hardened steel vials (50 ml capacity) and balls (6 mm Ø) were used and sealed under an Argon atmosphere. The ball-to-powder weight ratio (BPR) was 7:1 for each milling/run. The 0h, 3h, 6h, and 15h milled powders were placed in an alumina crucible and annealed in a Protherm™ tube furnace for 2h at various temperatures (600, 800, and 1000°C) under a flowing Ar atmosphere. The heating and cooling rates were

10°C/min for each run. The purification process of reacted powders was conducted using a dilute HCl solution (Merck™, 37% concentrated). The concentration and solid-to-liquid ratio of HCl solution were selected as 2 M and 1 g/10 ml, respectively. After centrifugation (Hettich™ Mikro 220/220R centrifuge, at 3500 rpm) for 20 min, decantation and filtration treatments were repeated three times, the powders were dried using an oven at 100°C.

Thermodynamic calculations were carried out using Factsage 7 thermochemical program. The FactPS database was used for thermodynamic calculations because of including all possible corresponding data in the gas, liquid, and solid phases. X-ray diffraction (XRD) patterns of powders were obtained using the Bruker™ D8 Advance Series X-ray diffractometer with $CuK\alpha$ (1.54Å) radiation. The morphological observations and microstructural characterization of powders were conducted using a FEI (Quanta FEG 250) scanning electron microscope (SEM) coupled with an energy-dispersive spectrometer (EDS). SEM analyses were operated at 15 kV under environmental mode.

3. Results and Discussion

The thermochemical predictions of the ZrO_2 - B_2O_3 -Si-Mg system were conducted by Factsage™ software to have a better understanding of the reaction probability and potential reaction products. The standard Gibbs free energy (ΔG°) and enthalpy (ΔH°) change of Eq.5 was calculated for different temperatures between 0 and 2000°C as given in Figures 1 (a) and (b), respectively. The large ΔG° and ΔH° values of Eq. 5 suggest that this reaction has a moral certainty. Figure 1(b) exhibits two sharp increase points in the ΔH° versus temperature curve at 630 and 1095°C which corresponds to the respective melting and boiling temperatures of Mg [29]. The ΔG° value of reaction (Eq.5) in Figure 1a shows a sharp increase around 1100°C caused by the vaporization of Mg.

Figure 1 pointed out that the reaction in Eq.5 could be started by a magnesiothermic reaction. Since our system has two oxides as ZrO_2 and B_2O_3 , the magnesiothermic reaction could progress as given in Eq.6 and 7.

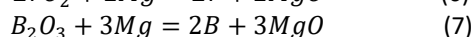
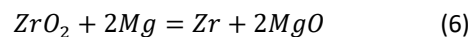


Figure 2 shows the probable reaction products predicted for varying amounts (from 0 to 15 mole) of magnesium input based on Eq.6. Below the stoichiometric mole of Mg (corresponds to 7 moles in Eq.6), the predicted reaction phases are ZrB_2 , $ZrSi$, MgO , Mg_2SiO_4 , $MgSiO_3$ together with residual ZrO_2 . According to the predictions, the Mg amount is below the stoichiometric proportion (7 moles for Mg), the reduction process of ZrO_2 and B_2O_3 dominates by the occurrence of silica (SiO_2) and silicate ($ZrSiO_4$, $MgSiO_3$, and Mg_2SiO_4) formations. The magnesiothermic reduction, as in Eq.2

and 3, takes place for a minimum of 3 moles of Mg. Above the stoichiometric proportion (7 moles of Mg) as in Eq.1, the only reduction mechanism is a magnesiothermic reaction, as understood by a sharp increase in the slope of the MgO curve in the graph (Figure 2). There is also a correlation between the initial Mg mole and magnesium silicate phases. When the amount of Mg addition increases, the MgSiO_3 curve decreases, and the Mg_2SiO_4 curve increases. The MgSiO_3 formations only exit up to three moles of Mg, which means the occurrence of Mg_2SiO_4 formations can be prevented with an increasing amount of Mg. In the stoichiometric

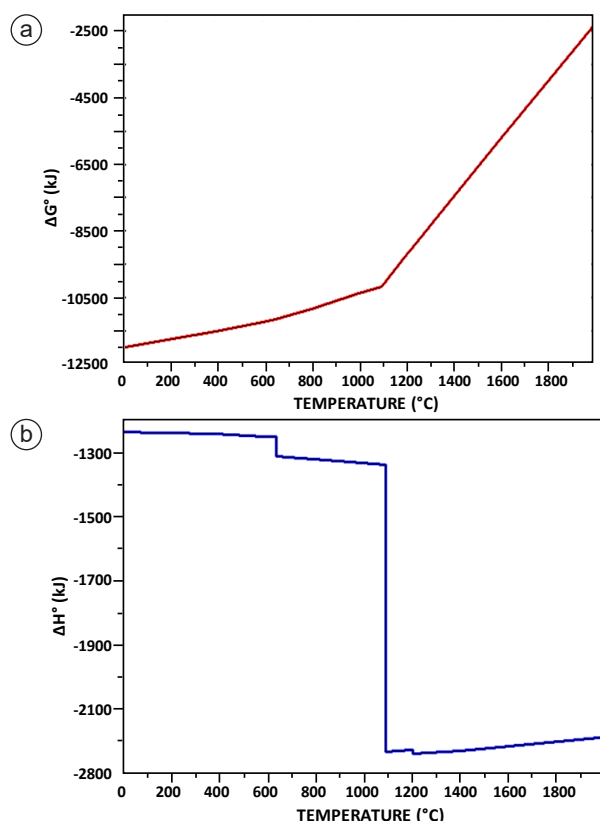


Figure 1. The graphs of (a) The ΔG° , and (b) ΔH° versus temperature based on Eq.5 were produced by the Factsage thermodynamic software.

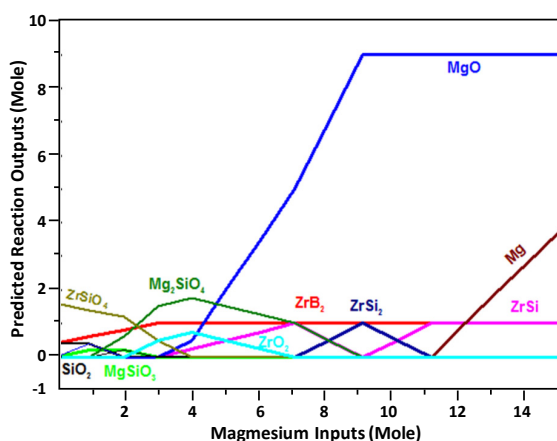


Figure 2. The amount of magnesium versus probable reaction products based on Eq.5 generated from the Factsage™ thermodynamic software.

proportion (7 moles of Mg), the thermodynamic predictions point to the ZrSi , ZrB_2 , Mg_2SiO_4 , and MgO phases. This result indicates the existence of the ZrSi phase as possible instead of ZrSi_2 for all initial powder proportions, except stoichiometric ones. Therefore, both of ZrSi and ZrSi_2 phases could be obtained for our system based on the thermodynamic predictions. The increased initial Mg amount (especially 9 moles of Mg) contributes to the ZrSi_2 formation.

The XRD pattern of initial powders after various times of ball milling is illustrated in Figure 3. All XRD patterns infer the ZrO_2 (ICDD number: 01-078-0047, Primitive Monoclinic Bravais Lattice, P21/c), Si (ICDD number: 71-9399, Face-centered Cubic Bravais Lattice, Fd3m), and Mg (ICDD number: ICDD Card number: 27-1402, Bravais lattice: primitive hexagonal Bravais Lattice, P63/mmc) phases. The existence of B_2O_3 peaks is not detected in the XRD pattern due to its amorphous nature [10]. The peaks of ZrO_2 , Si, and Mg phases are broadened and their intensities are decreased by increasing high-energy milling durations. In addition to this, the ZrO_2 peak at 28.17° and Si peak at 28.42° in the XRD pattern of as-blended powders (referred to as 0 h) are overlapped by intense milling prolonged to 15h of milling. The main peak of Mg at 36.5° are drastically decreased by 3h and a longer time of milling, which is a good sign for the stored energy during milling. Since the reductive metal is magnesium in this study, the stored energy is an important indicator of a probable reaction during the annealing process [30].

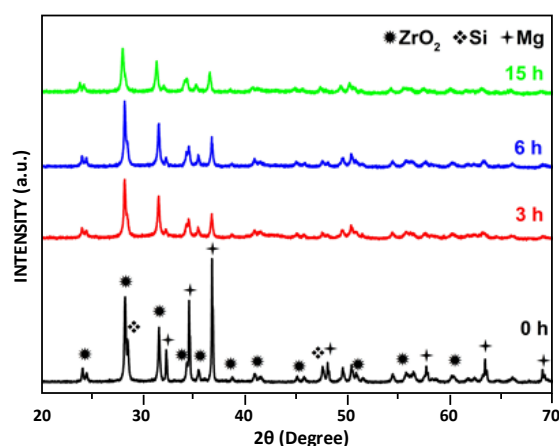


Figure 3. XRD patterns of high-energy ball-milled powders for 0h, 3h, 6h, and 15h.

XRD patterns of powders after various hours of high-energy milling and annealing at 600°C are illustrated in Figure 4. The existing phases of as blended powders (addressed with 0h) are ZrO_2 (ICDD number: 01-078-0047, Primitive Monoclinic Bravais Lattice, P21/c), and Mg_2Si (ICDD number: 00-035-0773, Face-centered Cubic Bravais Lattice, Fm3m) with a small intensity peak of ZrB_2 (ICDD number: 01-089-3930, Primitive Hexagonal Bravais Lattice, P6/mmm). Since the XRD reflections of ZrO_2 have high intensities and there are small peaks belonging to ZrB_2 and MgO phases, it can

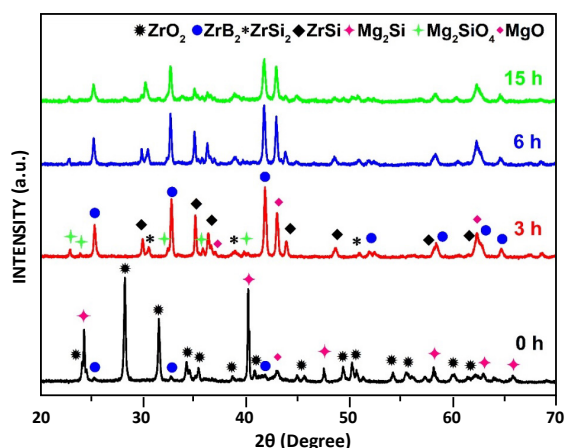


Figure 4. XRD patterns of high-energy ball milled powders for 0h, 3h, 6h, and 15h after annealing at 600°C for 2h.

be said that the magnesiothermic reduction of ZrO_2 slightly occurred. There are also no indications of a completed reduction in B_2O_3 at this stage. Therefore, it means the aimed reaction slightly takes place for the initial powder batch annealed at 600°C without milling. In the literature, the initial temperature for ZrB_2 phase formations in most synthesis studies starts above 800°C [10, 22, 26]. Some of them require extreme temperatures, such as 1650°C to obtain ZrB_2 formations synthesized from ZrO_2 and B_2O_3 initials [31, 32]. In this study, using ZrO_2 , B_2O_3 , Si, and Mg initials, the first formation temperature of the ZrB_2 phase was drawn up to 600°C. The XRD patterns of high-energy milled powders for 3, 6, and 15h (Figure 4) present mainly ZrB_2 (ICDD number: 01-078-0047, Primitive Monoclinic Bravais Lattice, P21/c), $ZrSi$ (ICDD number: 01-078-0047, Primitive Monoclinic Bravais Lattice, P21/c), $ZrSi_2$ (ICDD number: 01-078-0047, Primitive Monoclinic Bravais Lattice, P21/c), and MgO (ICDD number: 01-078-0047, Primitive Monoclinic Bravais Lattice, P21/c) phases together with a small intensity belonging to Mg_2SiO_4 . Since no peaks can be detected for ZrO_2 , it can be said that the magnesiothermic reduction completely occurred for high-energy milled powders. The zirconium silicide phase exists in two different stoichiometries as $ZrSi_2$ and $ZrSi$ compatible with thermodynamic prediction in Figure 2. The studies about synthesis of metal silicides showed it is quite possible to obtain metal silicide phases in a variety of stoichiometries especially the synthesis procedure involved a milling process [33, 34]. The thermodynamic predictions in Figure 2 also pointed to a possible Mg_2SiO_4 formation, as seen in the XRD patterns in Figure 4. A study revealed that the Mg_2SiO_4 phases easily formed with the initial powder batches containing Mg and Si phases [35]. Although zirconium boride and silicide phases were obtained for 3h milling and annealing, extended milling was applied up to 15h for the purpose of detecting any probable degradation or formation of a new phase. The peak intensities are slightly decreased by prolonged milling time, which suggests a decline in the crystallite size of powders based on the XRD patterns [30].

XRD patterns of high-energy ball milled powders annealed at 800°C and 1000°C are given in Figures 5a and b, respectively. The ZrB_2 , $ZrSi_2$, and $ZrSi$ phases are formed for 0h milled powders after annealing at 800°C and 1000°C. However, the existence of ZrO_2 and Si phases in the XRD pattern of 0h milled and annealed powders reveals the uncompleted reaction. With the effects of high-energy ball milling, the XRD patterns of annealed powders at 800°C and 1000°C reveal the reflections of ZrB_2 , $ZrSi_2$, $ZrSi$, and MgO structures together with a small one that arose from Mg_2SiO_4 phase. There is no distinguished difference between the XRD reflections of annealed powders at 600°C (Figure 4), 800°, and 1000°. It is understood that the structures formed in this study are stable and not affected by a higher temperature or an extended milling time. Since there is no significant difference, the minimum milling time (3h) and middle annealing temperature (800°C) can be described as optimum process conditions. In literature, most reaction temperatures to obtain the ZrB_2 phase from ZrO_2 and B_4C initials are above 1600°C [36]. With the help of milling, this reaction temperature was reduced to 1200°C [10]. Another study reduces the required annealing temperature to 800°C combining ZrO_2 with other elements/compounds such as Zr, B_4C , Si, and ZrC [26]. In this study, the ZrB_2 phase is obtained using ZrO_2 , B_2O_3 , Si, and Mg powders after the annealing process at 600°C with the help of milling. In a study, ZrB_2 powders were driven from ZrO_2 - B_2O_3 -Mg system by volume combustion synthesis method [37]. They stated the reaction temperature as 900°C. Comparing to initial systems, the reaction temperature was reduced to 600°C with addition of Si in this study.

A purification process with HCl acid solution was applied in order to remove the MgO phase from the powder structure synthesized via the magnesiothermic reduction. The XRD patterns of leached powders are given in Figures 6a and b. After purification, some undetected phases could be noticeable in the XRD patterns. For this reason, both 3h and 15h high-energy milled powders (annealed at 800°C) were leached. All peaks were sharp and had high intensities. After leaching, there is no new formation detected in the patterns. However, the undistinguishable ZrO_2 peaks in Figure 5a become clear view of the XRD patterns in Figure 6a and b. In another word, it is not possible to observe the ZrO_2 peaks detected at 28.5° and 31.5° because of its small intensity in Figure 5a (3h and 15h milled and annealed powders). The Figure 6b demonstrates that MgO phase is completely removed from powder structure by leaching. However, the Mg_2SiO_4 phase was remained in the powder structure because acid leaching could not eliminate it. By comparing the Figures 6a and b, it can be seen that the ZrO_2 peaks intensities of 3h milled powders are relatively higher than those in 15h milled powders, which suggests that milling causes a slight decrement in the residual ZrO_2 content. This can be attributed to the grain refinement caused by the fracture mechanism exposed during the

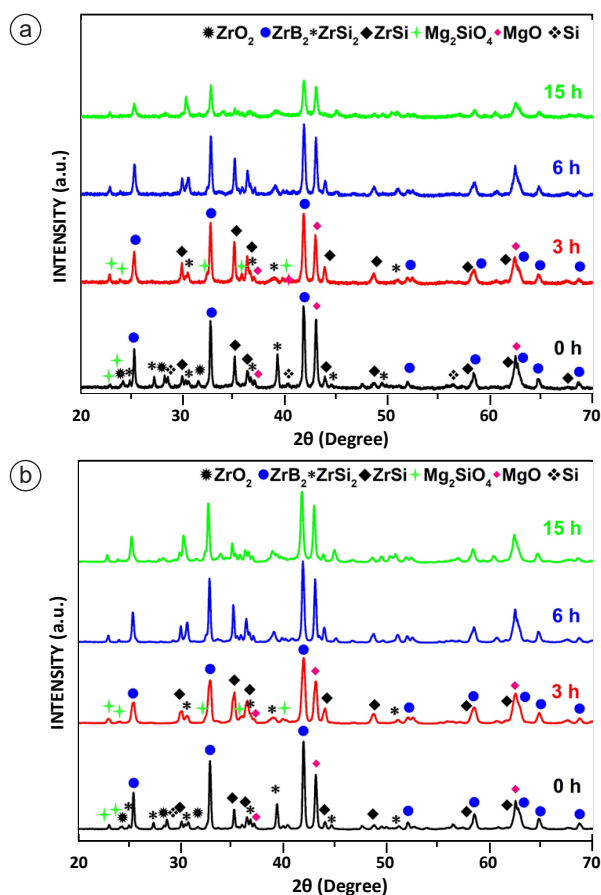


Figure 5. XRD patterns of high-energy ball milled powders for 0h, 3h, 6h, and 15h after annealing for 2h: a) at 800°C and b) at 1000°C.

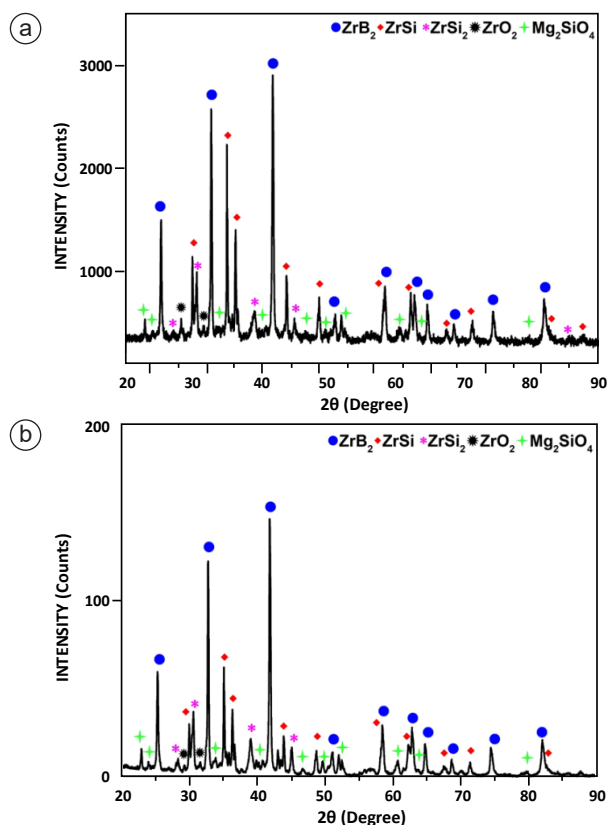


Figure 6. XRD pattern of powders after high-energy ball milled, annealed at 800°C, and leached powders: a) 3h MA and b) 15h MA.

milling process. These studies prove an excess Mg addition to the stoichiometric proportion can inhibit the MgSiO_4 formation during the synthesis procedure [33, 34]. Therefore, excess Mg added initial powder samples were milled for 3h and annealed at 800°C for 2h. Figure 7a and b presents the XRD analysis results of high-energy milled and annealed powders with excess Mg addition and those after leaching procedure, respectively. In the XRD pattern of milled and annealed powder, there are ZrB_2 , ZrSi_2 , ZrSi , ZrO_2 , and MgO phases. After removing MgO phases by leaching, all peaks in the XRD pattern belong to ZrB_2 , ZrSi_2 , ZrSi , and ZrO_2 phases. It is clear evidence for the inhibition of Mg_2SiO_4 formation by excess Mg addition. Comparing to Figure 6a, and 7b, there is a significant difference between the proportions of ZrB_2 , ZrSi_2 , ZrSi and ZrO_2 formations regarding to their peak intensities. For example, the reflections of ZrSi_2 in Figure 7b are quite higher than those in Figure 6b. Hence, it is obviously seen that excess Mg addition influences the zirconium boride, silicide and oxide phase composition in the synthesized powder structure. The XRD patterns of synthesized powder with excess Mg addition in Figure 7a present any reflection belonging to the residual Mg phase as unreacted initial if it is under the detection limit of XRD analysis. However, in the case of excess magnesium existence, the HCl leaching also removes it from the synthesized powder structure. Excess Mg addition attributes the ZrSi_2 occurrence instead of the ZrSi phase. The thermodynamic predictions in Figure

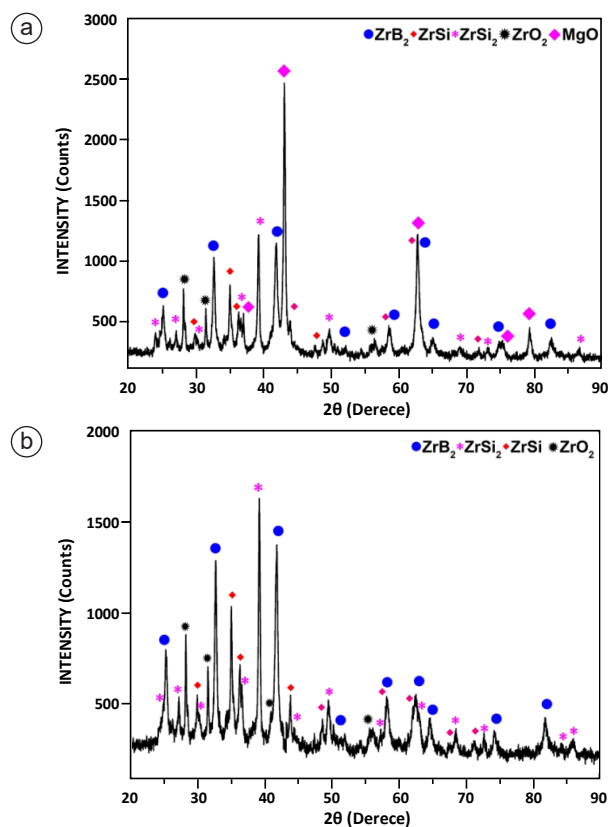


Figure 7. a) XRD pattern of excess Mg added powders after high-energy ball milling for 3h, annealing at 600°C and, b) those after leaching procedure.

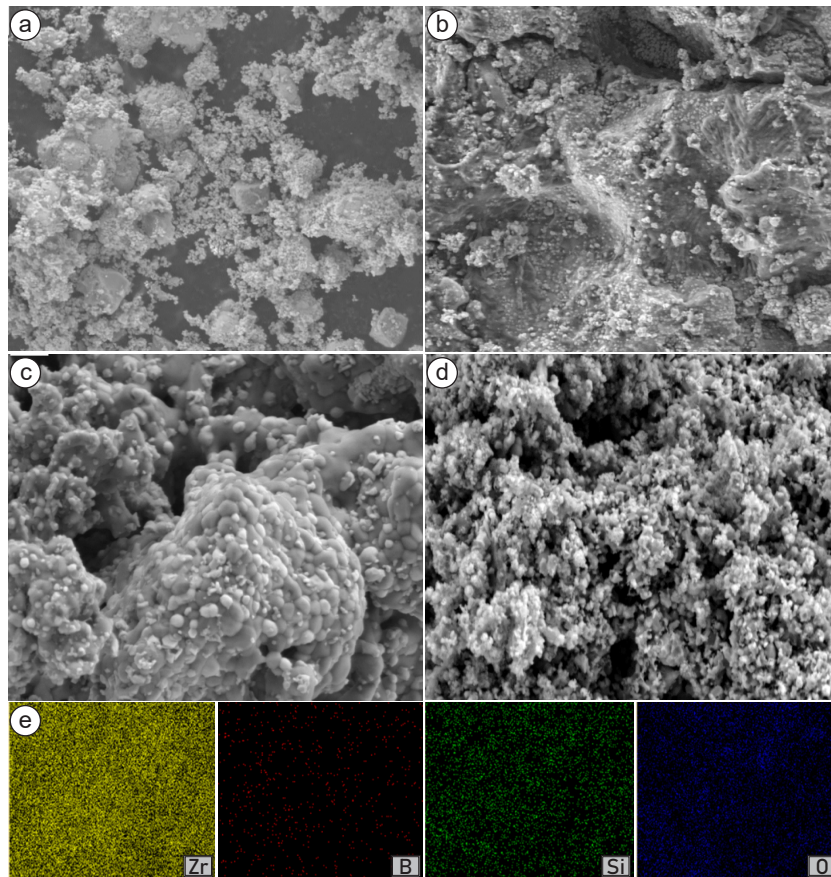


Figure 8. SEM images of excess Mg added powders: a) As-blended, b) High energy milled for 3h, c) High energy milled and annealed at 600°C, d) High energy milled, annealed at 600°C and leached, and e) Zr, B, Si and O elemental mapping of d.

2 show the constitution of $ZrSi_2$ formation rather than $ZrSi$ in the presence of excess Mg addition for 9 moles. The existence of $ZrSi$ is possible for other mole rates of Mg based on the Figure 2. Mg_2SiO_4 and $ZrSi_2$ phases have relation to the common Si content. Inhibition of Mg_2SiO_4 formation supports the formation of $ZrSi_2$ because there is more Si source to induce the existence of the zirconium silicide phase. Therefore, the $ZrSi$ phase exists in Figures 6 and 7 is probably originated from the residual of ZrO_2 . For solid state reactions, the initial powder composition plays a prominent role in the obtained powder embody [38].

Figure 8 displays the secondary electron SEM images of excess Mg added powders. The as-blended powders placed in Figure 8a have irregular and different particle sizes presenting a homogenous morphology of ZrO_2 , B_2O_3 , Si, and Mg initials. The 3h milled particles, as seen in Figure 8b, have a uniform distribution. After annealing at 800°C for 2h, the zirconium boride/silicide/oxide particles are embedded into large agglomerated MgO particles. The leaching process provides the division of zirconium-based ceramic particles by dissolving the MgO phase in the HCl acid solution. Therefore, the SEM images of leached zirconium boride/silicide/oxide particles can be seen in Figure 8d. The synthesized zirconium-based ceramic particles have a spherical shape and their particle sizes are smaller than 0.5 μm , as seen in Figure 8d. The

elemental mapping of Zr, B, Si, and O conducted for zirconium boride/silicide/oxide particles was given in Figure 8e. The maps of Zr, B, Si, and O elements coincide almost entirely with each other, which suggests the presence and homogenous distribution of the zirconium boride, silicide, and oxide phases.

4. Conclusions

Milling, annealing and following leaching process of the ZrO_2 , B_2O_3 , Si and Mg were successfully used in the fabrication of zirconium boride/silicide/oxide ceramic powders with fine microstructure. Synthesis procedure was studied in terms of different milling duration, annealing temperature and excess Mg addition. The results of experimental studies and thermodynamic analysis are compatible with each other regarding the formation of probable phases. The formation of ZrB_2 starts after milling for 3h and annealing at 600°C. Results showed that the application of milling has significant effects on the resultant composition; however, further milling and different annealing temperatures displayed any determinant difference. The ZrB_2 , $ZrSi_2$, $ZrSi$, ZrO_2 and Mg_2SiO_4 phases were obtained using the stoichiometric proportion of initial powders after the synthesis and purification process. Applying excess Mg addition to the stoichiometric proportion, the occurrence of Mg_2SiO_4 formation was prevented and the final structure of powders comprised ZrB_2 , $ZrSi_2$,

ZrSi and ZrO₂ phases based on the XRD results. The SEM analysis showed the powder products have homogenous distribution and fine structure.

Acknowledgement

The author wishes to express her gratitude to Prof. Dr. Lütfi Öveçoğlu for permission of using the Particulate Materials Laboratory infrastructure for milling and XRD analyses. The author thanks to Assoc. Prof. Dr. Nazlı Akçamlı for thermodynamic analysis. The author acknowledges the Namık Kemal University Center Laboratory (NABİLTEM) for conducting SEM analysis.

References

- [1] Golla, B. R., Mukhopadhyay, A., Basu, B., & Thimmappa, S. K. (2020). Review on ultra-high temperature boride ceramics. *Progress in Materials Science*, 111, 100651.
- [2] Zhang, G. J., Ni, D. W., Zou, J., Liu, H. T., Wu, W. W., Liu, J. X., ... & Sakka, Y. (2018). Inherent anisotropy in transition metal diborides and microstructure/property tailoring in ultra-high temperature ceramics-A review. *Journal of the European Ceramic Society*, 38(2), 371-389.
- [3] Sonber, J. K., & Suri, A. K. (2011). Synthesis and consolidation of zirconium diboride: review. *Advances in Applied Ceramics*, 110(6), 321-334.
- [4] Fahrenholtz, W. G., Hilmas, G. E., Talmy, I. G., & Zaykoski, J. A. (2007). Refractory diborides of zirconium and hafnium. *Journal of the American Ceramic Society*, 90(5), 1347-1364.
- [5] Predel B (2012) *B - Zr (Boron - Zirconium)* (Vol. 12B, pp 87-88). In: Predel B (Ed.). Springer.
- [6] Karasev, A. I. (1973). Preparation of technical zirconium diboride by the carbothermic reduction of mixtures of zirconium and boron oxides. *Soviet Powder Metallurgy and Metal Ceramics*, 12(11), 926-929.
- [7] Zhu, S., Fahrenholtz, W. G., & Hilmas, G. E. (2007). Influence of silicon carbide particle size on the microstructure and mechanical properties of zirconium diboride-silicon carbide ceramics. *Journal of the European Ceramic Society*, 27(4), 2077-2083.
- [8] Ağaoğulları, D., Balcı, Ö., Mertdinç, S., Tekoğlu, E., & Öveçoğlu, M. L. (2018). Synthesis of VB₂-V₃B₄-V₂B₃/VC hybrid powders via powder metallurgy processes. *Journal of Boron*, 3(3), 180-187.
- [9] Aguirre, T. G., Lamm, B. W., Cramer, C. L., & Mitchell, D. J. (2022). Zirconium-diboride silicon-carbide composites: A review. *Ceramics International*, 48(6), 7344-7361.
- [10] Balcı, Ö., Ağaoğulları, D., Duman, İ., & Öveçoğlu, M. L. (2012). Carbothermal production of ZrB₂-ZrO₂ ceramic powders from ZrO₂-B₂O₃/B system by high-energy ball milling and annealing assisted process. *Ceramics International*, 38(3), 2201-2207.
- [11] Balcı, Ö., Akçamlı, N., Ağaoğulları, D., Öveçoğlu, M. L., & Duman, İ. (2017). Otoklavda sentezlenen ZrB₂-ZrO₂ tozlarının farklı tekniklerle sinterlenmesi ve yığın yapıların mikroyapısal ve bazı mekanik özelliklerinin incelenmesi. *Journal of Boron*, 2(1), 1-10.
- [12] Xu, L., Guo, W., Liu, Q., Zhang, Y., Wu, L., You, Y., & Lin, H. (2022). Fully dense ZrB₂ ceramics by borothermal reduction with ultra-fine ZrO₂ and solid solution. *Journal of the American Ceramic Society*, October 2021, 1-8.
- [13] Sha, J. J., Wei, Z. Q., Li, J., Zhang, Z. F., Yang, X. L., Zhang, Y. C., & Dai, J. X. (2014). Mechanical properties and toughening mechanism of WC-doped ZrB₂-ZrSi₂ ceramic composites by hot pressing. *Materials and Design*, 62, 199-204.
- [14] Yen, B. K. (1998). X-ray diffraction study of mechanochemical synthesis and formation mechanisms of zirconium carbide and zirconium silicides. *Journal of Alloys and Compounds*, 268(1-2), 266-269.
- [15] Silvestroni, L., Meriggi, G., & Sciti, D. (2014). Oxidation behavior of ZrB₂ composites doped with various transition metal silicides. *Corrosion Science*, 83, 281-291.
- [16] Zamora, V., Guiberteau, F., & Ortiz, A. L. (2020). Effect of high-energy ball-milling on the spark plasma sinterability of ZrB₂ with transition metal disilicides. *Journal of the European Ceramic Society*, 40(15), 5020-5028.
- [17] Wang, M., Wang, C. A., & Zhang, X. (2012). Effects of SiC platelet and ZrSi₂ additive on sintering and mechanical properties of ZrB₂-based ceramics by hot-pressing. *Materials and Design*, 34, 293-297.
- [18] Sha, J. J., Li, J., Wang, S. H., Wang, Y. C., Zhang, Z. F., & Dai, J. X. (2015). Toughening effect of short carbon fibers in the ZrB₂-ZrSi₂ ceramic composites. *Materials and Design*, 75, 160-165.
- [19] Guo, S. Q., Kagawa, Y., Nishimura, T., & Tanaka, H. (2008). Pressureless sintering and physical properties of ZrB₂-based composites with ZrSi₂ additive. *Scripta Materialia*, 58(7), 579-582.
- [20] Guo, S. Q. Q., Kagawa, Y., & Nishimura, T. (2009). Mechanical behavior of two-step hot-pressed ZrB₂-based composites with ZrSi₂. *Journal of the European Ceramic Society*, 29(4), 787-794.
- [21] Jia, Y., Mehta, S. T., Li, R., Chowdhury, M. A. R., Horn, T., & Xu, C. (2021). Additive manufacturing of ZrB₂-ZrSi₂ ultra-high temperature ceramic composites using an electron beam melting process. *Ceramics International*, 47(2), 2397-2405.
- [22] Mousavi, S. M., Zakeri, M., Kermani, M., Rahimipour, M. R., & Tayebifard, S. A. (2019). A comparative study on the synthesis of oxide-free ZrB₂-xZrC composites. *Ceramics International*, 45(3), 3760-3766.
- [23] Adibpur, F., Zaferi, M., & Tayebifard, S. A. (2013). Feasibility study of metallic reductant element replacement by mechanical activation process in ZrB₂-ZrC composite synthesis from raw oxide materials by SHS. *Life Science Journal*, 10(8s), 336-341.
- [24] Astapov, A. N., Pogozhev, Y. S., Prokofiev, M. V., Lifanov, I. P., Potanin, A. Y., Levashov, E. A., & Vershinnikov, V. I. (2019). Kinetics and mechanism of high-temperature oxidation of the heterophase ZrSi₂-MoSi₂-ZrB₂ ceramics. *Ceramics International*, 45(5), 6392-6404.
- [25] Liu, C., Chang, X., Wu, Y., Li, X., Xue, Y., Wang, X., & Hou, X. (2020). In-situ synthesis of ultra-fine ZrB₂-ZrC-SiC

- nanopowders by sol-gel method. *Ceramics International*, 46(6), 7099-7108.
- [26] Qu, Q., Han, J., Han, W., Zhang, X., & Hong, C. (2008). In situ synthesis mechanism and characterization of ZrB₂-ZrC-SiC ultra high-temperature ceramics. *Materials Chemistry and Physics*, 110(2-3), 216-221.
- [27] Shao, G., Zhao, X., Wang, H., Chen, J., Zhang, R., Fan, B., ... & Chen, D. (2016). ZrB₂-ZrSi₂-SiC composites prepared by reactive spark plasma sintering. *International Journal of Refractory Metals and Hard Materials*, 60, 104-107.
- [28] Liu, H. L., Liu, J. X., Liu, H. T., & Zhang, G. J. (2015). Contour maps of mechanical properties in ternary ZrB₂-SiC-ZrC ceramic system. *Scripta Materialia*, 107, 140-144.
- [29] Ağaoğulları, D., Balcı, Ö., Akçamlı, N., Suryanarayana, C., Duman, İ., & Öveçoğlu, M. L. (2019). Mechanochemical synthesis and consolidation of nanostructured cerium hexaboride. *Processing and Application of Ceramics*, 13(1), 32-43.
- [30] Balcı, Ö., Ağaoğulları, D., Ovalı, D., Öveçoğlu, M. L., & Duman, İ. (2015). In situ synthesis of NbB₂-NbC composite powders by milling-assisted carbothermal reduction of oxide raw materials. *Advanced Powder Technology*, 26(4), 1200-1209.
- [31] Baris, M., Simsek, T., Simsek, T., Ozcan, S., & Kalkan, B. (2018). High purity synthesis of ZrB₂ by a combined ball milling and carbothermal method: Structural and magnetic properties. *Advanced Powder Technology*, 29(10), 2440-2446.
- [32] Ran, S., Van der Biest, O., & Vleugels, J. (2010). ZrB₂ powders synthesis by borothermal reduction. *Journal of the American Ceramic Society*, 93(6), 1586-1590.
- [33] Ovalı, D., Ağaoğulları, D., & Öveçoğlu, M. L. (2019). Mechanochemical synthesis and characterisation of niobium silicide nanoparticles. *Ceramics International*, 45(8), 10654-10663.
- [34] Ovalı, D., Ağaoğulları, D., & Öveçoğlu, M. L. (2017). Effects of excess reactant amounts on the mechanochemically synthesized molybdenum silicides from MoO₃, SiO₂ and Mg blends. *International Journal of Refractory Metals and Hard Materials*, 65, 19-24.
- [35] Ovalı, D., Ağaoğulları, D., & Öveçoğlu, M. L. (2019). Room-temperature synthesis of tungsten silicide powders using various initial systems. *International Journal of Refractory Metals and Hard Materials*, 82, 58-68.
- [36] Guo, W. M., & Zhang, G. J. (2009). Reaction processes and characterization of ZrB₂ powder prepared by boro/carbothermal reduction of ZrO₂ in vacuum. *Journal of the American Ceramic Society*, 92(1), 264-267.
- [37] Akgün, B., Çamurlu, H. E., Topkaya, Y., & Sevinç, N. (2011). Mechanochemical and volume combustion synthesis of ZrB₂. *International Journal of Refractory Metals and Hard Materials*, 29(5), 601-607.
- [38] Balcı, Ö., Ağaoğulları, D., Öveçoğlu, M. L., & Duman, İ. (2016). Synthesis of niobium borides by powder metallurgy methods using Nb₂O₅, B₂O₃ and Mg blends. *Transactions of Nonferrous Metals Society of China*, 26(3), 747-758.

YAZAR KILAVUZU

1. KAPSAM

Bor Dergisi, bor alanında aşağıda nitelikleri açıklanmış makaleleri Türkçe ve İngilizce olarak kabul etmektedir.

Araştırma Makalesi: Orijinal bir araştırmayı bulgu ve sonuçlarıyla yansıtan yazılardır. Çalışmanın özgün ve mutlaka uluslararası bilime katkısı olmalıdır.

Tarama Makalesi: Yeterli sayıda bilimsel makaleyi tarayıp, konuyu bugünkü bilgi ve teknoloji düzeyinde özetleyen, değerlendirme yapan ve bulguları karşılaştırarak yorumlayan yazılardır.

Her makale, konusu ile ilgili en az iki hakeme gönderilerek şekil, içerik, özgün değer, uluslararası literatüre ve bilime/teknolojiye katkı bakımından incelenir. Hakem görüşlerinde belirtilen eksikler tamamlandıktan sonra, dergide yayınlanabilecek nitelikteki yazılar, son baskı formatına getirilir ve yazarlardan makalenin son halinin onayı alınır. Dergide basıldığı haliyle makale içinde bulunabilecek hataların sorumluluğu yazarlara aittir.

Kabul edilen makaleler, ücretsiz olarak dergi internet sayfasında (online) ve/veya basılı şekilde yayınlanmaktadır.

2. BAŞVURU FORMLARI

Makale; Kapak Sayfası, Makale Kontrol Listesi Formu, Makale Metni, Telif Hakkı Devir Formu ve Benzerlik Oran Dosyası olmak üzere beş ayrı formdan oluşmalıdır. Başvurular da iletişimde bulunulacak yazar ve diğer yazarların iletişim bilgileri (adres, e-posta, cep ve sabit telefon no) kapak sayfasında verilmelidir.

3. GÖNDERİ KONTROL LİSTESİ

Başvuru sürecinde yazarlar gönderilerinin aşağıdaki listede bulunan tüm maddelere uygunluğunu kontrol etmelidirler, bu rehber uymayan başvurular değerlendirmeye alınmayacaktır.

1. Gönderilecek makale daha önceden yayınlanmadı ve/veya yayımlanmak üzere herhangi bir dergiye sunulmadı.
2. Makale Microsoft Office Word 2010 ve üzeri bir kelime işlemci ile hazırlandı.
3. Makale A4 sayfasında, kenar boşlukları, üstbilgi ve altbilgi boşlukları ve satır aralığı dergi formatına uygun olarak ayarlandı.

4. Ana başlıklar ve alt başlıklar İngilizceyle birlikte dergi formatına uygun olarak düzenlendi.
5. Tablolar dergi formatına uygun olarak hazırlandı, metin içerisinde bahsedildi, makalenin metin bölümüne yerleştirildi.
6. Şekiller dergi formatına uygun olarak hazırlandı, metin içerisinde bahsedildi, makalenin metin bölümüne yerleştirildi.
7. Eşitlik ve Reaksiyon numaralandırmaları sıralı olarak dergi formatına uygun olarak verildi.
8. Orijinal şekiller bütünüyle yazım kurallarına uygun hazırlandı.
9. Şekil boyutları formata uygun olacak biçimde düzenlendi.
10. Metin içinde şekiller ardışık numaralandı.
11. Kaynaklar yazım kurallarına uygun yazıldı.
12. Kaynaklar metin içinde ardışık sıralandı.
13. Kaynaklar metin sonunda, metin içinde verildiği sırada listelendi.
14. Türkçe makale başlığı/Özet/Anahtar kelimeler/Bölüm başlıkları/Tablo ve Şekil adlandırmaları ile İngilizce makale başlığı/Özet/Anahtar kelimeler/Bölüm başlıkları/Tablo ve Şekil adlandırmalarının birbirleri aynı olduğu kontrol edildi.
15. "Kapak Sayfası" oluşturuldu.
16. Telif Hakkı Devir Formu imzalandı ve gönderildi.
17. Muhtemel yazım hataları kelime işlemcinin "Yazım ve Dilbilgisi" denetimi ile kontrol edildi.
18. "Editöre Not" alanına makalenin özgün yönü ve makalenin bilime somut katkısı yazıldı.

4. TELİF HAKLARI

Makalelerin telif hakkı devri, dergi internet sayfasında sunulan Telif Hakkı Devir Formu doldurulup imzalanmak suretiyle alınır. Form imzalandıktan sonra "ek dosyaları yükle" bölümünde PDF olarak yüklenmelidir. Bu formu göndermeyen yazarların makaleleri basılamaz.

5. GİZLİLİK BEYANI

Bu dergi sitesindeki isimler ve elektronik posta adresleri bu derginin belirtilen amaçları doğrultusunda kullanılacaktır ve diğer amaçlar veya başka bir bölüm için kullanılmayacaktır.

YAZIM KURALLARI

GENEL BİLGİ

Makale; Kapak Sayfası, Makale Kontrol Listesi Formu, Makale Metni, Telif Hakkı Devir Formu ve Benzerlik Oran Dosyası olmak üzere beş ayrı formdan oluşmalıdır. Başvurular da iletişimde bulunulacak yazar ve diğer yazarların iletişim bilgileri (adres, e-posta, cep ve sabit telefon no) kapak sayfasında verilmelidir.

KAPAK SAYFASI

Başvuru esnasında yazar isimleri ayrı bir dosya olarak yüklenen Kapak Sayfası hazırlanmalı ve online olarak dergimizin internet sayfasına ayrı bir dosya olarak yüklenmelidir. İlk başvuru esnasında yazarları sadece dergi editörlerimiz görebilecektir.

Makalenin başlığının ilk harfi büyük ve diğerleri küçük harflerle sayfaya ortalı olarak yazılmalıdır. Başlık metne uygun, kısa ve açık olmalıdır. Başlığın altına, makalenin yazar ya da yazarlarının adı, soyadı, e-posta adresleri, posta adresleri, posta kodu ve ORCID numaraları yazılmalıdır.

İngilizce makale başlığı: Makaleyi kapsayıcı ve anlaşılır bir başlık kullanılmalıdır. Başlık büyük harfle başlamalı ve diğer tüm harfleri küçük yazı karakterinde yazılmalıdır. Başlık, gerektiğinde standart kısaltmalarla birlikte en çok 15 kelimedenden oluşmalıdır.

Türkçe makale başlığı: İngilizce makale başlığıyla uyumlu olmalıdır.

Yazar adları ve adres bilgileri: Yazar adlarının ve soyadlarının ilk harfleri büyük diğer tüm harfleri küçük olacak şekilde yazılmalıdır. Çalışmanın yürütülmüş olduğu yer yazar isimlerinden sonra gelmelidir. Yazarı ve çalışmanın yürütüldüğü yeri ilişkilendirebilmek amacıyla yazarın soyadından sonra ve çalışmanın yürütülmüş olduğu yerden önce üstsimgesi (1, 2, 3 vb.) ile numaralandırılmalıdır. Sorumlu yazar, soyadından sonra " * " simgesi ile belirtilmelidir. Adres bilgileri içerisinde çalışmanın yürütüldüğü yer, şehir, posta kodu ve ülke adı yer almalıdır. Adres bilgilerinden sonraki satıra her bir yazarın e-posta adresi yazar isimlerinin sırasına uygun olarak verilmelidir.

Özet: Ana metne atıf yapmadan makalenin konusu anlaşılır bir şekilde özetlemelidir. Özet 220 kelimeyi geçmemelidir. Standart olmayan kısaltmalar ilk kullanıldığında tam olarak yazılmalıdır.

Anahtar Kelimeler: Özetten hemen sonra gelmelidir. En fazla 5 anahtar kelime, harf sırasıyla verilmelidir. Anahtar Kelimeler konuyu açıklayıcı kelimelerden seçilmelidir. Her bir anahtar kelime ", " ile ayrılmalıdır. Anahtar kelimeler cümle içermemelidir.

Abstract: Özette verilen metnin İngilizceye çevrilmesiyle oluşturulmalıdır. Ondalık sayılar kullanılıyorsa bu sayıların Türkçe Özette " , " İngilizce özetinde " . " olmasına dikkat edilmelidir.

Key Words: İngilizce özetten sonra verilmelidir. Türkçe anahtar kelimelerle uyumlu olmalıdır. Konu ile ilgili en çok 5 anahtar kelime alfabetik olarak yazılmalıdır.

MAKALE KONTROL LİSTESİ FORMU

Makalenin metin bölümünün dergi yazım kurallarına uygunluğunun kabul edildiğini gösteren formdur. Başvurular yapılmadan önce Makale Kontrol Formunun doldurulması gerekmektedir. Kontrol formu makalenin ilk sayfası olarak verilmelidir. Dergi formatına uygun olmayan veya kontrol listesi doldurulmamış olan başvuru değerlendirilmeye alınmayacaktır.

MAKALE METNİ

Makale Kontrol Listesi Formundan hemen sonra Makale Metni başlamalıdır. Makaleler aşağıda verilen detaylar göz önünü alınarak hazırlanmalıdır.

- Makalenin metin bölümü Times New Roman 12 punto Yazı Tipi karakterinde, Microsoft Office Word 2010 ve üzeri bir kelime işlemci ile hazırlanması ve Microsoft Office Word'un Yazım ve Dilbilgisi bölümünden yazım hatalarının kontrol edilmesi ve düzeltilmesi gerekmektedir.
- Makale tek sütun halinde mümkün olduğunca yalın olarak, 2,5 cm kenar boşlukları kullanılarak A4 sayfasında oluşturulmalıdır.
- Makale düzenlenirken sayfa düzeninin değiştirilmemesi gerekmektedir.
- Satır aralıkları 1,5 olarak ayarlanmalı ve paragraflar arasında bir satır boşluk bırakılmalıdır. Paragraflar öncesi veya sonrasında otomatik aralık bırakılmamalıdır.
- Sayfa geçişlerinde bölüm sonları eklenmemeli ve tüm Makale tek bir bölümden oluşmalıdır.
- Tüm başlıkların yanında İngilizce karşılıkları parantez içerisinde yazılmalıdır.
- Makale metni referanslar dahil araştırma makaleleri için 14.000 kelimeyi tarama makaleleri için ise 22.000 kelimeyi geçmemelidir.
- Tablolar ve Şekiller Dergimizin istemiş olduğu formata uygun olarak hazırlanmalıdır.
- Makale metni, ana başlıklarla bölümlere ayrılmalı ve her bölüm başlığı numaralandırılmalıdır. Numaralandırma işlemleri ana bölümler için 1.'den başlamalı ve tüm ana başlıklar (Özet, Teşekkür, Kaynaklar ve Ekler bölümleri hariç) için devam etmelidir. İkincil başlıklar ana bölüm numaralandırmasına uygun olarak 1.1., 1.2., 1.3., ... şeklinde devam etmelidir. Üçüncü başlıklar ikinci başlıklara uygun olarak 1.1.1., 1.1.2., 1.1.3., ... şeklinde devam etmelidir.

Örnek bir makale formatı aşağıda verilmiştir:

Kapak sayfası

1. Giriş (Introduction)
2. Malzemeler ve Yöntemler (Materials and Methods)
3. Sonuçlar ve Tartışma (Results and Discussion)
4. Sonuçlar (Conclusions)
5. Simgeler (Symbols)
- Teşekkür (Acknowledgment)
- Kaynaklar (References)
- Ekler (Appendices)

1. Giriş (Introduction)

Detaylı bir literatür özeti, çalışmanın amacını ve kurulmuş olan hipotezi içermelidir. Kaynaklar toplu olarak ve aralıklı verilmemeli (örnek [1-5] veya [1, 2, 3, 5, 8]), her kaynağın çalışmaya katkısı irdelenmeli ve metin içerisinde belirtilmelidir.

2. Malzemeler ve Yöntemler (Materials and Methods)

Yürütülmüş olan çalışma deneysel bir çalışma ise deney prosedürü/metodu anlaşılır bir şekilde açıklanmalıdır. Teorik bir çalışma yürütülmüşse teorik metodu detaylı bir şekilde verilmelidir. Yapılan çalışmada kullanılan metod daha önce yayınlanmış bir metod ise diğer çalışmaya atıf yapılarak bu çalışmanın diğer çalışmadan farklı belirtilmelidir.

3. Sonuçlar ve Tartışma (Results and Discussion)

Elde edilen verilen açık ve öz bir şekilde verilmelidir. Elde edilen tüm veriler literatür ile karşılaştırılmalıdır.

4. Sonuçlar (Conclusions)

Elde edilen verilen açık ve öz bir şekilde verilmelidir. Elde edilen tüm veriler literatür ile karşılaştırılmalıdır.

5. Simgeler (Symbols)

Makalede kullanılan imgeler açıklamalarıyla birlikte alfabetik sıraya uygun olarak düzenli bir şekilde verilmelidir. Kullanılan diğer imgeler alfabetik sıralamadan sonra gelebilir. Gerektiğinde "Yunan Harfleri", "Alt İndis" gibi alt başlıklar kullanılabilir.

Teşekkür (Acknowledgment)

Makalenin sonunda ve kaynaklar bölümünden önce verilir.

Kaynaklar (References)

- Basılmış kaynakların DOI ve ISBN numarası belirtilmelidir.
- İnternet sitesi adresleri (URL) kaynak olarak verilmemelidir. Ancak metin içerisinde verinin geçtiği yerde veriden sonra belirtilebilir.
- Kaynaklar listesi metin içerisinde kullanılma sırasına uygun olarak numaralandırılmalıdır.
- Kaynaklar, "APA Publication Manual, Seventh Edition" kurallarına uygun olarak hazırlanmalıdır.
- Kaynaklar İngilizce olarak hazırlanmalıdır. Türkçe kaynakların İngilizce karşılıkları köşeli parantez içerisinde belirtilmelidir.

Kaynaklar için örneklere <https://apastyle.apa.org/style-grammar-guidelines/references/examples> adresinden ulaşılabilir.

Kaynaklar için örnekler aşağıda verilmiştir:

- **Kaynak bir makale ise:** Yazarın soyadı, Adının baş harfi. (Yıl). Makalenin tam başlığı. *Derginin Tam Adı*, Cilt no (Sayı no), makalenin başlangıç ve bitiş sayfa no.

Uysal, İ., Yılmaz, B., & Evis, Z. (2020). Boron doped hydroxyapatites in biomedical applications. *Journal of Boron*, 5(4), 192-201.

- **Kaynak yazarı verilen bir kitap ise:** Yazarın soyadı, Adının baş harfi. (Yıl). *Kitabın Adı*. (cilt no, varsa editörü). Yayınevinin adı. ISBN veya DOI numarası.

Yünlü, K. (2019). *Bor: Bileşikleri, Sentez Yöntemleri, Özellikleri, Uygulamaları*. [Boron: Its Compounds, Synthesis Methods, Properties and Applications] (2nd Ed.). Aydıllı Advertising Agency. ISBN 978-605-5310-93-6.

- **Kaynak editörü verilen bir kitap ise:** Editörün soyadı, Adının baş harfi (Eds.). (Yıl). *Kitabın Adı*. (cilt no). Yayınevinin adı. ISBN veya DOI numarası.

Korkmaz, M. (Eds.). (2020). *Bor ve İnsan Sağlığı [Boron and Human Health]*. Kuban Printing and Publishing. ISBN 978-605-9516-69-3.

- **Kaynak kitaptan bir bölüm ise:** Bölüm yazarının soyadı, Adının baş harfi. (Yıl). Kitabın Adı. In bölüm editörünün Soyadı, Adının baş harfi (Eds.), *Bölümün Adı* (Varsa cilt no, alıntılanan sayfalar). Yayınevinin adı.

Hakkı, S., & Nielsen, F. N. (2020). Boron and Human Health., Anti-Inflammatory and Anti-Microbial Potentials of Boron in *Medicine and Dentistry* (pp. 67-82). Nobel Academical Publishing, Education, Consultancy Ltd.

- **Kaynak basılmış tez ise:** Yazarın soyadı, Adının baş harfi. (Yıl). *Tez Başlığı* [Tezin kategorisi, Üniversite]. Tezin kayıtlı olduğu arşiv. Varsa tezin bağlantısı.

Akbaba, S. (2018). *Biopolymer modified polypropylene mesh for hernia treatment* [M. Sc. thesis, Middle East Technical University]. Council of Higher Education Thesis Center (Thesis Number 527833).

- **Kaynak kongreden alınmış bir tebliğ ise:** Yazarın soyadı, Adının baş harfi. (Yıl). Tebliğin adı. *Kongrenin Adı*, Yapıldığı yer, Tebliğin başlangıç ve bitiş sayfa no.

Akbaba, S., Atila, D., Tezcaner, T., & Tezcaner A. (2018). *BIOMED2018-TR 23. Biyomedikal Bilim ve Teknoloji Sempozyumu [BIOMED2018-TR 23rd Biomedical Science and Technology Symposium]*, Turkey, p. 43.

Ekler (Appendices)

Makaledeki ekler EK A (Appendix A), EK B (Appendix B) ve EK C (Appendix C) vb. olarak adlandırılmalıdır. Ekler içerisindeki denklem numaralandırmaları A1, A2, A3 vb. olarak, Tablo ve Şekil numaralandırmaları Tablo A1, Tablo A2, Şekil A1, Şekil A2 vb. olarak adlandırılmalıdır.

Diğer Hususlar

Eşitlik Numaraları: Metin içerisinde eşitlikler Eş. 1, Eş. 2 şeklinde verilmelidir. Eşitlik numaralandırmaları parantez içerisinde (1), (2), (3) vb. olarak, reaksiyon numaralandırmaları (R1), (R2), (R3) vb. olarak numaralandırılmalıdır.

Birimler: Metin, şekil ve tablo içerisinde SI birim sistemi kullanılmalıdır.

Şekiller ve Tablolar:

- Tablo içermeyen bütün görüntüler (fotoğraf, çizim, diyagram, grafik, harita vs.) şekil olarak belirtilir.
- Tablo ve şekiller metin içinde geçişlerine göre numaralandırılmalı, bütün tablo ve şekiller ilgili paragraftan hemen sonra verilmelidir. Tablo ve şekillerin her birinin metin içerisinde bahsedildiğinden emin olunmalıdır.
- Tablo başlıkları tablonun üstüne ve şekil başlıkları şeklin altına konulmalıdır. Tabloların ve Şekillerin Türkçe başlıklarından sonra İngilizce başlıkları parantez içerisinde verilmelidir.
- Makaleye eklenecek şekiller (fotoğraf, çizim, diyagram, grafik, harita vs.) mutlaka yüksek çözünürlükte (300dpi veya üstü) olmalıdır. Kabul edilen görüntü formatları jpeg, png, tiff, bmp, eps, wmf, emf veya pdf'dir. Dosya boyutları 1 Mb'tı geçmemelidir.
- Boyutlandırma işlemi orijinal veri üzerinde yapılmalıdır. Eksen başlıkları, etiketlendirme ve açıklamaları (metin kutusu, oklar, üste resim vb. şekilde) Word içerisinde yapılmamalıdır. Grafik, Word belgesine tek bir öge halinde eklenmelidir.
- Tablolar resim olarak verilmemelidir. Büyük tabloların tek bir sayfaya sığması tercih edilir. Şekillerde el yazısı kullanılmamalıdır. Renkli fotoğraflar kabul edilebilir ancak baskı siyah-beyaz formata olacaktır. Grafiklerin siyah-beyaz baskıda belirgin olabilmesi için uygun simgelerin kullanılmasına özen gösterilmelidir.

Yapısal Diyagramlar ve Matematiksel Denklemler: Molekül yapılarının yanı sıra matematiksel denklemler metin içinde ait oldukları yerde çizilmiş veya yazılmış olmalı ve ayrı bir satırda gösterilmelidir. Bu molekül yapıları veya matematiksel denklemler sağ yanında ve parantez içinde numaralandırılarak daha sonraki kullanımlarda bu numaralara atıf yapılmalıdır.

Eşitlikler ve denklemler için MS Word Equation Editor fonksiyonu, simgeler için ise MS Word'de Insert/Symbol fonksiyonu kullanılmalıdır.

TELİF HAKKI DEVİR FORMU

Yazıların telif hakkı devri, dergi internet sayfasında sunulan form doldurulup imzalanmak suretiyle alınır. İmzalı Telif Hakkı Devir Formunu göndermeyen yazarların yayınları değerlendirilmeye alınmaz.

BENZERLİK ORAN DOSYASI

Makalenizin referanslar bölümü dahil Tam Metni "iThenticate" veya "Turnitin" programları ile taranmalıdır. İlgili programdan alacağınız benzerlik oranı sonucunun PDF formatında sistemimize yüklenilmesi gerekmektedir.

AUTHOR'S GUIDE

1. SCOPE

Journal of Boron; accepts articles in the field of boron, whose qualifications are explained below, in Turkish and English.

Research Article: These are articles that reflect an original research with its findings and results. The study must be original and must contribute to international science.

Scan Article: These are articles that scan a sufficient number of scientific articles, summarize the subject at the current knowledge and technology level, evaluate and compare the findings.

Each article is sent to at least two referees on its subject and has it examined in terms of form, content, original value, contribution to international literature and science / technology. After the deficiencies stated in the referee opinions are completed, the articles that can be published in the journal are brought to the final print format and the approval of the final version of the article is obtained from the authors. The responsibility of the errors that may be found in the article as it is printed in the journal belongs to the authors.

Accepted articles are published free of charge on the journal's website (online) and/or in print.

2. APPLICATION FORMS

It should consist of five separate forms: Cover Page of Article, Article Checklist Form, Article Text, Copyright Form and Similarity Ratio File. Contact information (address, e-mail, mobile and fixed phone number) of the author and other authors to be contacted during the applications must be given on the cover page.

3. SUBMISSION CHECKLIST

During the application process, authors must check the compliance of their submissions with all the items in the list below, applications that do not comply with this guideline will not be evaluated.

1. The article to be sent has not been published before and/or has not been submitted to any journal for publication.
2. The article was prepared using Microsoft Office Word 2010 or higher word processor.
3. Margins, header and footer spacing and line spacing on the A4 page of the article have been adjusted according to the journal format.

4. Main headings and sub-headings were arranged in accordance with the journal format, together with their English translations.
5. The tables were prepared in accordance with the journal format, they were mentioned in the text and placed in the text section of the work.
6. Figures were prepared in accordance with the journal format, they were mentioned in the text, and placed in the text section of the work.
7. Equation and Reaction numbers were given in order in accordance with the journal format.
8. Original figures were prepared entirely in accordance with the spelling rules.
9. Figure sizes are arranged to fit the format.
10. Figures in the text are numbered consecutively.
11. References are written according to the spelling rules.
12. References are listed consecutively in the text.
13. References are listed at the end of the text, in the order given in the text.
14. It was checked that Turkish Article Title / Abstract / Keywords / Section Titles / Table and Figure titles and English Article Title / Abstract / Keywords / Section Titles / Table and Figure titles are the same.
15. The "Cover Page" containing the title of the work, the names of the authors and contact information was created.
16. The Copyright Form was signed and sent.
17. Possible spelling errors were checked with the word processor's "Spelling and Grammar" check.
18. The original aspect of the article and its concrete contribution to science are written in the "Note to the Editor" field.

4. COPYRIGHTS

The copyright transfer of the articles is taken by filling and signing the Copyright Transfer Form presented on the journal website. After the form is signed, it should be uploaded as PDF in the "upload additional files" section. Works of authors who do not submit this form cannot be published.

5. PRIVACY NOTICE

Names and e-mail addresses on this journal site will be used in line with the stated purposes of this journal and will not be used for other purposes or any other section.

WRITING RULES

GENERAL INFORMATION

An article is composed of 5 individual forms which are cover page, article checklist form, article manuscript, copyright transfer form and plagiarism score file. Contact information (address, e-mail address and phone number) of the corresponding author must be given in cover letter.

COVER PAGE

A cover page must be prepared and submitted to journal's webpage as an individual file. Author information will be visible only to journal editors during initial application.

Title of the article must start with a capital letter and centered to the page. The title must be brief, clear and appropriate for the manuscript. Name, surname, e-mail, affiliation, postal code, city and ORCID number of author(s) must be given below the title.

Title of the article in English: An inclusive and understandable title must be used. The title must start with a capital letter and the rest must be lowercase. The title must be no longer than 15 words including required standard abbreviations.

Title of the article in Turkish: Must be in concordance with the Turkish title.

Author Names and Address Information: Authors' names and surnames must start with a capital letter. Author names are followed by the institution where the author is affiliated. Uppercase numbers must be used in order to relate the author to the institution. Corresponding author must be denoted with the asterisk sign " * ", after their surname. Address information must include institution, city, postal code and country name. E-mail address must be added after the address line for all authors, according to author order.

Abstract: Topic of the article must be summarized without citing the article. An abstract must not exceed 220 words. Non-standard abbreviations must be explained when used for the first time.

Keywords: Must be placed after abstract. Maximum 5 words must be given with alphabetical order. Keywords must be chosen from explanatory words about the topic. Every keyword must be separated from each other with " , ". Keywords must not include full sentences.

Abstract in English: Must be formed by translating the text in abstract. If decimal are used, " , " must be used for Turkish abstract and " . " must be used for English numbers.

Keywords in English: Must be placed after Abstract in English. Must be in concordance with Turkish keywords. Maximum of 5 words must be written with the alphabetical order, about the topic.

ARTICLE CHECKLIST FORM

It is the form that shows approval of the article manuscript to the journal's writing rules. Article Checklist Form must be filled before submission. Article Checklist Form must be given as the first page of the manuscript. Applications that are not in accordance with the journal's format or submitted without Article Checklist Form will not be evaluated.

ARTICLE MANUSCRIPT

Article Manuscript must be placed after Article Checklist Form. Article manuscript must be prepared by considering details given below.

- Article manuscript must be prepared with Times New Roman font and 12 font size by using Microsoft Office Word 2010 or later version word processor. Misspellings and grammatical errors must be checked and corrected by using Microsoft Office Word's proofing errors section.
- Article manuscript must be prepared in A4 size page with 2.5 cm margins from each side, as a single column.
- Page order must not be changed when article is reviewed.
- Line and paragraph spacing must be set to 1.5 and there must be 1 line space between paragraphs. There must be no automatic line spacing before and after paragraphs.
- There must be no page breaks between pages and whole manuscript must consist of a single section.
- In case the article is in Turkish, translation of all headings must be given in parentheses.
- The manuscript must not exceed 14,000 words for research articles and 22,000 for review articles including references.
- Tables and figures must be prepared according to the journal's requirements.
- The manuscript must be divided into main sections and each section must be numbered. Numbering must start from 1 and go on for all main sections (Except for Abstract, Acknowledgements, References and Appendices sections). Secondary headings must be numbered as 1.1., 1.2., 1.3., etc. in concordance with main headings. Tertiary headings must be numbered as 1.1.1., 1.1.2., 1.1.3., etc. in concordance with secondary headings.

Manuscript format sample is given below:

Cover page
1. Introduction
2. Materials and Methods
3. Results and Discussion
4. Conclusions
5. Symbols
Acknowledgments
References
Appendices

1. Introduction

Must include detailed literature review, purpose and hypothesis of the conducted study. Contribution of a reference must be examined and placed individually in the manuscript, must not be given collectively.

2. Materials and methods

If the manuscript is for a research article, experimental methods must be explained in an understandable and detailed manner. Theoretical approach must be explained in detail, if a theoretical study was conducted. If the method that was used is already published, related source must be cited and differences must be pointed.

3. Results and discussion

Obtained data must be presented clearly. Data interpretation and literature comparison must be done.

4. Conclusions

Main conclusions of the conducted study must be given briefly.

5. Symbols

Symbols that are used in the manuscript must be given with an alphabetical order. Other symbols can be given after the alphabetical order. Greek letters and subscripts can be used, if required.

Acknowledgment

Acknowledgements is given after the manuscript and before the references.

References

- DOI or ISBN numbers of published sources must be given.
- Webpages (URL) must not be used as a reference. They can be used only in manuscript after data.
- References must be numbered with the same order as mentioned in the manuscript.
- References must be prepared according to "APA Publication Manual, Seventh Edition" rules.
- References must be prepared in English. English translation of Turkish sources must be denoted with square brackets.

Sample references can be found from the URL address <https://apastyle.apa.org/style-grammar-guidelines/references/examples>

- **If the source is an article:** Author's Last Name, Initial of Author's First Name. (Year). Article's full title. *Journal's Full Title*, Volume number (Issue number), Page numbers.

Uysal, İ., Yılmaz, B., & Evis, Z. (2020). Boron doped hydroxyapatites in biomedical applications. *Journal of Boron*, 5(4), 192-201.

- **If the source is a book with author:** Author's Last Name, Initial of Author's First Name. (Year). *Book's Name*. (Volume number, Editor, if present). Publisher. ISBN or DOI number.

Yünlü, K. (2019). *Bor: Bileşikleri, Sentez Yöntemleri, Özellikleri, Uygulamaları*. [Boron: Its Compounds, Synthesis Methods, Properties and Applications] (2nd Ed.). Aydıli Advertising Agency. ISBN 978-605-5310-93-6.

- **If the source is a book with editor:** Editor's Last Name, Initial of Editor's First Name (Eds.). (Year). *Book's Name*. (Volume number). Publisher. ISBN or DOI number.

Korkmaz, M. (Eds.). (2020). *Bor ve İnsan Sağlığı [Boron and Human Health]*. Kuban Printing and Publishing. ISBN 978-605-9516-69-3.

- **If the source is a chapter from a book:** Chapter Author's Last Name, Initial of Chapter Author's First Name. (Year). *Book's Name*. In Last Name of Chapter's Editor, First Name of Chapter's Editor (Eds.), *Chapter's Name* (Volume number if present, Pages). Publisher.

Hakkı, S., & Nielsen, F. N. (2020). Boron and Human Health., *Anti-Inflammatory and Anti-Microbial Potentials of Boron in Medicine and Dentistry* (pp. 67-82). Nobel Academical Publishing, Education, Consultancy Ltd.

- **If the source is a published thesis:** Author's Last Name, Initial of Author's First Name. (Year). *Thesis title* [Thesis category, University]. Archive that the thesis is registered (Thesis Number). Link to the thesis, if present.

Akbaba, S. (2018). *Biopolymer modified polypropylene mesh for hernia treatment* [M. Sc. thesis, Middle East Technical University]. Council of Higher Education Thesis Center (Thesis Number 527833).

- **If the source is from a conference proceeding:** Author's Last Name, Initial of Author's First Name. (Year). Name of the proceeding. *Name of the Conference*, Place of the Conference, Proceeding page numbers.

Akbaba, S., Atila, D., Tezcaner, T., & Tezcaner A. (2018). BIOMED2018-TR 23. *Biyomedikal Bilim ve Teknoloji Sempozyumu [BIOMED2018-TR 23rd Biomedical Science and Technology Symposium]*, Turkey, p. 43.

Appendices

Appendices in the manuscript must be named as AP A (Appendix A), AP B (Appendix B) and AP C (Appendix C) etc. Equation numbering within the appendix must be as A1, A2, A3 etc., whereas Table and Figure numbering must follow as Table A1, Table A2, Figure A1, Figure A2 etc.

Other Issues

Equality Numbers: Equations in the manuscript must be given as Eq. 1, Eq. 2. Equations must be numbered in brackets as (1), (2), (3), etc., and reaction numbers as (R1), (R2), (R3), etc.

Units: The SI unit system must be used in the text, figures and tables.

Figures and Tables:

- All images (photographs, drawings, diagrams, graphs, maps, etc.) that do not contain tables are considered as figures.
- Each table and figure must be numbered according to their transition in the text, and all tables and figures must be given right after mentioned paragraph in manuscript. It must be made sure that each table and figure was mentioned in the text.
- Table captions must be placed above the table and figure captions must be placed under the figure. Table and figure captions must also be noted in English and given in parentheses if the manuscript is in Turkish.
- Figures (photograph, drawing, diagram, graphic, map, etc.) to be added to the article must be at high resolution (300dpi or higher). Accepted image formats are jpeg, png, tiff, bmp, eps, wmf, emf or pdf. File sizes must not exceed 1 Mb.
- The sizing process must be done on the original data. Axis titles, labelling and explanations (such as text box, arrows, picture on top, etc.) must not be added with Word. The plot must be added to the Word document as a single element.
- Tables must not be added as pictures. Large tables are preferred to be fit in a single page. Handwriting must never be used in figures. Although colorized figures are acceptable, printing will be done in black-white format. Appropriate symbols must be used in order for figures to be prominent in black-white printing.

Structural Diagrams and Mathematical Equations: Mathematical equations as well as molecular structures must be drawn or written where they belong in the text and displayed on a separate line. These molecular structures or mathematical equations must be numbered on the right side and in parentheses for later referring.

MS Word Equation Editor function must be used for equations, and Insert/Symbol function in MS Word for symbols.

COPYRIGHT FORM

Copyright transfer of the articles is taken by filling and signing the form presented on the journal website. The publications of the authors who do not send the signed Copyright Form will not be evaluated.

SIMILARITY RATIO FILE

The manuscript, excluding the references section, must be scanned using the "iThenticate" or "Turnitin" programs. The similarity ratio result received from the relevant program must be uploaded to system in PDF format. It is expected that similarity ratio is not more than 10%.



İÇİNDEKİLER/CONTENTS

Effects of different boron salt treatments on micropropagation and genetic stability in <i>in vitro</i> cultures of <i>Liquidambar orientalis</i> Miller	521
..... Taner Mercan, Selin Galatalı, Damla Ekin Ozkaya, Onur Celik, Ergun Kaya	
Effect of soil application and foliar boron (Etidot-67) on hazelnut yield and kernel ratio	528
..... Faruk Özkutlu, Kürşat Korkmaz, Özlem Ete Aydemir, Mehmet Akgün, Fatmagül Akdin, Bayram Özcan, Özge Şahin, Mehmet Burak Taşkın	
B ₂ O ₃ katkısının PET'in kimyasal bozunma davranışı, termal ve mekanik performansı üzerine etkisi.....	535
..... Bilal Demirel, Ali Yaraş, Fatih Akkurt, Sedat Sürdem	
Investigation of the effects of borogypsum and silica fume on ceramic material's sintering and final properties.....	543
..... Çetin Öztürk, Atilla Evcin	
Co-synthesis of zirconium boride/silicide/oxide composite powders by magnesiothermic reduction	552
..... Didem Ovalı-Döndaş	

TENMAK Bor Araştırma Enstitüsü

Dumlupınar Bulvarı (Eskişehir Yolu 7. km), No:166, D Blok, 06530, Ankara

Tel: (0312) 201 36 00

Faks: (0312) 219 80 55

e-mail: boren.journal@tenmak.gov.tr

web:<https://dergipark.org.tr/boron>